AD NUMBER: AD0857519

LIMITATION CHANGES

TO:

Approved for public release; distribution is unlimited.

FROM:

This document is subject to special export controls; 01 Jun 1969, and each transmittal to foreign governments or foreign nationals may be made only with prior approval of RADC (ECMVM-1), GAFB, NY 13440.

AUTHORITY

ST-A RADC, USAF LTR, 17 SEP 1971

RADC-TR-65-161
Technical Report
June 1965

EMC DATA COLLECTION TECHNIQUES

Test Methods C2 and C5

Final Report

K. H. Dalla

G. M. Stevens

et al

University of Pennsylvania

D D C

EMC DATA COLLECTION TECHNIQUES

Test Methods CE and CS

Fred Haber
K. H. Dolle
R. M. Showers
et al

University of Pennsylvania

FOREWORD

This report presents the results of research on the second phase of Contract F30602-68-C-0178 entitled "EMC Data Collection Techniques." This report was prepared by The Moore School of Electrical Engineering, University of Pennsylvania, Philadelphia, 19104, for Rome Air Development Center, Griffiss Air Force Base, New York, under Project 4540, Task 454001.

RADC Effort Engineer was Mr. Robert White, EMCVM-1.

The authors gratefully acknowledge the assistance and cooperation given by members of the Air Force and their laboratories, and Mr. Frank Giordano of the U.S. Navy Applied Physics Laboratory, Brooklyn, New York, for the loan of a power line impedance bridge.

The contributors to this report were: P.A. Beekman, K.H. Dolle, R.J. Doviak, D.E. Groff, Fred Haber, D. Loomis, R.M. Showers, L.P. Sinha, and C.S. Yablik.

Distribution of this report is restricted to protect techniques for establishing new test specification limits for evaluation of military equipments.

This technical report has been revieved and is approved.

Approved: Robert L. White
ROBERT L. WHITE
Effort Engineer

Approved: Richard M. Cosel
RICHARD M. COSEL, Colonel, USAF
Chief, Communications Division

FOR THE COMMANDER: Irving J. Gabelman
IRVING J. GABELMAN
Chief, Advanced Studies Group

ABSTRACT

An evaluation of the present specifications for conducted interference in MIL-STD-461A and 462 is reported. The basis for setting limits is reviewed, and the test methods presently called for are applied to several types of communications and radar equipment. Statistical data on power line and equipment internal impedances permit a comparison of present emission and susceptibility limits and permit the computation of new limits by inserting the data into a theoretical interference model.

A radiation model is used to arrive at an absolute limit of current from an interference source. This limit is converted to a measured emission current limit through use of a statistical circuit model, assuming an allowable 2.3% probability of interference. A corresponding susceptibility limit is derived.

From the standpoint of efficiency in predicting compatibility, the optimum value of emission test load impedance is the average actual load impedance, and not a short circuit as is presently used. Limits derived for both test terminations, and accuracies of the two techniques are compared.

Certain new emission and susceptibility limits are proposed and specific recommendations are presented on test methods.

BLANK PAGE

TABLE OF CONTENTS

continued

continued

TABLE OF CONTENTS

LIST OF FIGURES

LIST OF FIGURES (cont.)

LIST OF FIGURES (cont.)

BLANK PAGE

Section 1

INTRODUCTION

1.0 Objective

The objective of this program is to"investigate, to establish, and to validate the electromagnetic emission and susceptibility limits specified in MIL-STD-461." The purpose is to provide sound engineering limits applicable to the test methods associated with particular equipment classes and environmental categories.

This report is primarily concerned with the conducted aspects of the work, namely, the examination of specifications related to conducted emissions (CE) and conducted susceptibility (CS). The emissions in question consist of any undesired signals emitted by electrical or electronic equipment on conductors connected to them, such as power lines, and input, output or antenna leads which might interfere with other equipment. The emissions may be conducted into other equipment or they may couple into other equipment by induction or radiation from the conductors under discussion and thereby affect susceptible equipment.

The general approach used in the development of this research program was discussed in the first technical report.* There, an "interaction model" was formulated which was used to describe the relationship between conducted and radiated emissions and susceptibility, and a partial listing of critical parameters relevant to the establishment of limits was given. That report should be consulted for further details. Because of the interdependence between radiated and conducted phenomena, it has been necessary to give some attention in this work to radiation as well as to conduction.

1.1 General Viewpoint

Before proceeding, it would be well to state the underlying viewpoint which motivated the approach taken here.

It was recognized at the outset that the effort toward developing satisfactory radio interference control specifications has a long history; the specifications dealt with here represent a distillation of the work of at least 20 years. In considering any proposed amendments to present practices, we have therefore carefully examined all possible bases for the existing specifications. Of considerable significance is the lack of documentation on the rationale behind the choice of limits and procedures. It is our belief that such documentation is essential if (1) the user is to have an adequate appreciation for the meaning inherent in the test procedure and the limit, and if (2) further work is to result in significant improvement.

1.2 Protection Afforded by Interference Testing

As discussed in the first report,** the purpose behind interference testing is to insure that electromagnetic incompatibility will arise only very infrequently. It is generally recognized that limits and procedures should be sufficient to cover most cases, not the "worst case," if the latter is uncommon. This means that there will be situations when equipments satisfying the specifications individually will not operate compatibly when initially installed. In such cases, additional steps will have to be taken to make the system work. To guarantee that this will never happen is impractical (and very likely impossible). It is only necessary to put the limits at a level at which there is no overall cost disadvantage--that is, at which the cost incurred in satisfying a specification with raised limits does not exceed the cost of achieving compatibility a posteriori.

We anticipate the need for occasional arbitrary decisions on the models to be used in the analysis, on levels and techniques. This ought not to suggest that the test results are the product of whim and need not be taken seriously. By describing the model used to arrive at a specification limit the compatibility engineer will know that in

---

* "EMC Data Collection Techniques," Report No. 1, Test Method CE, Dec. 1968.

** Id.

a particular configuration the interference conditions may be below the stated limit level. This knowledge should be a useful guide to him in making decisions on his specific configuration. Where such arbitrary choices are made they are based, to whatever extent possible, on typical configurations, and the limits so obtained are checked to see if compliance can be expected in view of the current state of the art.

It has been observed by some that the specification limits should perhaps be variable, depending on the configuration in which the equipment is to be employed. This has obvious disadvantages for general specifications such as MIL-STD-461A and 462. Rather than go in this direction it is advisable to fix the limit; in special situations the engineer responsible for the system would know what protection he needs and could specify other limits.

1.3 Technical Approach

The approach to this work was three-fold. The theoretical and practical rationale for choosing the quantities to be measured and the limits to be placed on these quantities were examined; measurements of environmental parameters to enable us to specify reasonable limits were made; and many of the tests specified were carried out to determine, at first hand, what problems of implementation and interpretation exist.

Section II of the report provides a review of present limits and discusses various aspects of the rationale behind them. These data are used as background material for recommendations made later in the report. Section III presents two analytical models upon which certain fundamental limit recommendations are based; one concerning a radiation basis for a conducted limit, and the other, a criterion for choice of a measurement method.

In Section IV measured data are inserted into the results of Section III to provide certain "theoretical" limits. In Section V an "evaluation" of these limits is made, taking into account certain "practical" considerations. Section V also develops other limit recommendations not explicitly discussed previously and comments on present test procedures and proposed revisions in them. Section VI summarizes the main conclusions and recommendations.

SECTION 2

A COMPARISON OF EMISSION AND SUSCEPTIBILITY LIMITS

A recent report* traces the development of electromagnetic compatibility standards and specifications over the past several decades. Much interesting data are presented on the various considerations involved in setting the limits established from time to time. A good background on the complexity of the situation can be obtained from this paper.

If one concerns himself with the situation in which a source of interference is coupled to a susceptible device only by means of conduction, a suitable means of control of interference can be established by providing limits for susceptibility and for emission having an appropriate relationship between each other. A discussion of this relationship is given in Pearlston's paper. With the limits, when expressed on commensurate scales, arranged so that the susceptibility limit is higher than the emission limit at all frequencies, interference would not be expected between equipments meeting the limits, unless there were actually a coupling gain between them. This concept becomes more complex in the case of broadband interference as compared to sine wave interference, since in the broadband case the condition for susceptibility is dependent upon the bandwidth of the receiver which is used, and the limits must be properly expressed in terms of appropriate parameters of the interacting devices in order that the criterion can be applied with confidence.

2.1 Summary of Emission Limits (Power Leads)

Present MIL-STD-461A conducted emission limits for both broadband and narrowband noise are shown in Figs. 1a and 1b. These limits are given in either decibels above 1 μA (in the case of narrowband limits) or in terms of decibels above 1 μA per MHz (in the case of broadband limits). As pointed out by Pearlston, the basis for the shapes of these curves is not well documented by published data. It is fair to state, however, that it is likely that equipment will be able to accept higher levels of interference at low frequencies than at high frequencies because of the improved efficiencies with which energy at higher frequencies can be transferred from one circuit to another by induction or radiation. Furthermore, it is likely that the general shapes of these curves are consistent with levels of spurious interference which are observed in equipments of various types. Thus, the shapes of the curves are partly based upon

---

* "What is Wrong with EMI Specifications," C. B. Pearlston, Jr., Electronic Engineer, July 1968, p. 66.

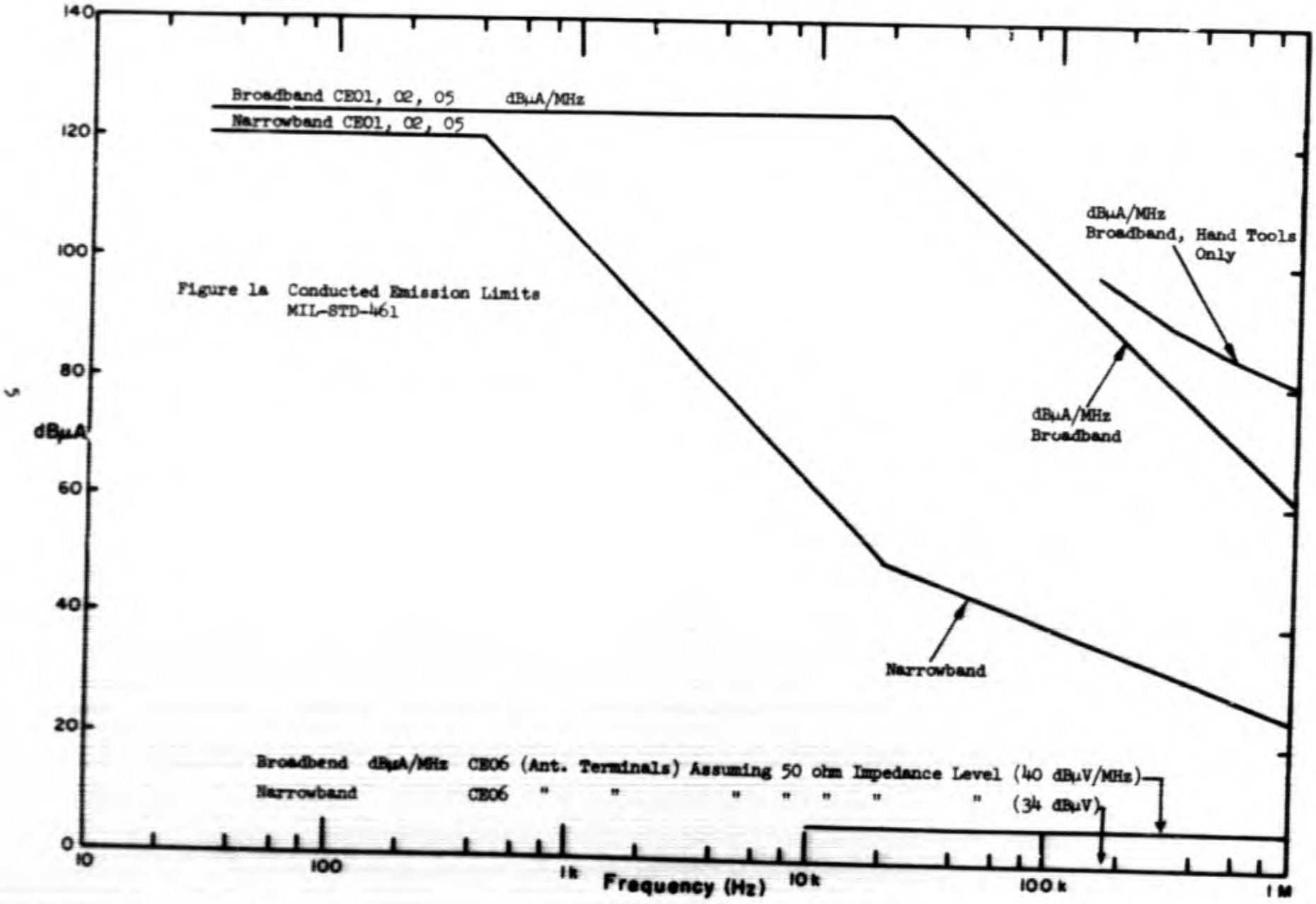

Figure 1a Conducted Emission Limits
MIL-STD-461

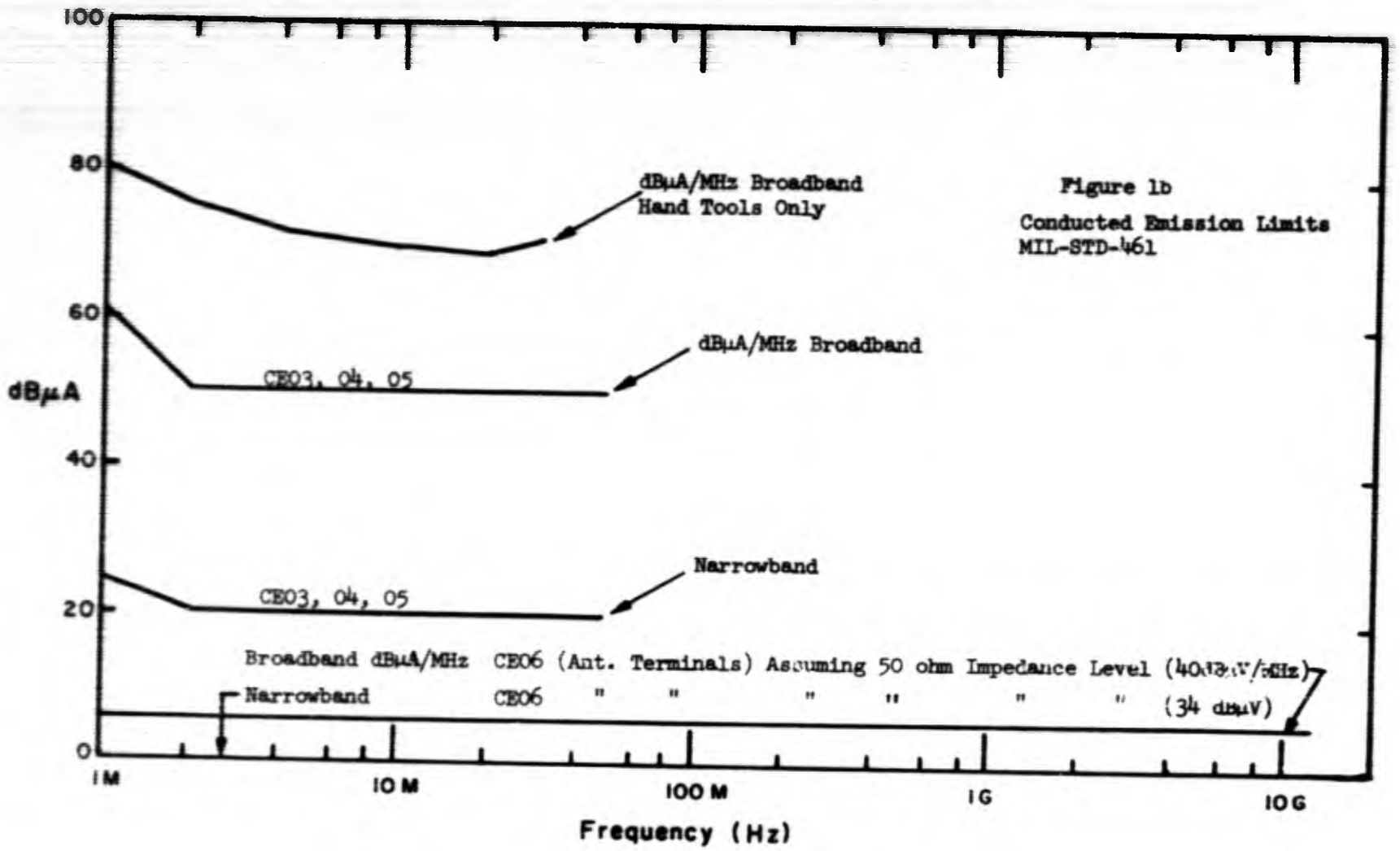

Figure 1b

Conducted Emission Limits
MIL-STD-461

what is obtainable in practice (a matter which deserves consideration from an economic point of view) and partly on susceptibility considerations.

The special limit for hand tools is apparently very specifically based upon what is obtainable; in fact, recently this limit has been considered for revision upward because of the difficulty of meeting it. From a practical point of view, it would seem that a high limit is permissible for hand tools since such tools are generally used for only a short period of time in susceptible locations, but a "use" discipline may be necessary in a critical operational situation.

The low values of emission permitted at antenna terminals are presumably justified on the basis that such currents would be directly connected to antennas which would radiate, or to other receivers which would be quite susceptible to relatively small currents when they are coupled directly to the antenna input terminals.

2.2 Summary of Susceptibility Limits (Power Leads)

Figures 2a and 2b show present susceptibility limits (curves labeled CS). The one labeled CS06 is a theoretical spectrum of a pulse, used in a spike test, which apparently is designed primarily to test the susceptibility of an equipment to a transient on a power line. (To calculate the spectrum conveniently it was necessary to approximate the actual pulse waveform given in MIL-STD-461.) The transient is approximately 10 μs long and has a peak value of 100 V or twice the line voltage, whichever is less. This test is not meant specifically as an evaluation of the performance of a device to broadband interference. No other broadband susceptibility requirement appears in this standard. It should be noted that the spectrum given in the figure drops off rapidly with frequency above 100 kHz.

The narrowband susceptibility level for power lines is also shown on Fig. 2. It is flat at about 1.0 V at frequencies above 50 kHz and somewhat higher at lower frequencies.

2.3 Correlation of Emission and Susceptibility Limits

Where only conduction is involved, in order to relate the susceptibility limit with the emission limit, one can multiply the permitted emission current (which is presumably short-circuit current) by the expected parallel impedance of the power line and internal impedance of the source. In studies described in later sections of this report, values of the power line impedance as a function of frequency were determined, as given in Fig. 8. Using the data on Figs. 1 and 8, one thus obtains the curves on Fig. 2

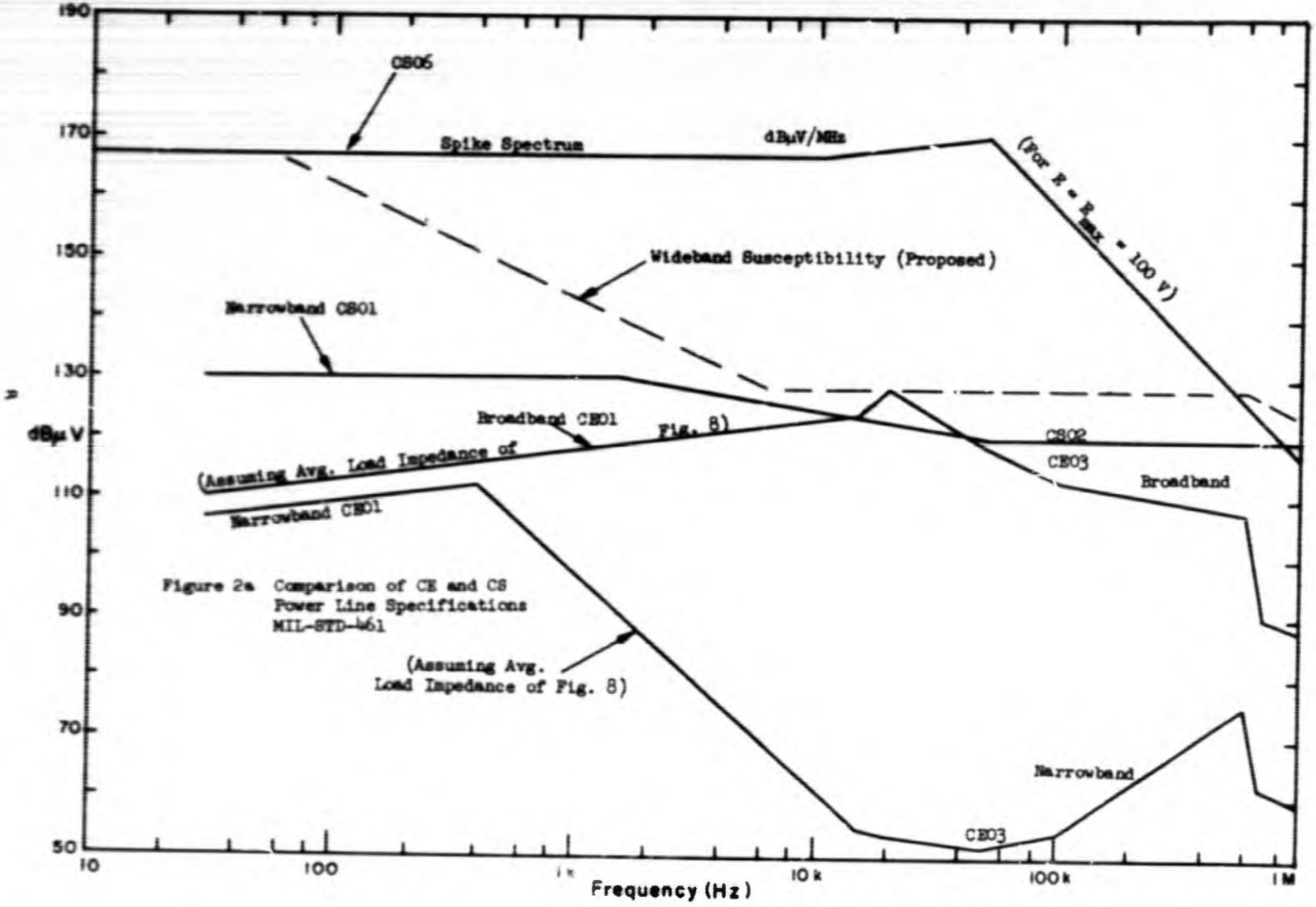

Figure 2a Comparison of CE and CS Power Line Specifications MIL-STD-461

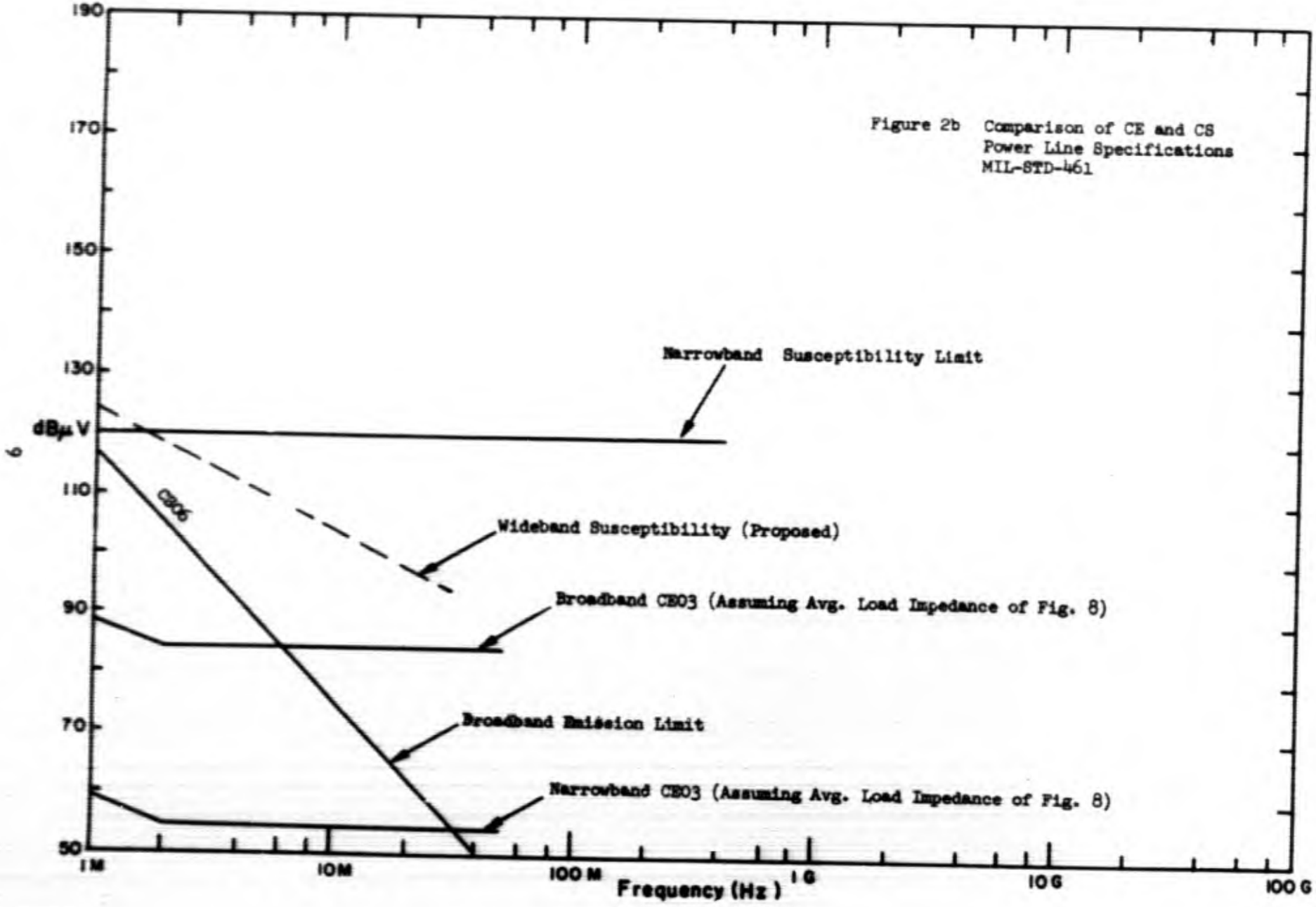

Figure 2b Comparison of CE and CS Power Line Specifications MIL-STD-461

identified by the words "(assuming average load impedance of Fig. 8)." Note that these impedance data are "unsmoothed" and therefore these curves show sudden changes in shape. Later in the report the curves of Fig. 8 are "smoothed" before being used in generating recommendations. Comparing the narrowband curve with the narrowband susceptibility limit curve, also given on Fig. 2, one observes that at a frequency of 400 Hz there is only about 18 dB of protection (that is, the difference between the susceptibility value and the emission value), at 50 kHz there is about 70 dB, and at higher frequencies the degree of protection is of the order of 65 dB. Some of the protection might be considered as needed to take into account the fact that the impedance values used in the emission curve are nominal and that they actually vary over a wide range. The apparently high degree of protection, however, underlies the fact that this concept was probably not used in establishing present limits.

The high value of the narrowband susceptibility limit which is taken out to 400 MHz is thought to be required for operating susceptible devices in the local field of transmitting antennas. Here a "mixed" radiation-conduction mechanism is involved where radiation from the antenna is coupled into unprotected power lines and thereby produces substantial voltages at the device power line terminals. Considerations of this type of coupling, although strictly speaking lying within the scope of the work on radiation planned for the next phase of this study, require special treatment in attempting to correlate emission and susceptibility limits. Figure 2 also compares the broadband voltage expected on the line at the limit value of the emission current and the spike spectrum specified in CS06. Although this comparison may not be valid, generally, the difference in these curves is large at low frequencies, but decreases at higher frequencies where they eventually reverse positions. In the frequency range up to 100 kHz these two tests, broadband emission and broadband susceptibility, do in fact measure comparable quantities and appear to be separated by an unjustifiable amount. It is conceivable that the explanation for this difference lies in the susceptibility criterion used in the spike test, where a major failure is implied (such as loss of information stored in a computer memory). Presumably, this type of spike is expected to occur very infrequently.

It would also be possible to compare the broadband emission limit with the narrowband susceptibility limit, on the assumption that the susceptible device has an effective bandwidth, and if one multiplies the emission strength by the effective bandwidth and obtains a level which exceeds the narrowband susceptibility level, one would expect to get some degradation in performance of the device. Just how much degradation would be obtained would depend upon the repetition rate of the broadband noise and other factors. To make this comparison, one must tabulate such effective bandwidths for the

various devices which might be connected to power lines of interest. A procedure of this kind is described in connection with new limit proposals in a later section of this report.

2.4 Signal and Control Leads

Figure 3 shows data corresponding to that on Fig. 2 for signal leads. Here, the susceptibility limits, as given in MIL-STD-461A, are in every case flat with frequency. In relating the emission limit for CE02, 04, 05 in terms of current to the susceptibility limit in terms of voltage, we have multiplied the current limits by 50, assuming that the impedance of the signal or control line is 50 ohms in each case. It is particularly interesting in this case to note that the emission and susceptibility curves cross, so that at low frequencies the allowed value of emission exceeds all susceptibility limit values. The difficulties of comparing the emission and susceptibility limits are obvious. Note also the susceptibility limits on intermodulation and spurious response are given in terms of receiver sensitivity ("standard reference output"). These levels are therefore comparable only if one assumes values for the corresponding sensitivity. Curves are shown on Fig. 3 for 0.1 μV sensitivity and 1.0 μV sensitivity receivers.

It should be further noted that there is no effective broadband susceptibility test, except for the evaluation of the squelch circuit. Here again one could relate the broadband emission limit to the narrowband susceptibility by an examination of the effective bandwidth of the devices which are involved. In such an evaluation, it would be assumed there were no significant spurious responses of a broadband nature. However, cases have been known where out-of-band spurious broadband responses of significant magnitude were observed.

2.5 Summary

A succinct discussion of present conducted emission and susceptibility limits has been presented along with some of the pertinent rationale underlying them.

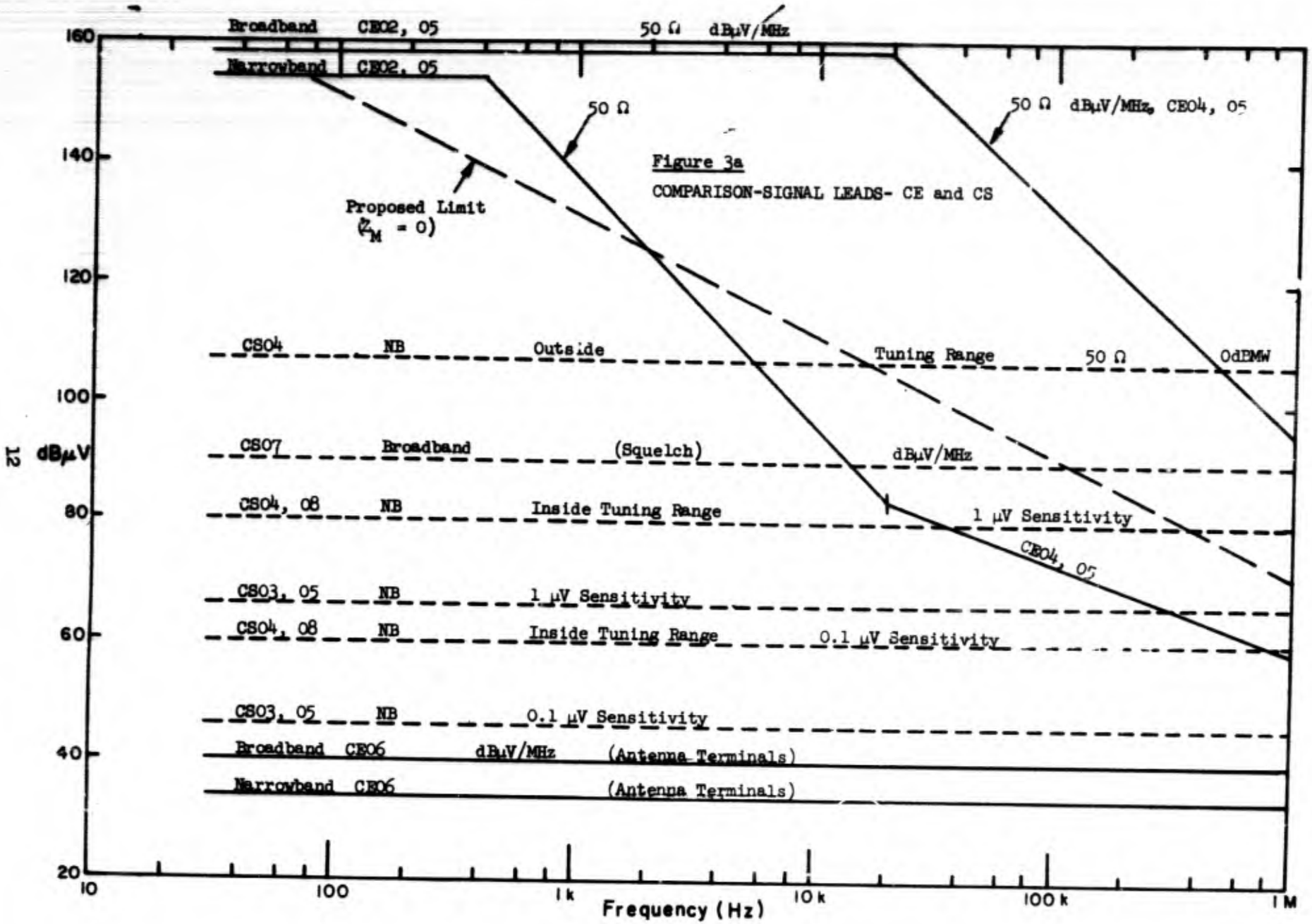

Figure 3a

COMPARISON-SIGNAL LEADS- CE and CS

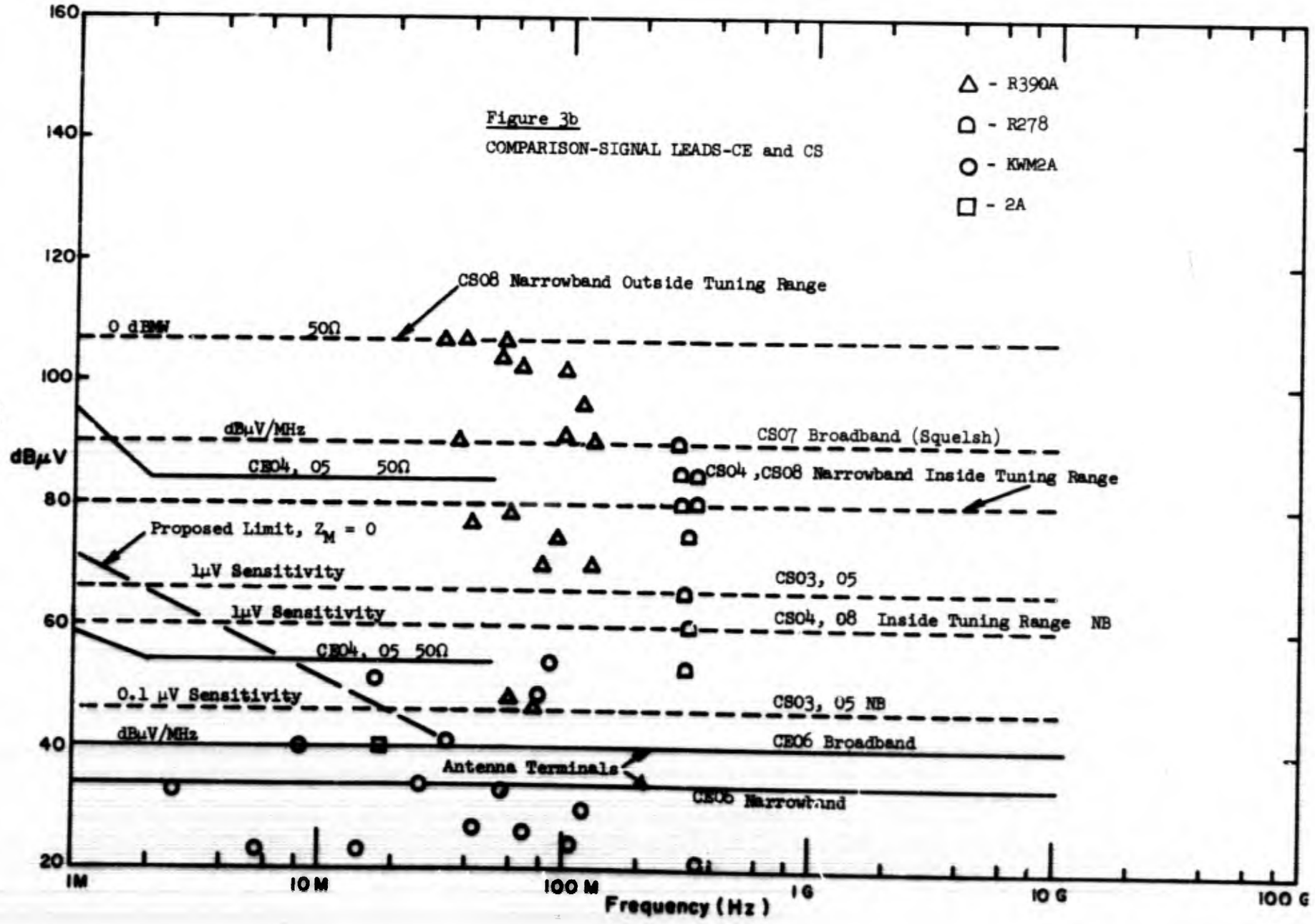
160
140
120
100
80
60
40
20
dBμV
Figure 3b
COMPARISON-SIGNAL LEADS-CE and CS
Δ - R390A
⌂ - R278
○ - KWM2A
□ - 2A
CS08 Narrowband Outside Tuning Range
0 dBW
50Ω
dBμV/MHz
CS07 Broadband (Squelsh)
CE04, 05 50Ω
CS04, CS08 Narrowband Inside Tuning Range
Proposed Limit, Z_M = 0
1μV Sensitivity
CS03, 05
1μV Sensitivity
CS04, 08 Inside Tuning Range NB
CE04, 05 50Ω
0.1 μV Sensitivity
CS03, 05 NB
dBμV/MHz
CE06 Broadband
Antenna Terminals
CE06 Narrowband
1M
10 M
100 M
1G
10 G
100 G
Frequency (Hz)

SECTION 3

ANALYSIS

3.1 Introduction

One possible basis for establishing an emission limit is the potential of any resulting current to radiate. The view may be taken that noise emanating from the power terminals, which are not observed in the usual radiation tests carried out in the vicinity of the equipment, may pass along the power leads to some more remote point and there be radiated to nearby sensitive equipment. In this case, the limit established is intended to maintain the noise emission current on power leads below a level which, in a certain assumed configuration, will induce or radiate fields considering potentially harmful. The analysis of this model is carried out in Section 3.2.

Another matter requiring analysis is the proper basis for correlating emission and susceptibility limits as just described in Section 2 of this report. The limit is chosen for the current measured in a laboratory emission test, so as to insure that, if the equipment satisfying such a test is connected to any line, the probability will be small of exceeding the allowable emission current. The laboratory emission test is carried out using a setup which is itself chosen to improve the quality, in a statistical sense, of the compatibility prediction. The analysis of this matter is carried out in Section 3.3.

3.2 Limit of Allowable Current on Power Leads

The model assumed was as follows. Noise emission current enters and passes along the power leads to a remote point. Here the wiring configuration is such that it behaves like a radiating, or inducing, one-turn loop, which we assumed to have an area of one square meter. Furthermore, it was assumed that a sensitive receptor will be found at a distance of 10 meters from the radiating source. Three different interference criteria were examined. In the first, the current in the radiating loop which results in a maximum electric field of 1 μV/meter at the receptor was determined. In the second, the receptor was assumed to be a 10 turn, 1 square meter, receiving loop (which is typical of low frequency loops) and the current in the radiating loop which would induce 1 μV in a coaxial receptor loop was found. The third scheme was similar to the second except that the two loops were assumed coplanar.

The equation governing the first configuration is given by*

$$|I| = \frac{(3 \times 10^8)^2 |E|}{120\pi^2 f^2} \frac{r}{A} \frac{1}{\left[1 + \frac{(3 \times 10^8)^2}{4\pi^2 f^2 r^2}\right]^{1/2}} \text{ Amp} \qquad (3.2.1)$$

where $|I|$ is the magnitude of the input current which causes an electric field magnitude of $|E|$ volts/meter,

r is the distance in meters between loop center and point at which $|E|$ is determined, and

f is frequency in Hertz.

With $|E| = 1\ \mu V/m$, $A = 1\ m^2$, $r = 10$ m

$$I = \frac{7.58 \times 10^8}{f^2} \frac{1}{\left[1 + \left(\frac{4.78 \times 10^6}{f}\right)^2\right]^{1/2}} \text{ Amp} \qquad (3.2.2)$$

for $f \ll 4.78$ MHz

$$I = \frac{1.85 \times 10^8}{f} \ \mu A \qquad (3.2.3)$$

for $f \gg 4.78$ MHz

$$I = \frac{7.58 \times 10^{14}}{f^2} \ \mu A \qquad (3.2.4)$$

These results are shown plotted in Fig. 4 curve I.

The equation governing the second configuration (coaxial loops

* Antenna Engineering Handbook by Henry Jasik, McGraw-Hill, 1961, pp. 2-4.

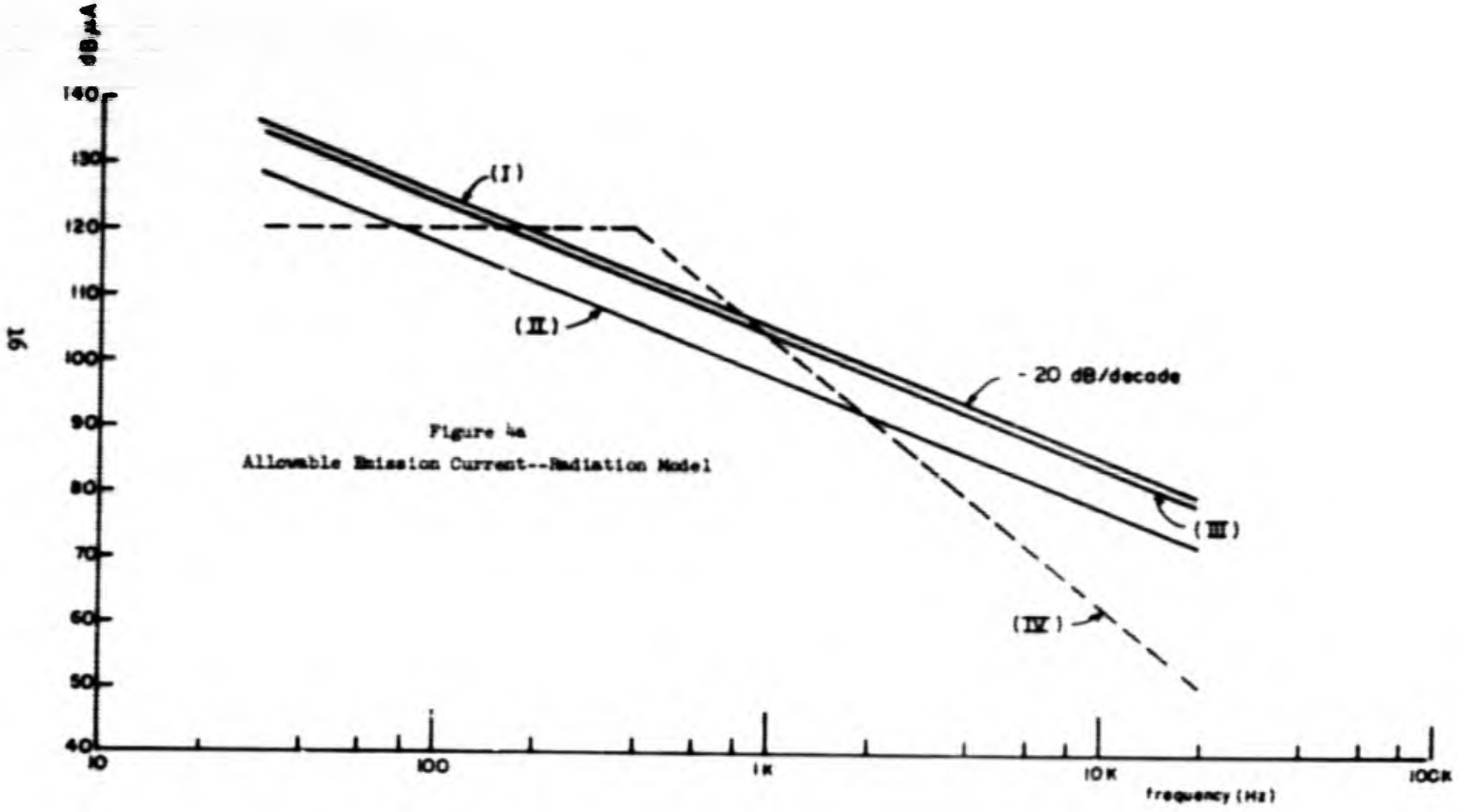

Figure 4a

Allowable Emission Current--Radiation Model

Figure 4b

Allowable Emission Current--Radiation Model

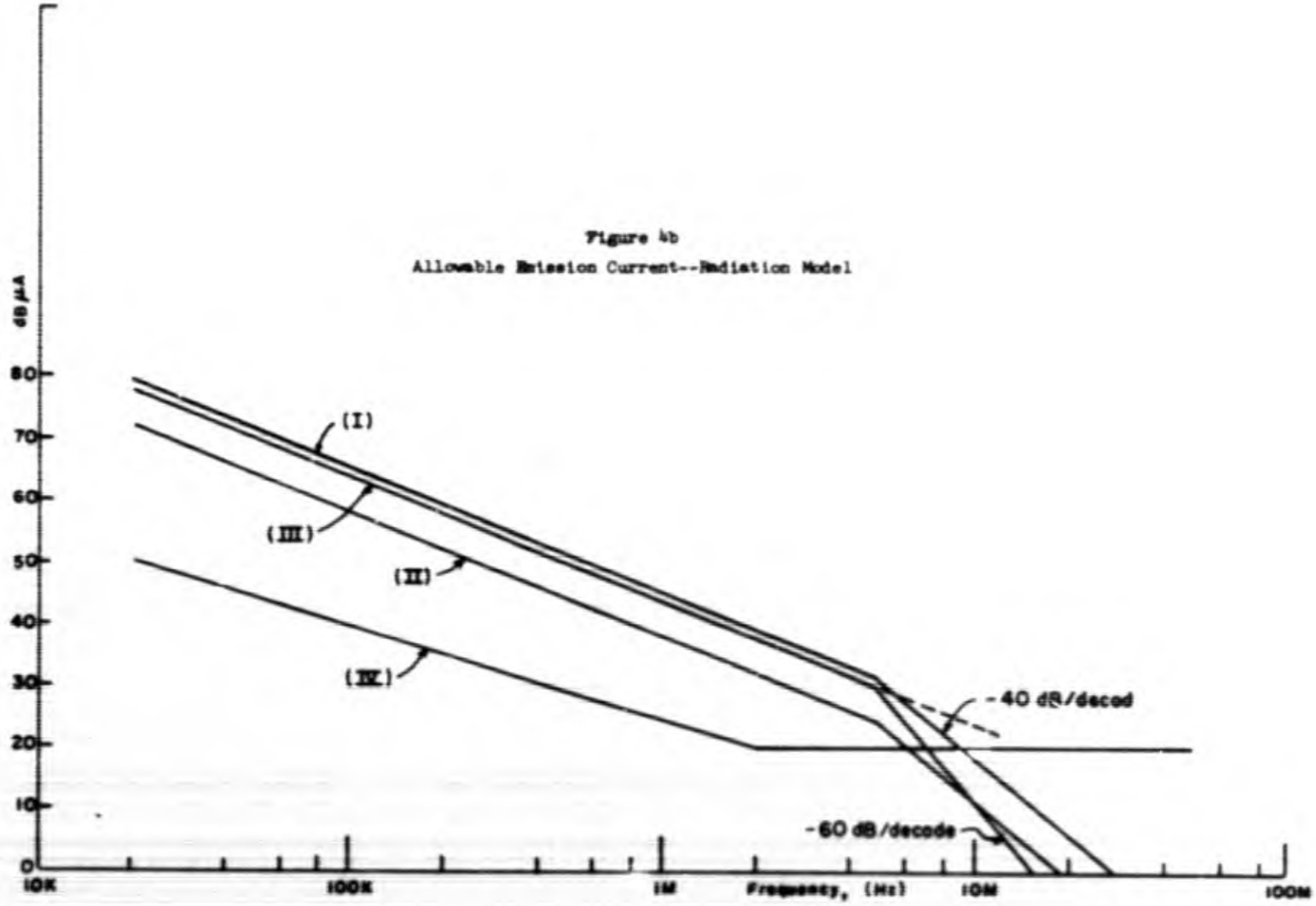

at 10 meters) is given by

$$I = \frac{Vr^3}{\mu_o NA^2} \frac{1}{\sqrt{1 + \left(\frac{2\pi fr}{3 \times 10^8}\right)^2}} \qquad (3.2.5)$$

where V is the induced voltage

N is the number of turns in the receptor loop

μ_o is the free space permeability, and the other symbols are the same as for (3.2.1).

$$I = \frac{80}{f} \frac{1}{\sqrt{1 + \left(\frac{f}{4.78 \times 10^6}\right)^2}} \text{ Amp} \qquad (3.2.6)$$

For $f \ll 4.78$ MHz

$$I = \frac{80}{f} \text{ Amp} = \frac{8 \times 10^7}{f} \mu A \qquad (3.2.7)$$

For $f \gg 4.78$ MHz

$$I = \frac{3.82 \times 10^{14}}{f^2} \mu A \qquad (3.2.8)$$

These results are shown plotted in Fig. 4 curve II.

The equation governing the third configuration (coplanar loops at 10 meters) is given by

$$I = \frac{2V r^3}{\mu_o NA^2 f} \frac{1}{\left|1 - \left(\frac{2\pi rf}{3 \times 10^8}\right)^2 + j\left(\frac{2\pi rf}{3 \times 10^8}\right)\right|} \qquad (3.2.9)$$

With $A = 1\ m^2$, $r = 10$ m, $V = 1\ \mu V$

$$I = \frac{160}{f} \frac{1}{\left|1 - \left(\frac{f}{4.78 \times 110^6}\right)^{\frac{1}{2}} + j\left(\frac{f}{4.78 \times 10^6}\right)\right|} \text{ Amp} \qquad (3.2.10)$$

for $f \ll 4.78 \times 10^6$ Hz

$$I = \frac{1.6 \times 10^8}{f}\ \mu A \qquad (3.2.11)$$

for $f \gg 4.78$ MHz

$$I = \frac{3.65 \times 10^{21}}{f^3}\ \mu A \qquad (3.2.12)$$

These results are shown plotted in Fig. 4 curve III.

First to be noted is that all three curves are within about 7 dB of one another. For reference, we show plotted on Fig. 4 curve IV the emission specification limit for CE01, CE02, and CE05 tests taken from MIL-STD-461A. At low frequencies there is, it will be noted, not much difference between the specification limit and the currents computed here. It should be emphasized that the specification limit represents current into a certain termination given by the specification test setup. The computation done here represents current in a line without consideration of the impedance.

We have adopted curve II, which is the most demanding of the three, as the allowable emission current from 30 Hz to 10 MHz. In most of this range the dropoff of the limit is 20 dB/decade; at the high frequency end it changes to 40 dB/decade. However, the currents determined here are those which appear at a point remote from the source. At low frequencies the same current will flow into the line at the source. At the high frequency end the line will act like a lossy filter so that a larger input current will generally be required than that shown in Fig. 4. Note for example the attenuation data shown plotted in Fig. A.5.4 of Appendix 5 . There is on the order

of a 6dB attenuation difference from 5 to 10 MHz on a 70 foot run of power transmission line. For this reason we have extended curve II at the 20 dB/decade level, as shown by the dotted extension on Fig. 4b, up to 10 MHz. In short, the allowable line emission current is taken to be 124 dB above 1μA at 30 Hz decreasing at the rate of 20 dB per decade to 10 dB above 1 μA at 10 MHz. In later discussions this limit is extended to 30 MHz.

3.3 Optimum Terminating Impedance, Emission Tests and Limits

3.3.1 Introduction

The present military specifications for power line conducted emission (in MIL-STD-461, 462) appear to call for the measurement of the short circuit current generated by the piece of equipment under test at frequencies from 30 Hz to 50 MHz (tests CE01 and CE03). (The current is effectively not the short circuit current at the extrema of the frequency range.) Acceptability of the equipment is ascertained by comparing the measured values with the limits, which are specified in terms of current.

The purposes of this section are to:

1) determine if the measurement of current (or voltage) into a known load other than a short circuit can result in a more accurate prediction of compatibility, and

2) determine emission limits, in terms of measured current (or voltage), once the load impedance has been decided upon, using the absolute limit on line current derived in the preceding section.

These problems are complicated by the statistical uncertainties in all of the circuit parameters involved. The results obtained are based upon certain approximations which provide what is felt to be a good indication of the results a more exact analysis would provide. What follows is an outline of this analysis and the results; details are given in Appendix 4.

3.3.2 Circuit Models

Under actual operating conditions, the equivalent circuit of the interference source and its load is as shown in Fig. 5(a) and its equivalent in 5(b).

I_S - equivalent current generator - short circuit current

Z_S - equivalent source impedance

Z_L - shunt line impedance

Z_R - driving point impedance of susceptible device

Z_T - net load on source, $\frac{Z_L Z_R}{Z_L + Z_R}$

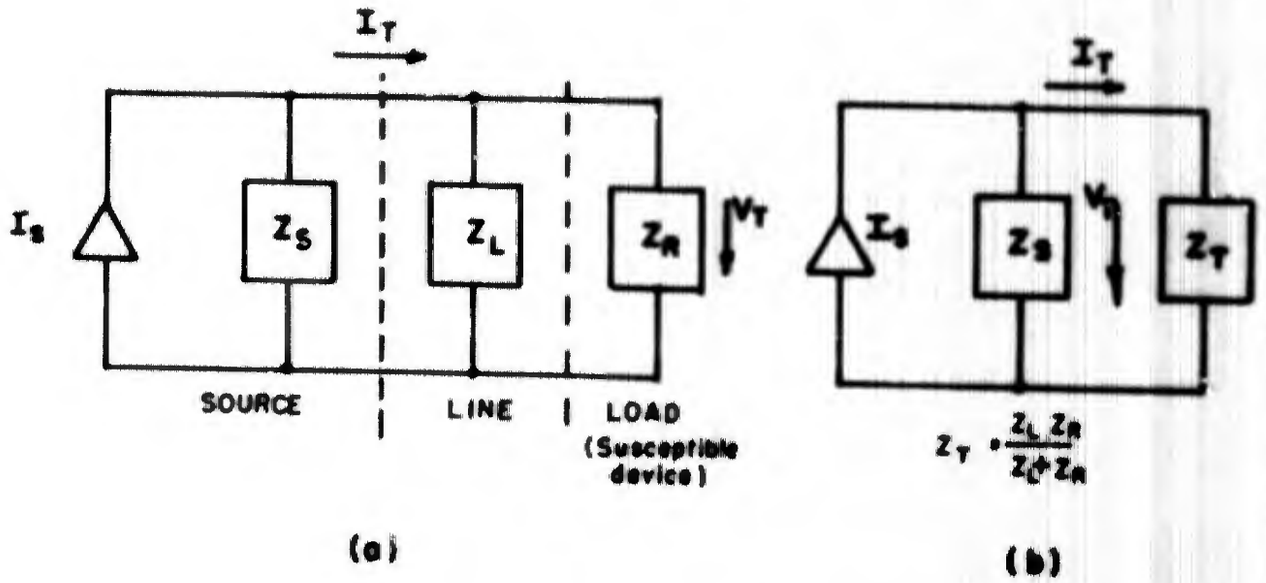

Figure 5 Circuit Model Showing (a) Susceptible Device
(b) Equivalent Circuit

This is a simplified model. Series line impedances have been neglected to facilitate the analysis. The difference is on the conservative side, since this will result in a larger theoretical signal at the susceptible device, except in rare cases where a resonant match occurs between the line and the source or load.

Also, we shall assume that the statistics of Z_S, Z_L, and Z_R are all the same, i.e. that the real parts have the same means and variances, and that the imaginary parts have the same means and variances. This is an assumption which is justified, within the statistical uncertainties involved, by our impedance data.

Under measurement conditions, the line and the load are replaced by a known impedance Z_M (see Fig. 6). The current I_M through Z_M or the voltage V_M across it is measured. For example, the test method specified in MIL-STD-462 is such that the current measured is nearly equal to the short circuit current at frequencies around 1 MHz, so that $Z_M = 0$ and $I_M = I_S$.

3.3.3 Specifying Limits on Measured Quantities

The basic purpose of measurement is to determine whether or not a given source will cause interference; that is, whether or not I_T will exceed the limit value I_{TL} set by use of the radiation model in the previous section.

This actual line current I_T is given by (from Fig. 5)

$$I_T = I_S \left| \frac{Z_S}{Z_S + Z_T} \right| = \frac{V_T}{|Z_T|} \qquad (3.3.1)^*$$

while the measured current is

$$I_M = I_S \left| \frac{Z_S}{Z_S + Z_M} \right| = \frac{V_M}{|Z_M|} \qquad (3.3.2)$$

Dividing (3.3.1) by (3.3.2), we find I_T in terms of I_M or V_M

$$I_T = I_M \left| \frac{Z_S + Z_M}{Z_S + Z_T} \right| = I_M A_M = \frac{V_M}{|Z_M|} A_M \qquad (3.3.3)$$

where

$$A_M = \left| \frac{Z_S + Z_M}{Z_S + Z_T} \right| \qquad (3.3.4)$$

* Currents and voltages should be understood to be magnitudes and not phasors.

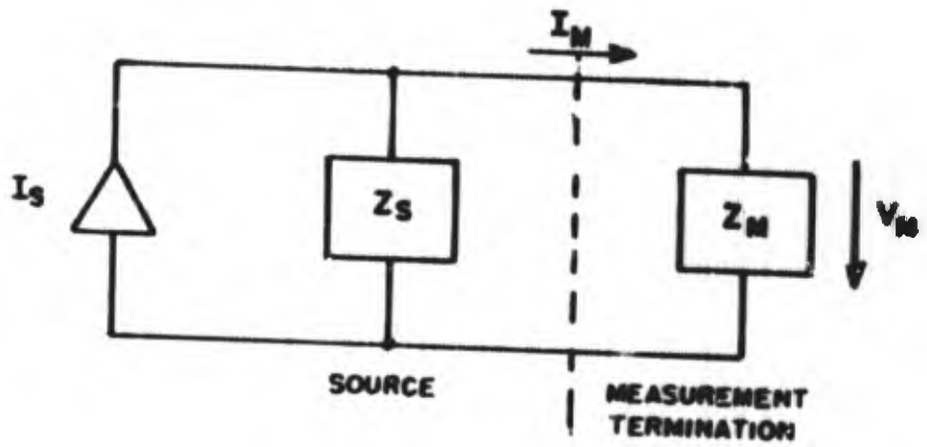

Figure 6 Equivalent Circuit, Measurement Conditions

The voltage appearing across the susceptible device is also the voltage across the net load, V_T, in our simplified model, and is given by

$$V_T = V_M \left|\frac{Z_T}{Z_M}\right| A_M = I_M \left|Z_T\right| A_M \qquad (3.3.5)$$

3.3.3.1 Statistical Uncertainties in I_T

For a given source, we measure I_M or V_M for a known load Z_M. From eq. (3.3.3), we see that I_T can still not be predicted exactly, due to uncertainties in Z_S and Z_T. Instead, I_T will have a statistical distribution about some mean value. From the statistics of Z_S and Z_T, if they are known, we can find the probability density function of I_T for a given I_M and Z_M. From eq. (3.3.3)

$$\bar{I}_T = I_M \bar{A}_M = \text{mean of } I_T \qquad (3.3.6)$$

$$\text{Var } (I_T) = I_M^2 \text{ Var}(A_M) = \text{variance of } I_T \qquad (3.3.7)$$

That is, the mean of the probability density function of I_T, given I_M, increases linearly with I_M, and the variance as the square of I_M. These quantities also vary with Z_M. Some possibilities are illustrated in Fig. 7, in which the effect of I_M and Z_M on means and variances is depicted.

Figure 7 also shows how a limit on I_M (or $V_M = I_M \left|Z_M\right|$) may be set. For a given Z_M, I_M determines the probability density function of I_T and consequently the probability of interference

$$p_I = P\left[I_T > I_{TL}\right].$$

We must decide beforehand what the acceptable limit on p_I is. Once this is done, we work backwards, finding which pdf of I_T will give this p_I, and, finally, the corresponding value of I_M. This value of I_M is set to be the limit value, $I_{M\ LIM}$. For all values of I_M below this limit, p_I will be less than $p_{I\ LIM}$.

Thus, while 100% compatibility can never be achieved, we can come arbitrarily close by choosing $p_{I\ LIM}$ small enough. The cost will increase as the percentage compatibility figure is increased due to the increased suppression necessary to pass the more restrictive emission tests that will result.

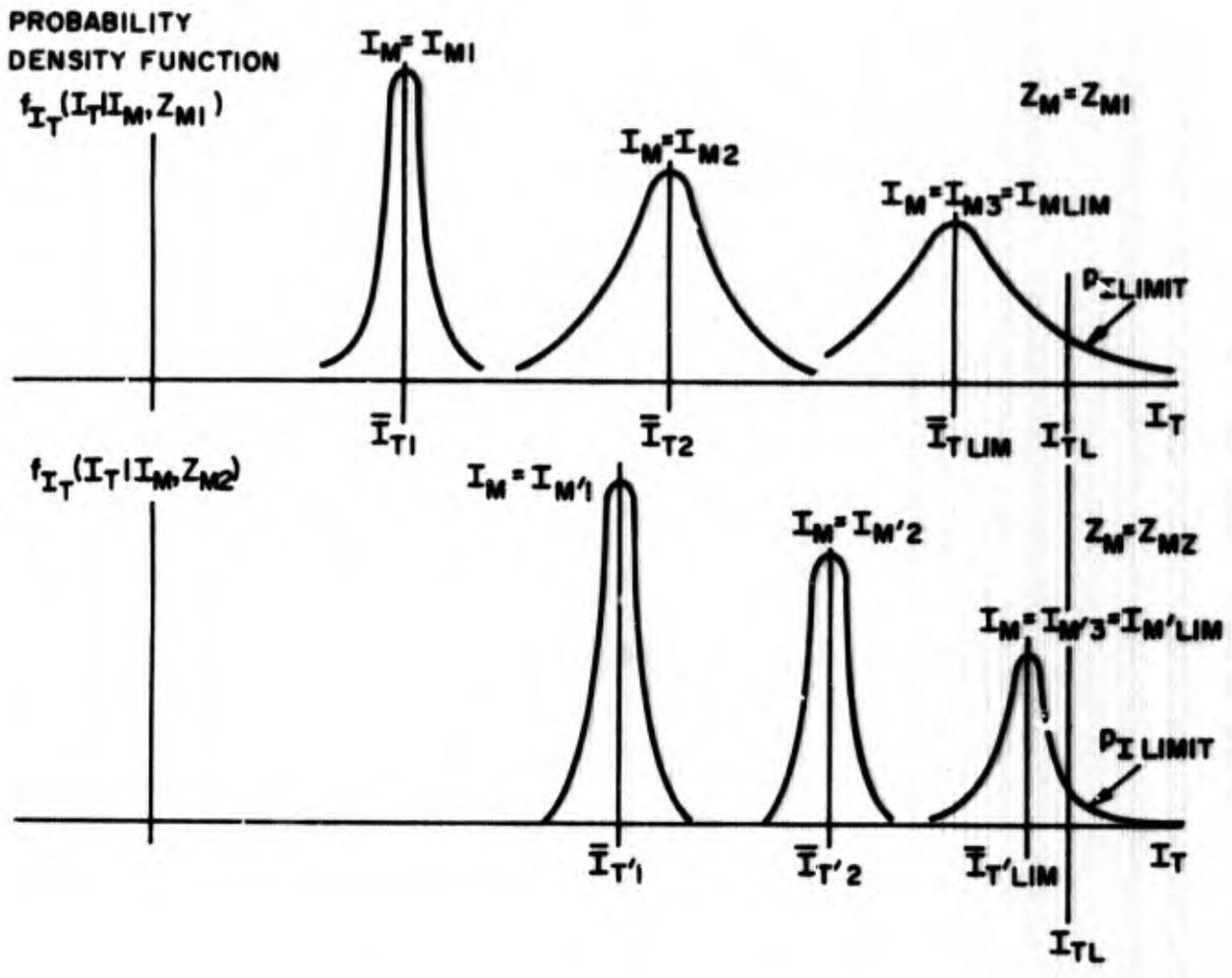

Figure 7 Some Possible Probability Density Functions of I_T Given I_M and Z_M

$I_{M3} > I_{M2} > I_{M1}$; $I_{M3}' > I_{M2}' > I_{M1}'$

3.3.4 Optimum Measurement Impedance Z_M

We are now ready to consider the question of whether or not some test load Z_M other than a short circuit is desirable, from the standpoint of accuracy in determining the probability of exceeding I_{TL}, or p_I.

It has just been asserted that, once Z_M is known, there is a correspondence between the measured current I_M and the probability of interference p_I. Theoretically, then, the latter quantity can be determined exactly by this simple measurement technique, regardless of the value of Z_M.

Practically, this is not the case, because it assumes perfect knowledge of the statistical distribution of I_T. This, in turn, requires exact knowledge of the statistics of Z_S and Z_T. This is never obtained, since it is based upon a finite number of observations of Z_S and Z_T. Consequently, there will always be some uncertainty in the distribution of I_T and hence in p_I.

In the literature on the estimation of distributions,[1] it is common practice to use the variance of the distribution of an estimator as a measure of its uncertainty. Thus, in order to minimize the uncertainty in estimating p_I, we must minimize the variance of the distribution of I_T given I_M. This can be done by properly selecting Z_M. The mathematical operation of minimizing $\mathrm{Var}(I_T)$ with respect to Z_M is carried out in detail in Appendix 4. The outline and results of this analysis are presented below.

To make the analysis tractable, it was necessary to make a linear approximation in which it was assumed that the random impedances Z_S and Z_T did not change appreciably from their mean values. The validity of this assumption will be commented upon in the next section. Using this approximation, the value of Z_M minimizing $\mathrm{Var}(I_T)$ about any mean value $\bar{I}_T$ turns out to be

$$Z_M = Z_{M\ \mathrm{Opt}} = \bar{R}_T + j\,\bar{X}_T = \bar{Z}_T \qquad (3.3.8)$$

That is, the uncertainty in predicting p_I will be a minimum if the test load Z_M equals the mean of the actual load Z_T.

---

1. Herman Kahn, "Use of Different Monte Carlo Sampling Techniques," Symposium on Monte Carlo Methods, N. Y., Wiley, 1956.

Section 4

IMPEDANCE DATA AND RECOMMENDED LIMITS

4.1 Introduction

The results of the analysis presented in Section 3 are used with measurement data to determine proper measurement techniques and limits. The statistical variations which have been encountered in the measurements made make interpretation somewhat uncertain, but it is believed that the conclusions drawn are valid within the accuracies normally considered attainable in this field. The actual measured data are described in detail in the Appendices. Summaries of the data presented there are given here as needed.

4.2 Values of Z_{Mopt} from Measured Data on Z_L

To determine Z_{Mopt} as a function of frequency, one must know $\bar{Z}_T$ as a function of frequency, or, since Z_T is the parallel combination of Z_L and Z_R, one must know the statistics of Z_L and Z_R and be able to obtain the statistics of Z_T from this relationship.

The measurements of line impedance (Z_L) and source and load impedance (Z_S and Z_R) are described in Sections A.2 and A.3.

Mean and standard deviation of line impedance in a three-terminal delta configuration are plotted in Figs. A.2.8, A.2.9 and A.2.10. Measured values of source impedance are presented in a two-terminal line-to-line form. **There was insufficient time to convert the source data to three-terminal form and compute means and standard deviations. However, checking average values at 1 MHz revealed that the average impedances between the two "hot" lines were as follows:**

Line: 80 + j100 ohms
Source: 75 + j 44 ohms

i.e., average impedances at 1 MHz were of the same order of magnitude. The trends in the source impedance data indicated that this relationship was maintained at all frequencies, so that, within the uncertainties involved, we may assume that

$$\left.\begin{aligned} \bar{R}_S &= \bar{R}_L = \bar{R}_R = \bar{R} \\ \bar{X}_S &= \bar{X}_L = \bar{X}_R = \bar{X} \\ \sigma_{R_S}^2 &= \sigma_{R_L}^2 = \sigma_{R_R}^2 = \sigma_{X_S}^2 = \sigma_{X_L}^2 = \sigma_{X_R}^2 = \sigma^2 \end{aligned}\right\} \quad (4.1)$$

With this assumption, the line impedance statistics may be used as the statistics of Z_S and Z_R as well. This is advantageous because of the greater volume of data available on Z_L. Specifically, data shall be used on the resistance and reactance of Z_2, the impedance between the two "hot" lines (differential mode).

From the plots of the mean and standard deviation of R_2 and X_2 given in Section A.3, it appears that, within the uncertainties involved, $\bar{R}_2$ and $\bar{X}_2$ as functions of frequency may be fitted by "log linear" functions as listed in Table 4.I.

Table 4.I

MEASURED VALUES OF IMPEDANCE

f	$\bar{R}_2$	$\bar{X}_2$
Hz	dB ohms	dB ohms
30 - 15k	$5.04 \log_{10} f(\text{kHz}) + 0.14$	$33.1 \log_{10} f(\text{kHz}) - 48.0$
15 - 600k	$14.1 \log_{10} f(\text{kHz}) - 10.6$	same as above
0.6M - 2M	$22.5 \log_{10} f(\text{MHz}) + 33.5$	0
2M - 10M	100	0

Comments on Table 4.I

1) The "log linear" functions are convenient because they are straight lines on semilog paper when the ordinates are in dB and abscissae in Hz, and they fit the measured data reasonably well.

2) Below 15 kHz, an extrapolation was made of the data above 15 kHz, assuming a value of line impedance at 60 Hz of $0.5\angle 0^\circ$ ohms.

3) Resistance in the range 2 MHz to 10 MHz and reactance in the range 0.6 MHz to 10 MHz appear to fluctuate about constant means of 100 ohms and 0 ohms, respectively. We therefore treat all of the data points in these ranges as coming from the same distributions, and may calculate variances by averaging overall the points. This provides less uncertainty than calculating the variance at one frequency. These variances will be used in comparing accuracies of measurement techniques and in establishing the limits.

4.2.1 Computation of $Z_{M\ opt} = \bar{Z}_T$

We note that

$$Z_T = \frac{Z_L Z_R}{Z_L + Z_R} \tag{4.2}$$

(See Fig. 5.) Applying a linear approximation, we find that

$$\bar{Z}_T = \frac{\bar{Z}_L \bar{Z}_R}{\bar{Z}_L + \bar{Z}_R}$$

Using the assumption (4.1) of equal statistics, i.e., $\bar{Z}_L = \bar{Z}_r$,

$$\bar{Z}_T = \frac{\bar{Z}_2}{2} = \frac{\bar{R} + j\bar{X}}{2}$$

Since we are taking our measured values of $\bar{R}_2$ and $\bar{X}_2$ for $\bar{R}$ and $\bar{X}$,

$$\left.\begin{aligned} R_{M\ opt} &= \bar{R}_T = \frac{\bar{R}}{2} = \frac{\bar{R}_2}{2} \\ X_{M\ opt} &= \bar{X}_T = \frac{\bar{X}}{2} = \frac{\bar{X}_2}{2} \end{aligned}\right\} \tag{4.3}$$

$\bar{R}_2$ and $\bar{X}_2$ are found from Table 4.I.

$R_{M\ opt}$ and $X_{M\ opt}$ as functions of frequency are plotted in Fig. 8, calculated from (4.3).

4.2.2 Implementation of Optimum Test Load

According to Figs. 8(a) and 8(b), the optimum test load must

1) have an inductive reactance that increases to 80 ohms at 600 kHz, then becomes zero,

2) have a resistance which increases from about 0.25 ohms at 60 Hz to 50 ohms at 2 MHz, thereafter remaining constant.

A simple circuit which approximates this impedance curve is shown in Fig. 9.

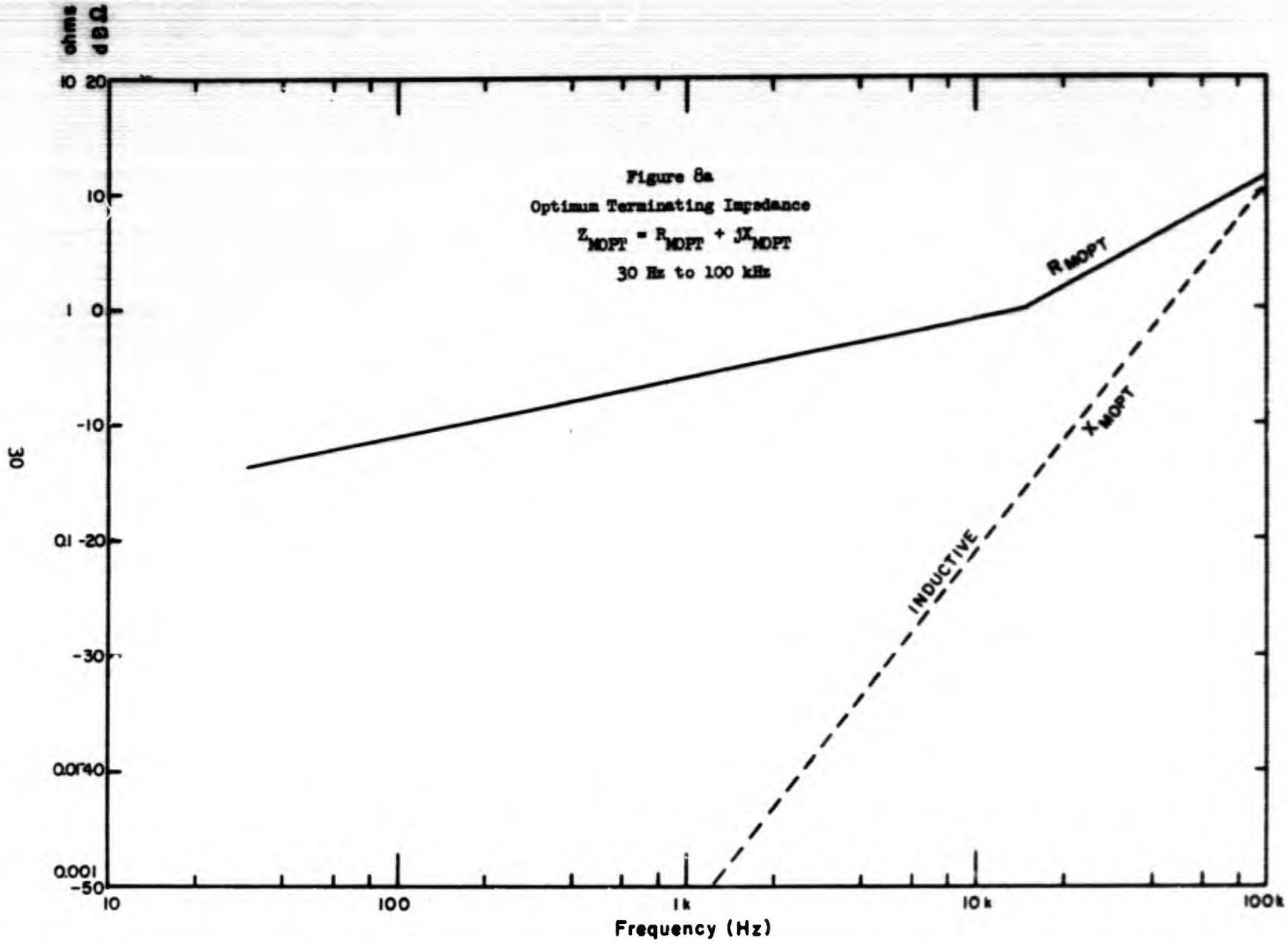

Figure 8a

Optimum Terminating Impedance

$Z_{MOPT} = R_{MOPT} + jX_{MOPT}$

30 Hz to 100 kHz

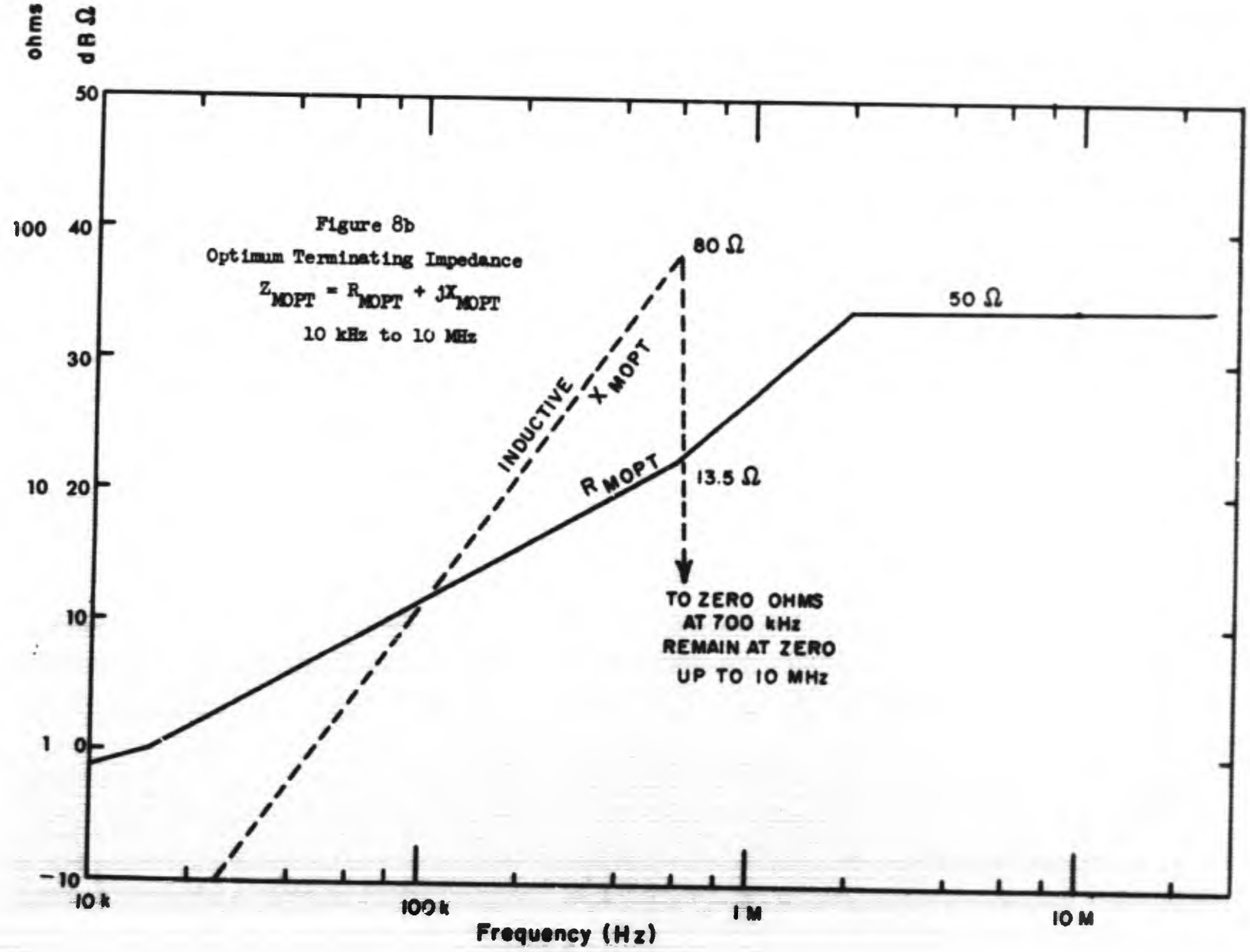
ohms
dB Ω
50
100 40
30
10 20
10
1 0
−10
Figure 8b
Optimum Terminating Impedance
$Z_{MOPT} = R_{MOPT} + jX_{MOPT}$
10 kHz to 10 MHz
80 Ω
50 Ω
INDUCTIVE
X MOPT
R MOPT
13.5 Ω
TO ZERO OHMS
AT 700 kHz
REMAIN AT ZERO
UP TO 10 MHz
10 k
100 k
1 M
10 M
Frequency (Hz)

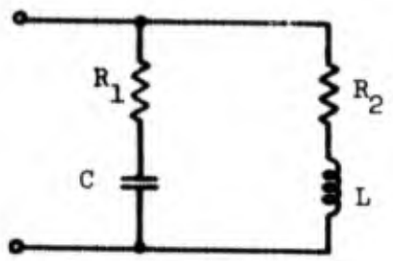

$R_1 = 50\ \Omega$

$R_2 = 0.25\ \Omega$

$C = 0.005\ \mu F$

$L = 14\ \mu H$

Figure 9 Optimum Test Load

The test procedure will remain unchanged except that current flowing into this load will be measured instead of current into 10 μF feedthrough capacitors.

4.2.3 Relative Accuracies of Optimum, Short-Circuit and Open-Circuit Tests

The question of whether or not the improved accuracy of the optimum load termination is significant will now be considered. As a measure of accuracy, we use the variance of the normalized actual load current, $I_T / \frac{I}{\pi} = A$. As mentioned above, the uncertainty in the predicted value of p_I varies monotonically with Var(A).

Accordingly, we compute Var(A) for the following values of Z_M

$Z_M = Z_{M\ opt}$ (Var(A) = Var(A) min)

$Z_M = 0$ (Short circuit test)

$Z_M = \infty$ (Open circuit test)

$Z_M = 0$ is the presently-used configuration in which short-circuit current is measured. $Z_M = \infty$ is included as a point of interest. In this case, open circuit voltage would be measured.

The details of this computation are carried out in Appendix 4. The results are presented in Table 4.II, assuming identical statistics for Z_S, Z_L and Z_R (i.e., that eq. (4.1) applies).

We may evaluate Var(A) and $Var(A)/Var(A)_{min}$ for the different frequencies by referring to our measured data on Z_2, the line impedance. The values of $\bar{R}$ and $\bar{X}$ needed in these computations are equal to $\bar{R}_2$ and $\bar{X}_2$ listed in Table 4.I. The values of σ^2 are found from the data in

Appendix 3 on standard deviations. Above 600 kHz, σ^2 is treated as constant and equal to

$$\sigma^2 = 3400 \text{ ohms}^2 \qquad f > 600 \text{ kHz}$$

which is an average of the variances at each frequency as well as the square deviations of the local means from the overall mean. Below 15 kHz, where little data are available, the value of σ^2 at 15 kHz was used.

The calculations are summarized in Table 4.III, where we see that the short-circuit test has a variance (uncertainty) which is at least 1.5 times as great as the optimum load test, whereas that for the open circuit test is nine times as great.

Table 4.II

NORMALIZED VARIANCE OF PREDICTED CURRENT

Z_M	Var(A)	$\text{Var(A)}/\text{Var(A)}_{min}$
$Z_{M\ opt} = \bar{R}_T + j\ X_T = \frac{\bar{R}}{2} + j\frac{\bar{X}}{2}$	$\frac{\sigma^2}{18(\bar{R}^2+\bar{X}^2)} = \text{Var(A)min}$	1
0	$\frac{\sigma^2(\bar{R}^6+\bar{X}^6)}{9(\bar{R}^2+\bar{X}^2)^4} + \frac{\sigma^2}{18(\bar{R}^2+\bar{X}^2)}$	$2\frac{\bar{R}^6+\bar{X}^6}{(\bar{R}^2+\bar{X}^2)^3} + 1$
∞	$\frac{\sigma^2}{2(\bar{R}^2+\bar{X}^2)}$	9

Table 4.III - COMPUTATION OF VARIANCES

	From Table 4.I		Sec. A.2	$Z_M = Z_{Mopt} = \frac{\bar{R}}{2} + j\frac{\bar{X}}{2}$		$Z_M = 0$ (S.C. Test)		$Z_M = \infty$ (O.C. Test)	
f	$\bar{R}$	$\bar{X}$	σ^2	$\frac{Var(A)}{Var(A)_{min}}$	$Var(A) = Var(A)_{min}$	$\frac{Var(A)}{Var(A)_{min}}$	Var(A)	$\frac{Var(A)}{Var(A)_{min}}$	Var(A)
Hz	ohms	ohms	$(ohms)^2$						
30	0.42	$\ll \bar{R}$		1.0	0.315	3	0.945	9.0	2.83
60	0.50	↓	↓	↓	0.222	↓	0.666	↓	2.00
100	0.56				0.177		0.531		1.59
300	0.76				0.0962		0.289		0.865
600	0.89				0.0701		0.210		0.630
1 k	1.0				0.0556		0.167		0.500
3 k	1.33	0.026			0.0314		0.0942		0.282
6 k	1.59	0.078			0.0219		0.0657		0.197
10 k	1.78	0.178			0.0173	2.94	0.0509		0.156
15 k	2.0	0.33	1.0		0.0135	2.85	0.0385		0.122
30 k	3.3	1.00	9.0		0.0421	2.54	0.110		0.378
60 k	5.3	3.2	9.0		0.0130	1.825	0.0237		0.117
100 k	7.9	7.1	25.0		0.0123	1.517	0.0187		0.111
300 k	16.8	47.0	100.0		0.0223	2.40	0.0535		0.0201
600 k	27.0	160.0	3400.0		0.00717	2.84	0.0204		0.0645
1 M	47.0	0	3400.0		0.0855	3.0	0.257		0.769
2 M	100.0	0	3400.0		0.0189	3.0	0.0567		0.170
10 M	100.0	0	3400.0	↓	0.0189	3.0	0.0567	↓	0.170

4.3 Setting a Limit on I_M

As pointed out in Section 3.3.3.1, setting a limit on the measured current I_M depends on three quantities: I_{TL}, $p_{I\ limit}$, and Z_M (see Fig. 7).

An implied factor is the form of the distribution of the actual line current I_T. We shall assume this to be normal for definiteness, with mean $\bar{I}_T$ and variance $\bar{I}_T^2\,\mathrm{Var}(A)$, so that the probability density function is

$$f_{I_T}(I_T) = \frac{1}{\sqrt{2\pi\,\bar{I}_T^{\,2}\mathrm{Var}(A)}}\ \exp\ -\frac{1}{2}\left\{\frac{(I_T - \bar{I}_T)^2}{\bar{I}_T^{\,2}\ \mathrm{Var}(A)}\right\} \qquad (4.4)$$

and the probability p_I, of exceeding the allowable line current given that the emission test current limit is just satisfied, is given by

$$p_I = \int_{I_{T_L}}^{\infty} f_{I_T}(I_T)\, dI_T \qquad (4.5)$$

where

$$A = \left|\frac{Z_S + Z_M}{Z_S + Z_T}\right| = \frac{I_T}{\bar{I}_T}$$

$$\bar{I}_T = I_M\, E\left\{\left|\frac{Z_S + Z_M}{Z_S + Z_T}\right|\right\} \approx I_M \left|\frac{\bar{Z}_S + Z_M}{\bar{Z}_S + \bar{Z}_T}\right| \quad \text{(using linear approx.)},$$

I_{T_L} = limit on actual line current, based on radiation model.

We now assume a value for p_I. For the normal distribution, we know that if $I_{T_L} - \bar{I}_T = 2\sigma$, then $p_I \approx 0.023$. Assuming this to be a satisfactory p_I, we can proceed to find I_M.

If $\quad p_I = 0.023$

then

$$I_{T_L} - \bar{I}_{T_{Lim}} = 2\sigma = 2\bar{I}_{T_{Lim}}\sqrt{\mathrm{Var}(A)}$$

or

$$\bar{I}_{T_{Lim}} = \frac{I_{TL}}{2\sqrt{Var(A)} + 1} = I_{M\ Lim} \left| \frac{\bar{Z}_S + Z_M}{\bar{Z}_S + \bar{Z}_T} \right|$$

so that

$$I_{M\ Lim} = \frac{I_{TL}}{2\sqrt{Var(A)} + 1} \left| \frac{\bar{Z}_S + \bar{Z}_T}{\bar{Z}_S + Z_M} \right| \qquad (4.6)$$

As before, we assume $\bar{Z}_S = \bar{Z}_R = \bar{Z}_L = \bar{R} + j\,\bar{X} = \bar{Z}_2$, so that

$$\bar{Z}_T = \frac{\bar{Z}_2}{2} = \frac{\bar{R} + j\bar{X}}{2}$$

and

$$I_{M\ Lim} = \frac{I_{TL}}{2\sqrt{Var(A)} + 1} \left| \frac{\frac{3}{2}\bar{Z}_2}{\bar{Z}_2 + Z_M} \right|$$

$$= \frac{3I_{TL}}{4\sqrt{Var(A)} + 2} \left| \frac{\bar{Z}_2}{R + R_M + j(\bar{X} + X_M)} \right| \qquad (4.7)$$

From the data on $\bar{R}$, $\bar{X}$, and Var(A) in Table 4.III, we calculate $I_{M\ Lim}$ from (4.7) as a function of frequency for $Z_M = Z_{M\ Opt}$ and $Z_M = 0$. For $Z_M = \infty$, we calculate $V_{M\ Lim} = \lim_{Z_M \to \infty} Z_M I_{M\ Lim}$. The results are presented in Table 4.IV. The following relationships are used:

1) For $Z_M = Z_{M\ Opt} = \bar{Z}_T = \frac{\bar{Z}_2}{2}$,

$$I_{M\ Lim} = \frac{3I_{TL}}{4\sqrt{Var(A)} + 2} \left| \frac{\bar{Z}_2}{\bar{Z}_2 + \frac{1}{2}\bar{Z}_2} \right| = \frac{I_{TL}}{2\sqrt{Var(A)} + 1}$$

2) For $Z_M = 0$

$$I_{M\ Lim} = \frac{3I_{TL}}{4\sqrt{Var(A)} + 2} \left| \frac{\bar{Z}_2}{\bar{Z}_2} \right| = \frac{3}{2} \left(\frac{I_{TL}}{2\sqrt{Var(A)} + 1} \right)$$

3) For $Z_M = \infty$

$$V_{M\ Lim} = \frac{3\left|\bar{Z}_2\right| I_{TL}}{4\sqrt{Var(A)} + 2}$$

Table 4.IV - EMISSION LIMITS

		$Z_M = Z_{M\ Opt}$		$Z_M = 0$		$Z_M = \infty$	
f	Z_2	$I_{M\ Lim}$	$I_{M\ Lim}$	$I_{M\ Lim}$	$I_{M\ Lim}$	$V_{M\ Lim}$	$V_{M\ Lim}$
Hz	ohms	Units of I_{TL}	dBμA	Units of I_{TL}	dBμA	Units of I_{TL}	dBμV
30	0.42	0.471 I_{TL}	I_{TL}(dBμA)-6.54	0.706 I_{TL}	I_{TL}(dBμA)-3.03	0.296 I_{TL}	I_{TL}(dBμA)-10.6
60	0.50	0.514	-5.77	0.771	-2.25	0.386	-8.28
100	0.56	0.543	-5.30	0.815	-1.78	0.456	-6.81
300	0.76	0.617	-4.19	0.926	-0.668	0.704	-3.05
600	0.89	0.654	-3.69	0.981	-0.168	0.873	-1.18
1k	1.0	0.680	-3.36	1.02	+0.162	1.02	+0.172
3k	1.33	0.738	-2.63	1.11	+0.892	1.48	+3.41
6k	1.59	0.772	-2.25	1.16	+1.27	1.84	+5.30
10k	1.79	0.792	-2.03	1.19	+1.49	2.13	+6.57
15k	2.03	0.811	-1.81	1.22	+1.71	2.48	+7.88
30k	3.45	0.709	-2.99	1.06	+0.532	3.66	+11.3
60k	6.19	0.814	-1.78	1.22	+1.74	7.55	+17.6
100k	10.62	0.818	-1.74	1.23	+1.78	13.1	+22.3
300k	49.9	0.770	-2.27	1.16	+1.25	57.9	+35.3
600k	162.0	0.855	-1.35	1.28	+2.17	207.0	+46.3
1M	47.0	0.631	-4.00	0.947	-0.478	44.5	+33.0
2M	100.0	0.784	-2.11	1.18	+1.41	118.0	+41.4
10M	100.0	0.784	-2.11	1.18	+1.41	118.0	+41.4

The recommended limits are plotted in Figs. 10(a) and (b), together with the present limits of MIL-STD-461A. The limit curves are the best straight lines fitting the results of Table 4.IV on the conservative side. Since the limit for $Z_M = Z_{M\ Opt}$ is at most about 6.5 dB below I_{TL} and at least about 2 dB below, the line drawn is a constant 6 dB below. Since the limit for $Z_M = 0$ is, for the most part, 1 or 2 dB above I_{TL}, I_{TL} itself is chosen for the limit.

I_{TL}, we recall, is the actual limit current derived from the radiation model of the previous section.

4.4 Susceptibility Limit

4.4.1 Introduction

In section 4.2 a limit for conducted emission of interference was specified. In this section, a corresponding limit is established for conducted susceptibility which is consistent with the emission limit plus a certain safety factor.

4.4.2 Circuit Model

We recall the circuit of Fig. 5, in which a model of the source, power line, and susceptible device is depicted. Using the same notation as used in conjunction with Fig. 6, V_T is the spurious signal voltage impressed by the source on the susceptible device, assumed equal in this model to the source output voltage. It is upon this voltage that the susceptibility limit is set.

4.4.3 Distribution of V_T

Recalling eq. (3.3.5), V_T is given by

$$V_T = I_M \left| Z_T \right| A_M \qquad (4.8)$$

where I_M = current measured during emission test

$A_M = \left| \frac{Z_S + Z_M}{Z_S + Z_T} \right|$, where Z_M = emission test load impedance.

For a given I_M, $\left| Z_T \right|$ and A_M are random variables. Consequently, V_T is distributed around some mean value with a certain variance (see Fig. 11).

As with the current I_T (see Section 3.3.1), the mean and variance of V_T depends on I_M and Z_M. It turns out (see Appendix 4) that the same value of Z_M which minimizes the variance of I_T about a

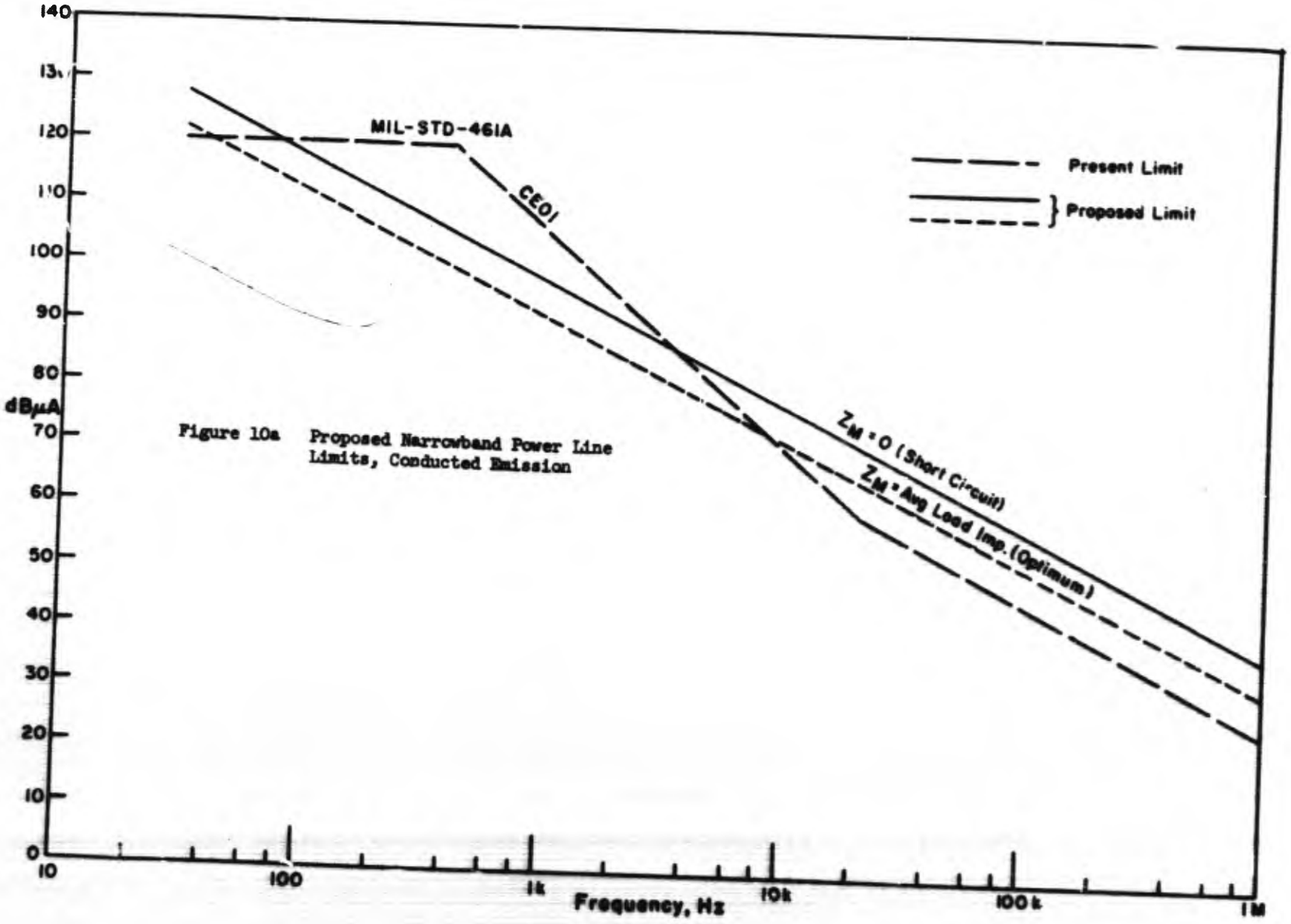

Figure 10a Proposed Narrowband Power Line Limits, Conducted Emission

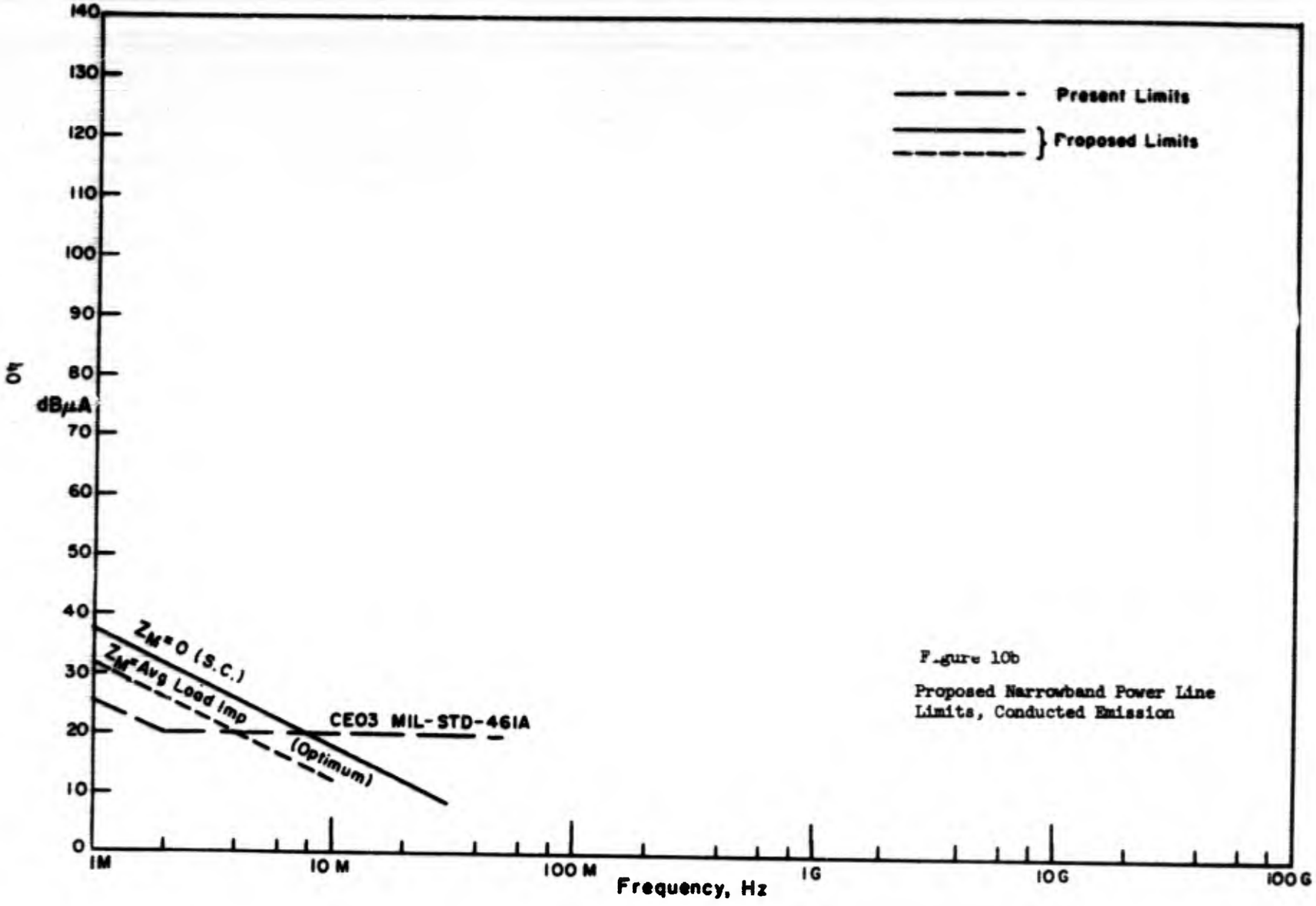

Figure 10b

Proposed Narrowband Power Line Limits, Conducted Emission

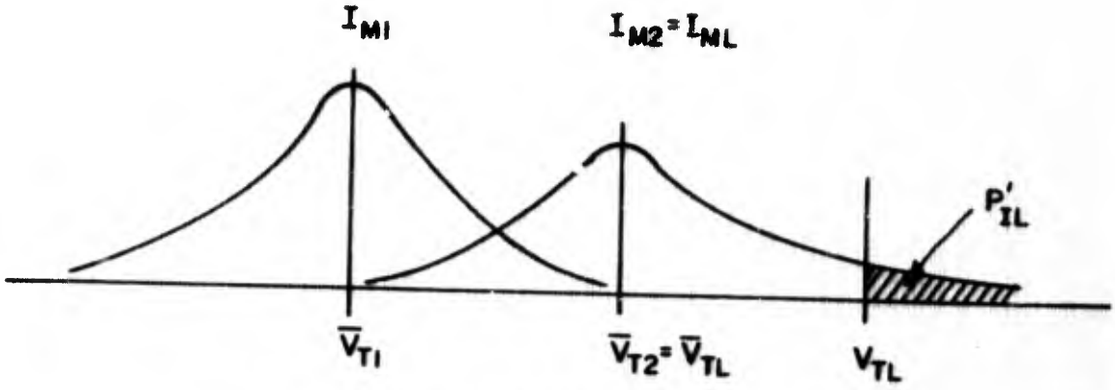

Figure 11 Distribution of V_T, $I_{M2} > I_{M1}$

given mean value, will also minimize the variance of V_T about a given mean value. The mean and variance both increase with I_M:

$$E\left[V_T\right] = \bar{V}_T = I_M \, E\left[\left|Z_T\right| A_M\right] \tag{4.9}$$

$$\text{Var}\left[V_T\right] = I_M^{\,2} \, \text{Var}\left[\left|Z_T\right| A_M\right] \tag{4.10}$$

4.4.4 Setting the Limit V_{TL}

If I_M is at its limit value I_{ML}, then the distribution of V_T has its largest mean and variance (by (4.9) and (4.10)), so that the probability of exceeding a given limit V_{TL} will have its maximum value.

Calling this probability p'_{IL}, we seek to choose V_{TL} such that p'_{IL} will equal some arbitrarily-set value. Assuming V_T is normally distributed,

$$p'_{IL} = \frac{1}{\sqrt{2\pi \, \text{Var}(V_T)}} \int_{V_{TL}}^{\infty} \exp\left\{-\frac{\left(V_T - \bar{V}_{TL}\right)^2}{2\text{Var}(V_T)}\right\} dV_T \tag{4.11}$$

If we choose

$$p'_{IL} = 0.023 \tag{4.12}$$

then

$$V_{TL} = \bar{V}_{TL} + 2\sqrt{\mathrm{Var}(V_T)} \tag{4.13}$$

$$= \bar{V}_{TL}\left[1 + 2\sqrt{\mathrm{Var}\left(\frac{V_T}{\bar{V}_{TL}}\right)}\right]$$

$$= I_{ML}\,\bar{C}_M\left[1 + 2\sqrt{\mathrm{Var}(C)}\right] \tag{4.14}$$

where

$$C_M \equiv |Z_T|\ A_M = \left|\frac{\frac{Z_S + Z_M}{Z_S}}{\frac{Z_S}{Z_T} + 1}\right| = \frac{V_T}{I_M} \tag{4.15}$$

$$C = \frac{C_M}{\bar{C}_M} \tag{4.16}$$

Once Var(C) and $\bar{C}_M$ are known, V_{TL} can be found from the emission limit I_{ML} and eq. (4.14). Adding a safety factor provides the final susceptibility limit V_{TL}'.

4.4.4.1 Statistics of C_M and C

The mean and variance of C_M and C, respectively, are found by making a linear approximation similar to the one made in finding the optimum emission test impedance in Section 3.3.1. From the linear approximation

$$\bar{C}_M = \left|\frac{\bar{Z}_S + Z_M}{\bar{Z}_S + \bar{Z}_T}\right| \left|\bar{Z}_T\right| \tag{4.17}$$

As in Section 3.3.1, we make the assumption of equal statistics:

$$\left.\begin{aligned} &\bar{Z}_S = \bar{Z}_L = \bar{Z}_R = \bar{R} + j\,\bar{X} \\ &\sigma_{R_S}^2 = \sigma_{R_L}^2 = \sigma_{R_R}^2 = \sigma_{X_S}^2 = \sigma_{X_L}^2 = \sigma_{X_R}^2 = \sigma^2 \end{aligned}\right\} \tag{4.18}$$

So that

$$\bar{Z}_T = \frac{\bar{Z}_L\,\bar{Z}_R}{\bar{Z}_L + \bar{Z}_R} = \frac{\bar{R} + j\,\bar{X}}{2} \tag{4.19}$$

and

$$\bar{C}_M = \left|\frac{(\bar{R} + R_M) + j(\bar{X} + X_M)}{3}\right| \tag{4.20}$$

Using the same approximation, it is shown in Section A.2 that

$$\frac{\mathrm{Var}(C)}{\mathrm{Var}(C)_{min}} = \frac{1}{16}\left[\frac{\mathrm{Var}(A)}{\mathrm{Var}(A)_{min}} + 15\right] \tag{4.21}$$

where

$$A = \left|\frac{Z_S + Z_M}{Z_S + Z_T}\right|$$

is the quantity whose variance was calculated in Section 3.3.1. $\mathrm{Var}(A)_{min}$ and $\mathrm{Var}(C)_{min}$ are the variances for $Z_M = Z_{M\ Opt} = \overline{Z}_T$. It is also shown in Section A.2 that $\mathrm{Var}(C)_{min} = 16\ \mathrm{Var}(A)_{min}$, so that

$$\mathrm{Var}(C) = \mathrm{Var}(A) + 15\ \mathrm{Var}(A)_{min} \tag{4.22}$$

$\mathrm{Var}(A)$ and $\mathrm{Var}(A)_{min}$ have been tabulated previously in Table 4.III, and we use these results to calculate $\mathrm{Var}(C)$ from (4.22). Also, we use the data on $\overline{R}$ and $\overline{X}$ in Table 4.III to compute C_M from (4.20). These computations are summarized in Table 4.V.

4.4.4.2 Computation of the Limit

The results of Table 4.V are now used to compute V_{TL} from (4.14). The results are in Table 4.VI and are plotted in Fig. 12, using the CE limits of Fig. 10 for I_{ML}.

These curves represent the susceptibility limits for a probability of susceptibility of 0.023, for emission test terminating impedances equal to: (1) a short circuit, and (2) the average actual load. The latter was shown in a previous section to be the optimum termination in terms of minimizing the variance of predicted current. In Fig. 12, it is seen that the limit for this termination is about 3 dB less strict than for the short circuit case.

It may be desirable to reduce the probability of susceptibility even further. This may be done by raising the limits by an appropriate amount. For example, assuming a normal distribution as above, an increase in the limit of 3.5 dB will reduce p'_{IL} to less than 0.0001.

Table 4.V

PREDICTED NORMALIZED VARIANCE OF VOLTAGE APPEARING ACROSS SUSCEPTIBLE DEVICE

	$Z'_M = Z_{M\ Opt} = \frac{\bar{R} + j\bar{X}}{2}$		$Z_M = 0$	
f	$\bar{C}_M$	Var(C)	$\bar{C}_M$	Var(C)
Hz	ohms	$= Var(C)_{min}$	ohms	
30	0.21	5.04	0.14	5.67
60	0.25	3.55	0.17	4.00
100	0.28	2.83	0.19	3.17
300	0.38	1.54	0.25	1.73
600	0.45	1.12	0.30	1.26
1k	0.5	0.890	0.33	0.834
3k	0.67	0.502	0.45	0.565
6k	0.80	0.350	0.53	0.394
10k	0.89	0.277	0.59	0.310
15k	1.01	0.216	0.67	0.241
30k	1.72	0.674	1.15	0.742
60k	3.10	0.208	2.07	0.219
100k	5.31	0.197	3.54	0.203
300k	25.0	0.357	16.7	0.388
600k	81.1	0.115	54.1	0.128
1M	23.5	1.37	15.7	1.54
2M	50.0	0.302	33.3	0.340
10M	50.0	0.302	33.3	0.340

Table 4.VI

SUSCEPTIBILITY LIMITS FOR 2.3% PROBABILITY OF INTERFERENCE PRODUCED BY DEVICES MEETING EMISSION LIMITS

	$Z_M = Z_{M\,Opt} = \frac{\bar{R} + j\bar{X}}{2}$		$Z_M = 0$	
f	V_{TL}	V_{TL}	V_{TL}	V_{TL}
Hz	Units of I_{ML}	dBμV	Units of I_{ML}	dBμV
30	1.15 I_{ML}	I_{ML}(dBμA)+1.21	0.806 I_{ML}	I_{ML}(dBμA)-1.87
60	1.19	+1.51	0.850	-1.41
100	1.22	1.73	0.867	-1.24
300	1.32	2.41	0.908	-0.84
600	1.40	2.92	0.973	-0.24
1k	1.44	3.17	0.933	-0.60
3k	1.62	4.19	1.13	+1.06
6k	1.75	4.86	1.20	+1.58
10k	1.74	4.81	1.25	+1.94
15k	1.94	5.76	1.33	+2.48
30k	4.54	13.10	3.13	+9.91
60k	5.93	15.45	4.01	+12.06
100k	10.02	20.01	6.73	+16.56
300k	54.9	34.8	37.5	+31.48
600k	136.1	42.7	92.8	+39.35
1M	78.5	37.9	54.7	+34.76
2M	105.0	40.4	72.1	+37.16
10M	105.0	40.4	72.1	+37.16

4.5 Summary

The more significant conclusions of the analysis presented so far are:

1. Optimum terminating impedance for conducted emission testing is the average actual load impedance and not a short circuit (see par. 3.3.4).

2. A plot of the optimum load impedance is shown in Fig. 8 and a simple circuit to implement it in Fig. 9.

3. The mean square error in predicting compatibility is roughly 1.5 to 3 times as large with the short circuit test, compared with the optimum load test.

4. Proposed narrowband limits on measured current based on the data on line impedance variation and the actual current limit of the previous section are shown in Fig. 10.

5. The narrowband susceptibility limits are shown in Fig. 12 for a probability of susceptibility of 0.023.

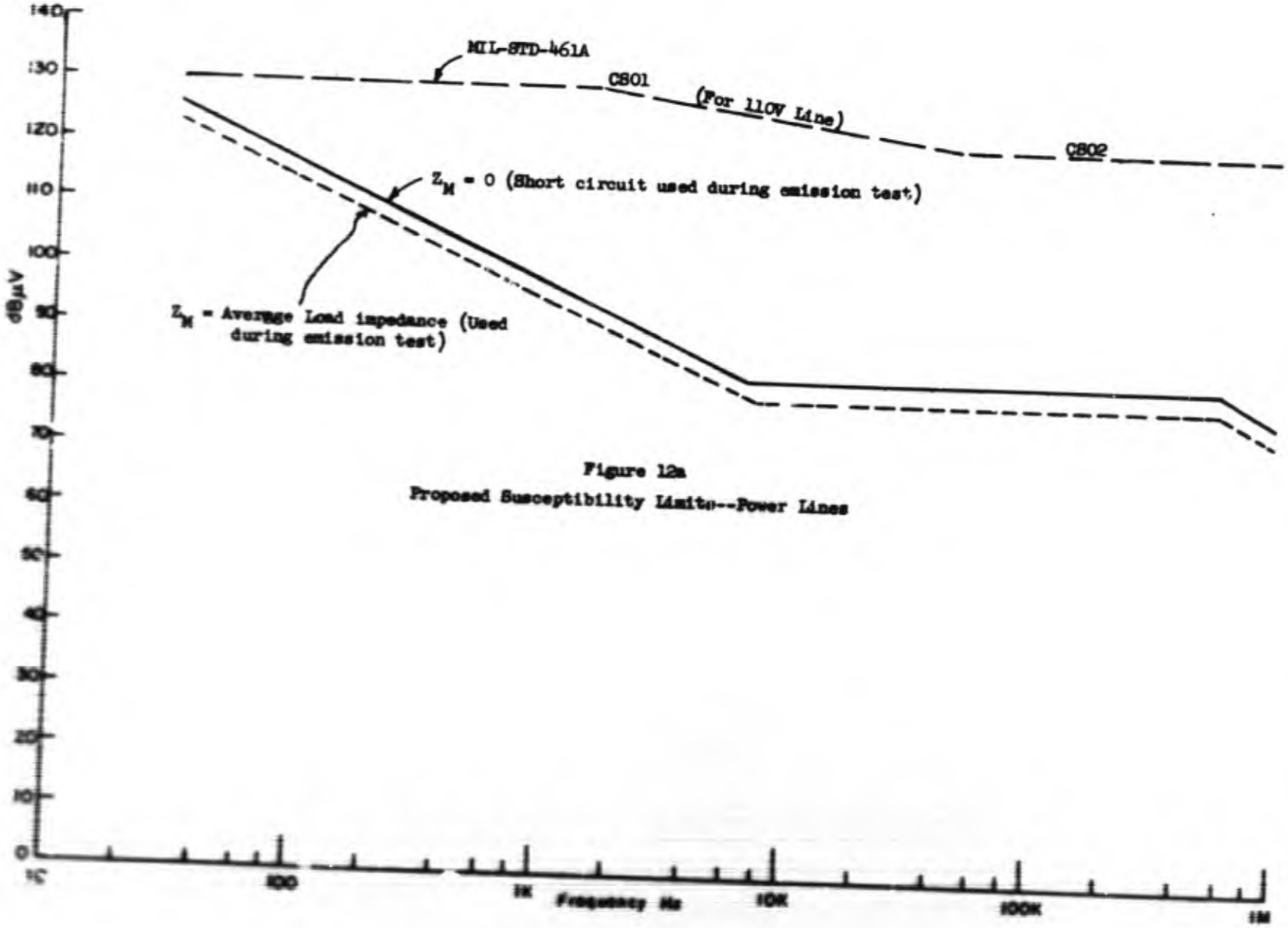

Figure 12a
Proposed Susceptibility Limits--Power Lines

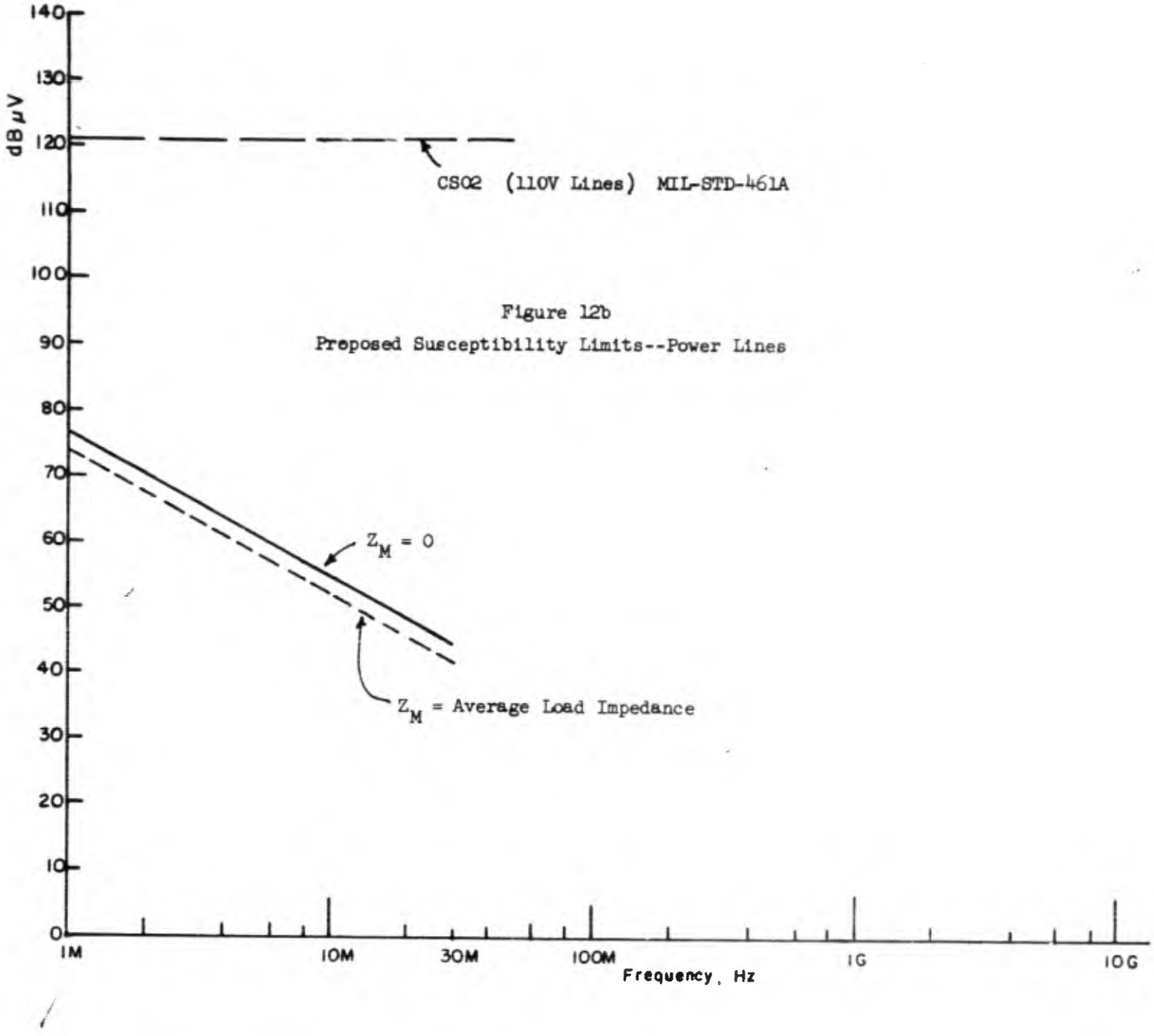

Figure 12b
Proposed Susceptibility Limits--Power Lines

SECTION 5

DEVELOPMENT OF LIMITS AND TEST PROCEDURES

5.1 Introduction

In this section the results of the analysis of the previous section are used to develop recommended limits and test procedures, and the consequences are discussed. The analysis given above dealt largely with narrowband emission and susceptibility testing on power lines. This work is here extended and modified to arrive at limits for broadband tests and for tests on signal and control leads. Some of the recommendations which are presented in this section are recommendations that apply to the present standards 461 and 462 regardless of whether or not the new recommendations are implemented. Such cases will be apparent from the text.

The discussion in this section is divided into two parts, the first associated with the recommendations on limits, and the second associated with recommendations on test procedures.

5.2 Recommendations on Power Line Limits

As shown in Fig. 10, which is the proposed narrowband conducted emission limit for power lines, the proposed limit is very little different (in the average) from that which now exists. The uniformly inverse frequency characteristic is more severe in its limit at frequencies in the vicinity of several hundred Hertz and above about 5 MHz, but is less severe at frequencies between 10 kHz and 5 MHz. On a per unit frequency range basis, the limit level is raised considerably, especially if one considers the short circuit current level. As has been established, however, it is best to measure the emission current at a typical value of impedance. Assuming source and line impedances are equal, this limit is 6 dB lower than the short circuit current level.

5.2.1 Narrowband Emission Limits (Power Line)

Figure 13 shows the present narrowband power line limit curve along with the proposed limit curve. For the purpose of comparing with present limits, however, the equivalent short circuit limit curve should be used. Shown on this figure are values of measured emission from the various equipments subjected to test. These tests are described in more detail in Appendix A.1. It can be seen that, except for the TPS-1D radar, almost all measured emission levels fall below the proposed limits. This may be a fortuitous result, but the indication is, at least for those equipments other than the TPS-1D, that the proposed limit curve would be desirable.

A point in question is the upper limit of frequency at which emission should be measured. It has been common in the field to indicate that conducted interference is of relatively little importance at frequencies above about 25 MHz. The proposed curve shows the limit at this frequency to be about 4 dB above a microampere when measured across the average load impedance. Reference to Fig. 13 shows that measured narrowband emissions generally fall at or below this proposed limit. It would appear that a cutoff of 25 or 30 MHz is reasonable, and we have taken 30 MHz as the upper frequency limit.

5.2.2 Broadband Emission Limits (Power Line)

As discussed previously the logical basis for establishing broadband limits is to refer to the narrowband limit and adjust the broadband spectral intensity so that the same peak voltage is obtained in a circuit having a bandwidth characteristic of a particular frequency range in question. Where several bandwidths are frequently used it is probably best to choose the most wideband circuit commonly used since it is the one that would likely suffer the most degradation. In the audio frequency range a fairly typical bandwidth is about 10 kHz. On the other hand, in the low radio frequency range (above about 15 kHz) a typical communications service bandwidth is less than 600 cycles while at frequencies above about 150 kHz several kilocycles is probably more reasonable. Unfortunately, it is difficult to decide on a specific bandwidth. For example, in some services fairly wideband video amplifiers, having bandwidths on the order of 100 kHz or one MHz, are not uncommon. But frequencly, such amplifiers operate at a relatively high signal level and are not as susceptible to interference as input circuits. Furthermore, the signal conducting cables in such circuits are usually shielded. Since it is a matter of judgement, as to what bandwidth should be used, we have adopted a 5 kHz bandwidth as typical over the entire frequency range. It is recognized that some services may find such a bandwidth inadequate and others may find it more than adequate. It is assumed that in such cases, where adopting the stated limit may be either economically or operationally unwise, special considerations can be used to obtain an adjustment in the necessary limit. To be consistent with the narrowband emission limit the broadband emission limit, assuming a bandwidth of 5 kHz, would be 200 times or 46 dB above the limit for narrowband interference. The broadband limit curve shown on Fig. 14 is drawn using this criterion. It also is terminated at 30 MHz. Also shown are the present broadband limits. In general the proposed limit represents a relaxation. Experimental data are shown here also for comparison. The communications receivers are well within the limits, however, the TPS-1D exceeds the limits in most cases. This is perhaps not unexpected from such a device.

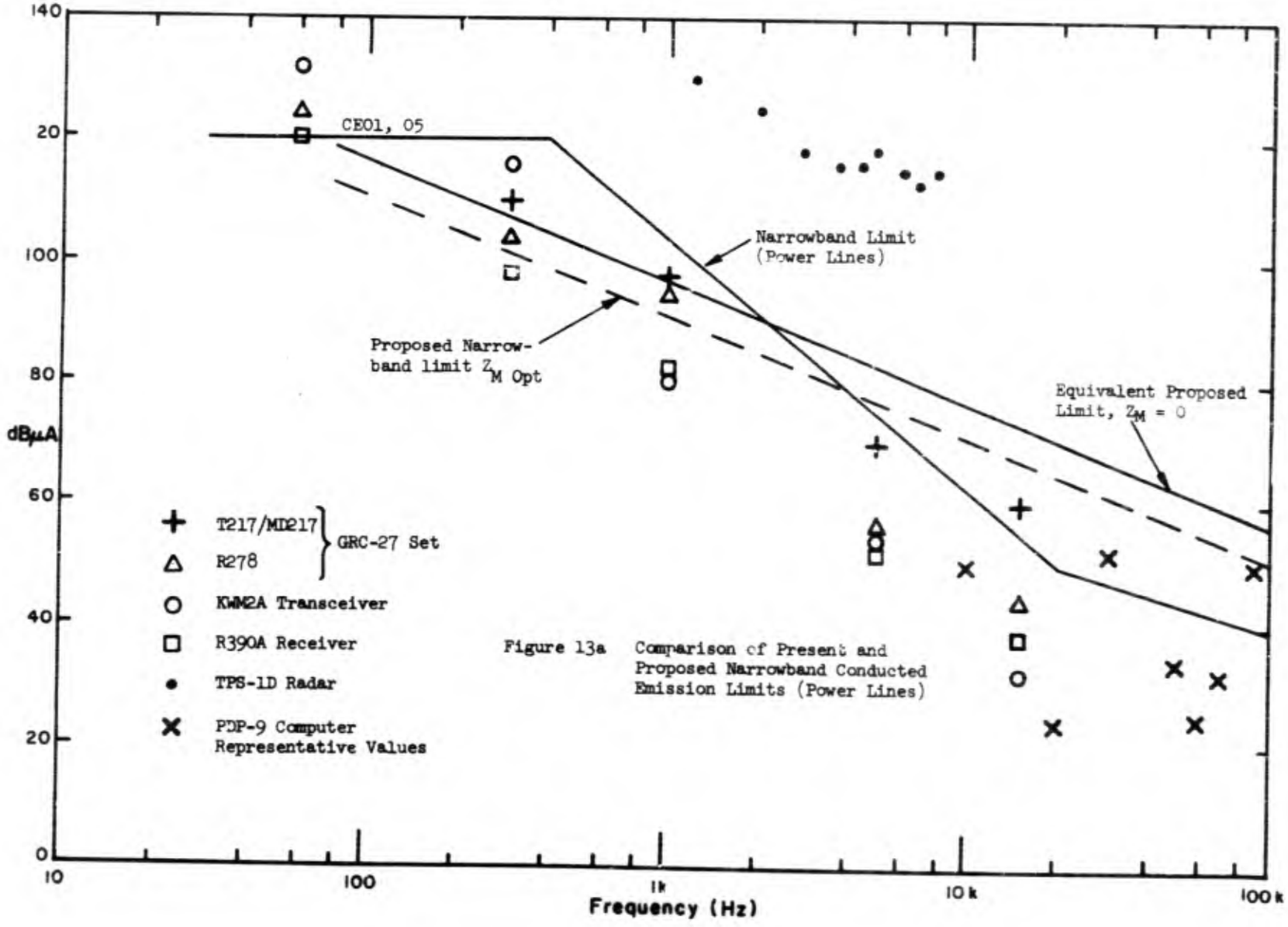

Figure 13a Comparison of Present and Proposed Narrowband Conducted Emission Limits (Power Lines)

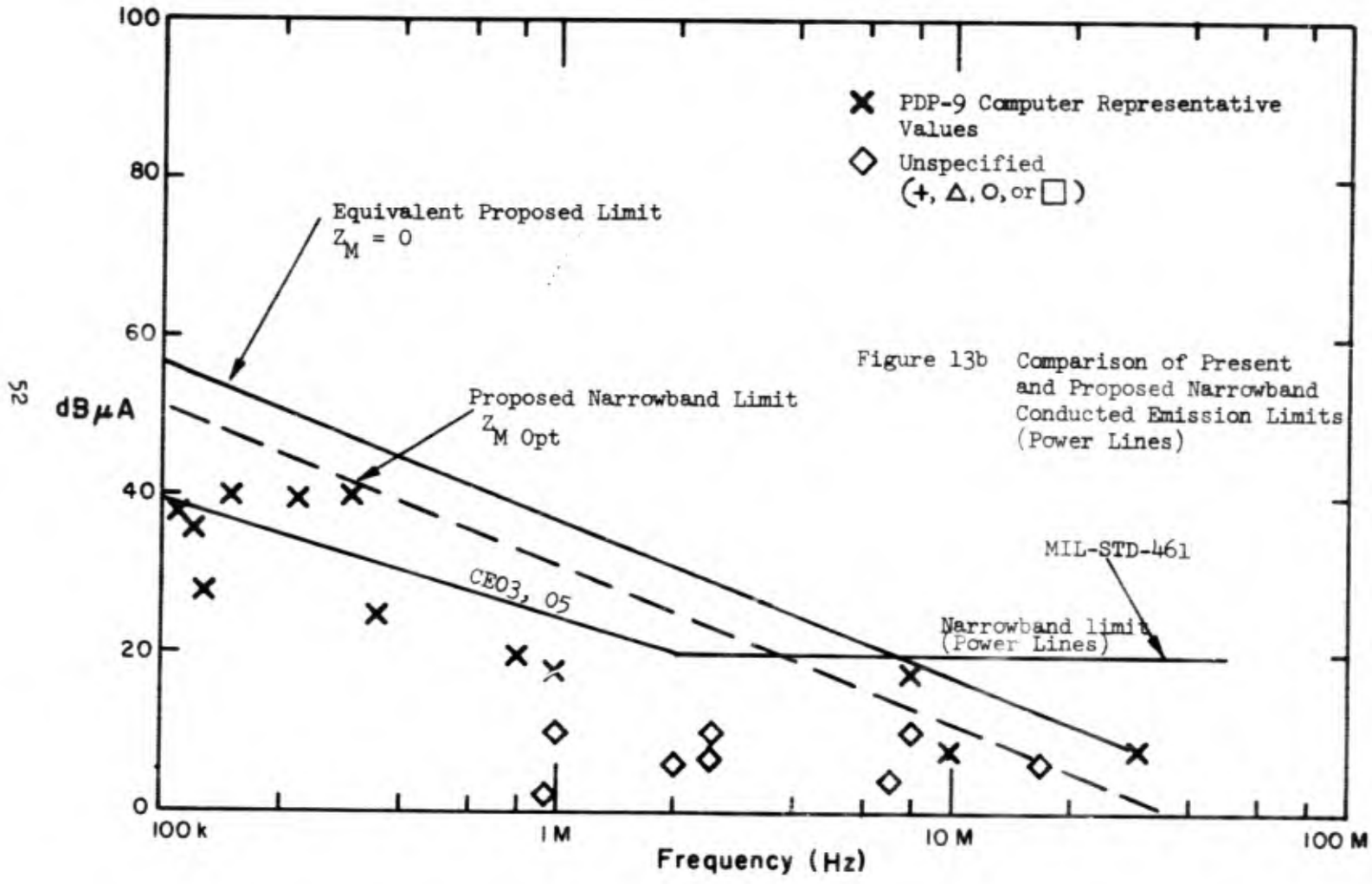

Figure 13b Comparison of Present and Proposed Narrowband Conducted Emission Limits (Power Lines)

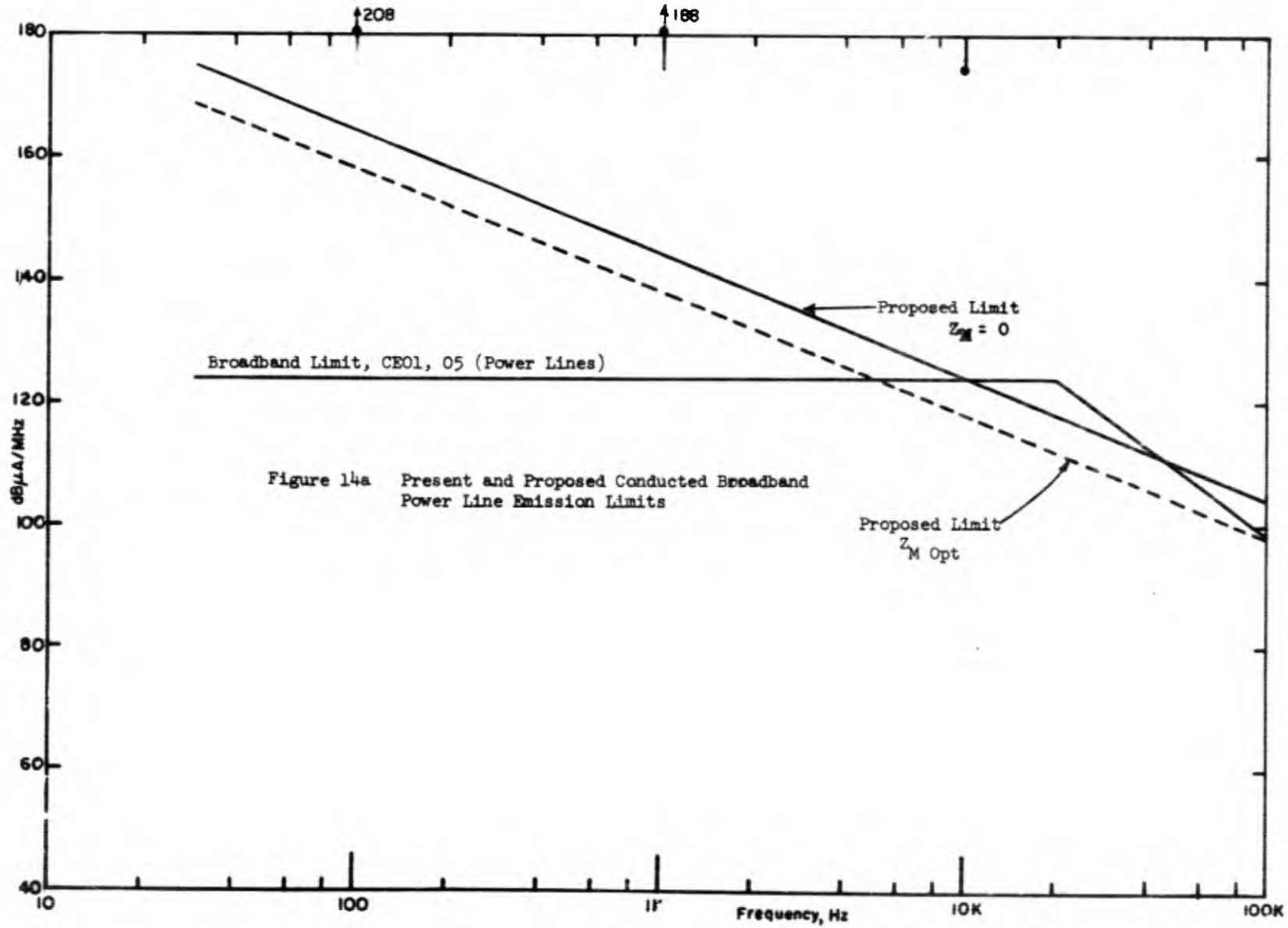

Figure 14a Present and Proposed Conducted Broadband Power Line Emission Limits

Figure 14b

Present and Proposed Conducted Broadband Power Line Emission Limits

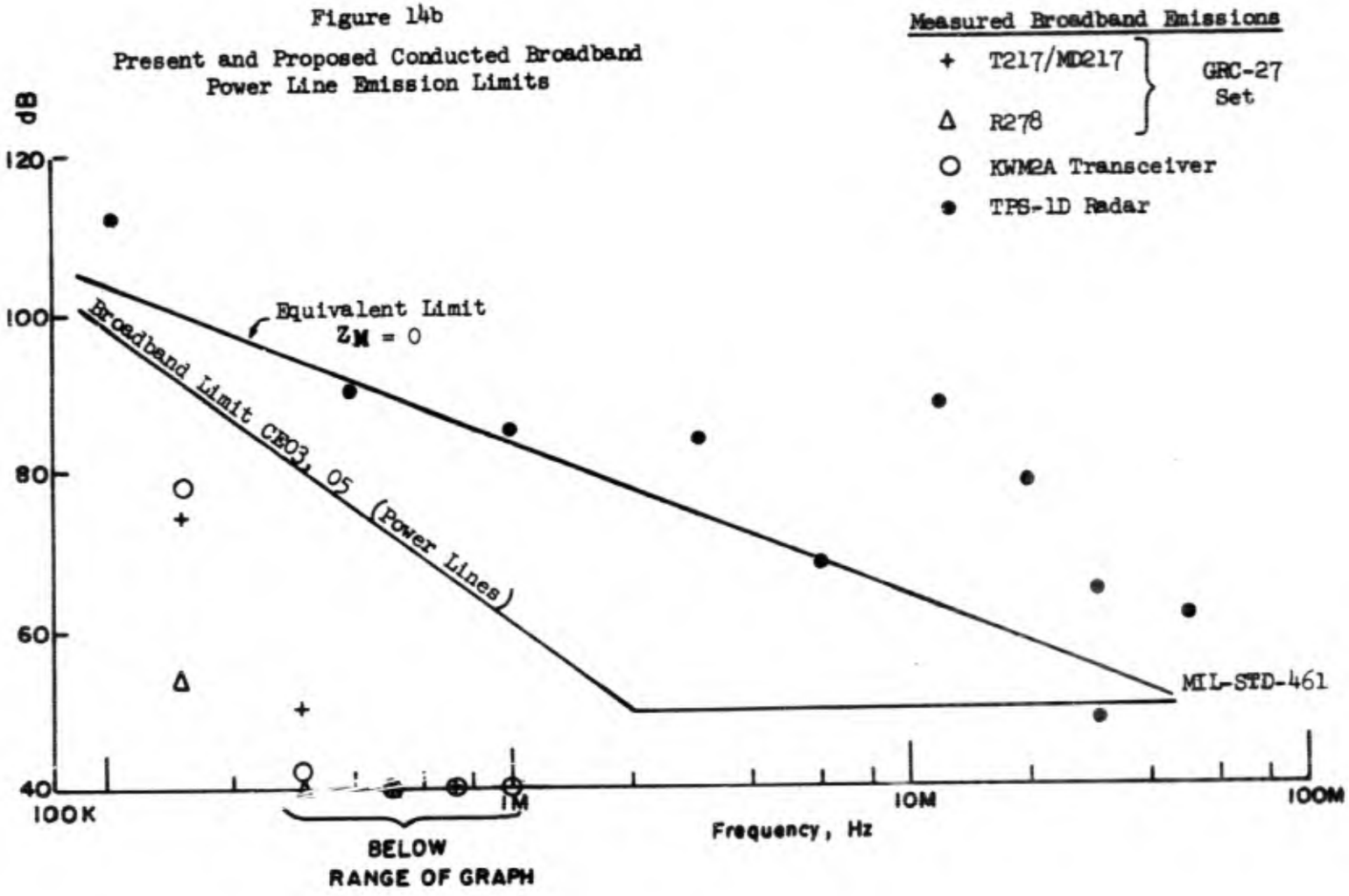

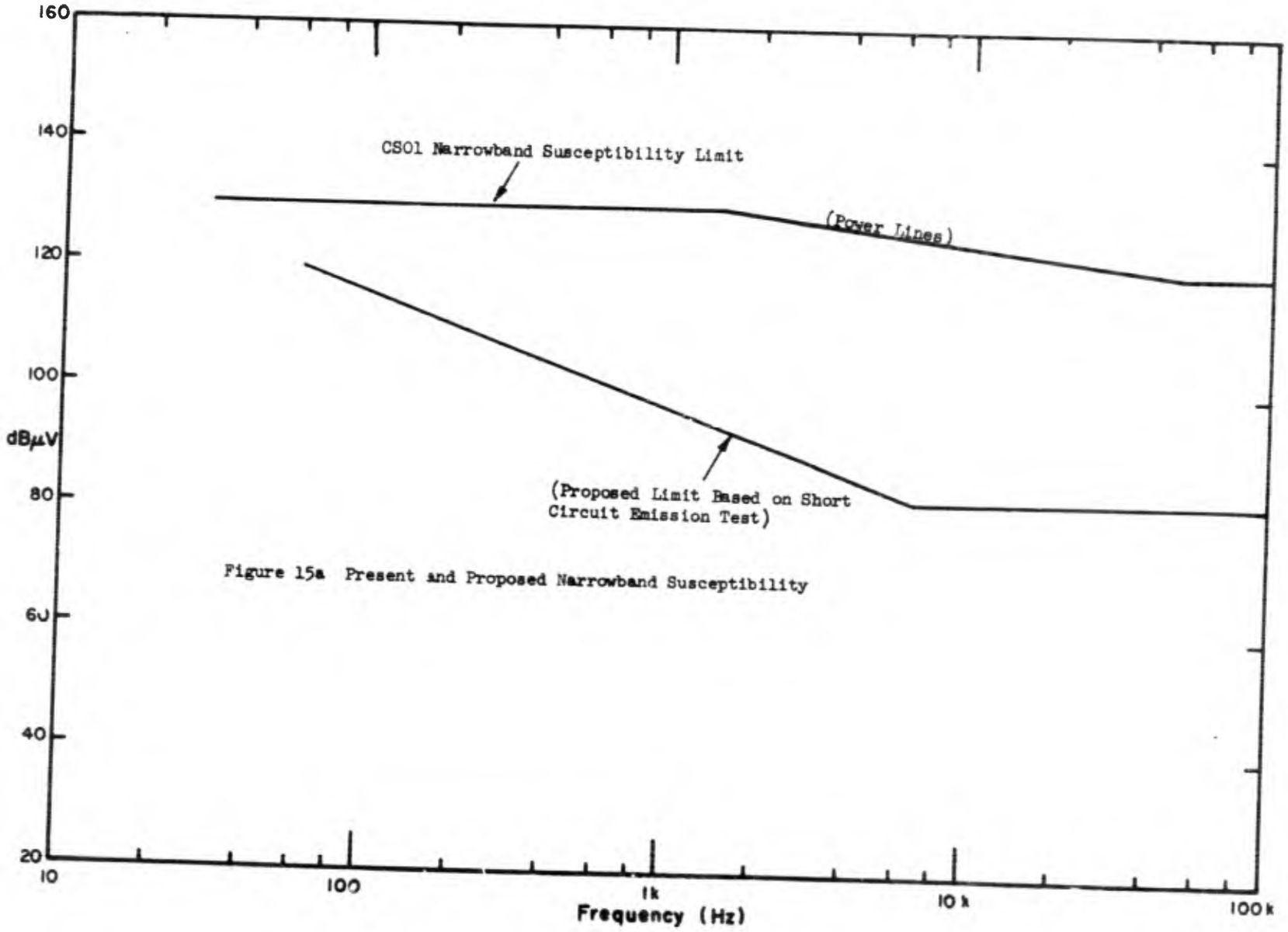

Figure 15a Present and Proposed Narrowband Susceptibility

5.2.3 Narrowband Susceptibility Limit (Power Lines)

The theoretically logical limit based upon correlation with conducted emission limits is shown on Fig. 12. At frequencies above 10 kHz it is lower than the present limit by about 40 dB. Figure 15 shows measured data (details on the measurements are given in Appendix A.1) along with the present and proposed limits. Except for the TPS-1D the measured susceptibilities are well outside the present limit. The proposed limit is more consistent with measured values but there are still a number of points outside it.

Thus it appears that the proposed limit is more consistent with present practice. Actually most of the points outside the proposed limit are from either old or relatively low quality receivers. However, a relatively modern receiver (the KWM2A) also shows some points outside the lower limit.

As pointed out previously one of the factors which is considered in the present susceptibility limit, particularly at UHF, is the coupling to the power line by radiation directly from a transmitting antenna in the vicinity. For example a situation considered typical is a UHF 1 kilowatt transmitter located within a distance of about 25 feet. The isolation between the transmitter antenna and the power line (here assumed to resemble a half-wave antenna with about 50 ohms load impedance) might be of the order of 30 dB. Thus approximately 1 watt or 7 volts would appear across the 50 ohms corresponding to the line voltage input terminals. Thus if protection from direct transmitter radiation of this kind is necessary it is quite illogical to lower the susceptibility limit unless special installation practices are adopted for such situations.

The fact that typical receivers do not appear to meet the more stringent requirements indicates that special care must be taken in the design of receivers intended for such a configuration if this limit is maintained.

5.2.4 Broadband Susceptibility Limits (Power Lines)

In the present specifications the only broadband susceptibility test is that of the spike test designed to provide protection against switching transients. If such limits were established in the same manner as the narrowband susceptibility limit by relating it to the emission limit one would obtain the curve shown dotted in Fig. 2. Since it, in fact, has been developed on the basis of a different concept than that of the spike spectrum test, direct comparison may not be appropriate. However, it may be noted that the most significant difference in level between the two arises,

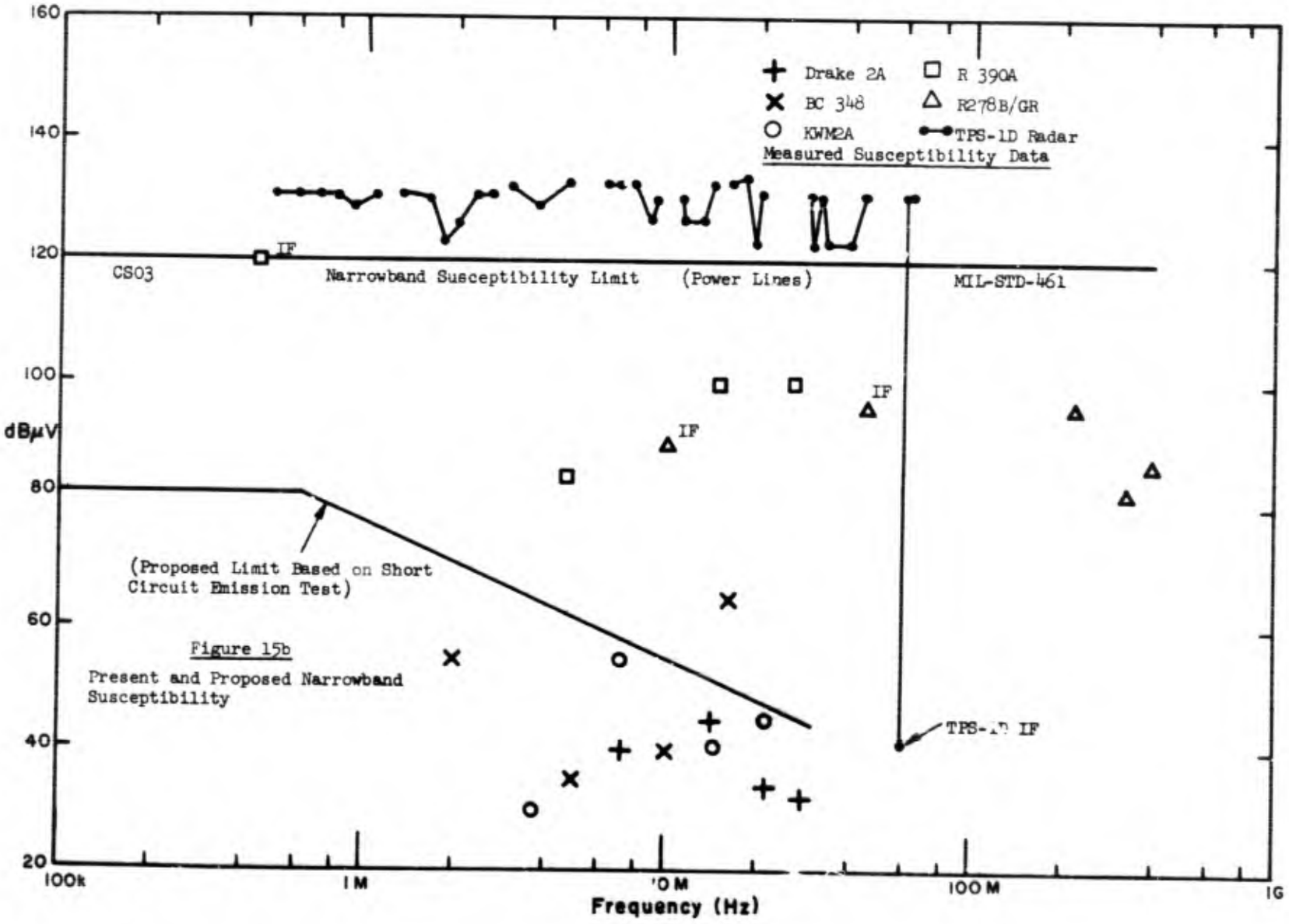

Figure 15b

Present and Proposed Narrowband Susceptibility

in part, from taking into consideration the impedance of the line as a function of frequency.

Because of inadequate data no particular recommendation is made on broadband susceptibility tests at this time. However, it is a subject that deserves further consideration, especially in view of the extensive use of digital devices capable of generating broad spectrum pulses. Furthermore, it is sometimes found that sinusoidal inputs--though not interfering when unmodulated--do cause interference when modulated. The mechanism involves detection by the rectifier circuit, and admission of the low frequency sideband components by the power supply filter.

5.3 Signal and Control Line Limits

Applying the same logic to the development of signal and control line limits as to power line limits one would expect the same emission limit with the exception that it would be measured over a different impedance. The determination of the proper impedance is not simple. Such lines can emit in two possible modes, frequently referred to in the 2 wire-line case as the common mode and the differential mode. The control or signal voltage itself is transmitted via the differential mode. If the line is a parallel line or a twisted pair the proper impedance usually lies between 100 and 300 ohms. If the line is a coaxial cable, it will most likely be 50 ohms. The differential mode is the mode primarily responsible for direct conducted coupling.

The common mode would be that primarily responsible for radiation.

The present test procedure is unclear as to which is to be measured. Figure CE02-1 might be interpreted as showing the current probe completely surrounding an interconnecting cable so as to measure the common mode; yet note c on method CE02 implies that differential mode should be measured (except for twisted pairs). No information is given pertaining to coaxial lines. The rationale for the different treatments should be clarified, if retained. There follows a recommendation to clarify the procedures.

5.3.1 Differential Mode

Limitation of differential mode current is of value to protect interconnected equipments. For compatible operation the emission current multiplied by the lead impedance equals the voltage appearing at the terminals of the interconnected device. Hence this voltage can be compared with the susceptibility limit. In view of the common use of coaxial cable for interconnection 50 ohms has been

chosen as a typical load impedance in the differential mode. As discussed in Section 2, with this impedance, Fig. 3 shows the comparison of present emission and susceptibility limits. If one uses the proposed limits for power lines (shown dotted on Fig. 3) one has an emission limit which exceeds various of the present susceptibility levels, and at frequencies below 20 kHz, exceeds all present susceptibility levels. As the frequency increases the proposed limit gives less protection than the present one up to about 8 MHz. Furthermore, the proposed emission limit should logically be extended above 30 MHz if coverage of radio input systems such as antenna feeds, couplers, etc. is involved. Therefore, a levelling off of the emission curve appears to be in order. Hence it appears to be difficult to justify using the same limits for power lines and for differential mode currents on signal and control lines.

This effect of constant impedance and unlimited frequency range has been implicitly recognized in present susceptibility limits for radio equipment and emission limits for antenna terminals. These limits are constant all across the band up to 12.4 GHz. The levels of emission and susceptibility in these cases appear to have been chosen on the basis of state of the art. For example, intermodulation occuring inside the tuning range of a receiver can be just as troublesome as that outside the range, but different limits are used. Thus, specifications of conducted antenna emission and susceptibility limits are a special problem since the various interconnection possibilities can create highly individual situations.

It was considered beyond the scope of the present program to attempt to relate the probability of interference under such variable conditions with any set of limits, particularly since the number of intermodulation products increases so rapidly as the number of receivers on common antennas increases. Some analysis in this area will be done in connection with the next phase of this program on radiation limits.

Considering available power levels, one way out of the present difficulties would be to divide "signal" leads and "control" leads into separate categories. The concept here is to consider the signal as any low level desired voltage out of a sensor, transducer, receiving antenna, pre-amplifier, etc. The level of such "signals" is usually less than a millivolt. "Control" voltages, however, are usually of the order of a volt or more and thus can tolerate substantially higher interference voltages. Thus on "control" leads one could tolerate interference voltages of, say, 90 dB/μV. Since on such circuits it should be quite possible to avoid any large signals the same limit could be used for intermodulation and other forms of spurious response.

The establishment of broadband emission and susceptibility limits is more difficult. Control circuits may be divisible into two classes, sine wave, and video. The video includes pulse circuits of various kinds. A typical pulse control voltage is about 5 volts peak (on interconnecting cables) and there should be no response to about 1 volt peak. If it is assumed that such circuits have a bandwidth of about one MHz a limit of 120 dB/μV/MHz would be appropriate. The corresponding emission limit would be approximately 68 dB/μA/MHz.

With regard to "signal" leads it is proposed to retain the present antenna terminal limits including CE04, 05, 06, 07, and 08.

5.3.2 Common Mode

As previously mentioned in the common mode the primary consideration is one of radiation. The limit here is, therefore, similar to that placed on power leads. Thus, it is proposed to use the same limits here as previously proposed.

A secondary consideration in the common mode situation is common-to-differential mode conversion. Any difficulties of this kind, however, would be subject to detection in the susceptibility test. Also this conversion is involved in the radiated susceptibility of the cable under conditions where longitudinal currents are induced by external fields.

5.4 Critique on Test Procedures

In this section criticisms and recommendations for changes on various aspects of the testing procedure outlined in MIL-STD-462 are discussed. These comments are based upon the experience gained in performing certain of the conducted emission and susceptibility measurements reported in Appendix A.1 as well as detailed review of all procedures. The number in parenthesis following the paragraph title identifies the pertinent clause in MIL-STD-462.

5.4.1 General Comments on Procedure Requirements, Section 4 of MIL-STD-462

Test Conditions (4.2.1)

In this section it is implied that a shielded enclosure is used; but the conditions under which this enclosure should be used are not explicitly stated. In some cases a test sample (e.g., radar set) may be too large to be practically tested in a shielded enclosure. In other cases a shielded enclosure may not be necessary because the ambient fields may be below the specified limit. It is recommended that a shielded enclosure be used if the ambient fields at the test site outside the enclosure exceed the ambient electromagnetic level specified in 4.2.1.1. If in this case the test sample is too large to test inside a shielded enclosure, then procedure 4.2.8 should be implemented.

Ground Plane (4.2.12)

It should be explicitly stated here that the use of a ground plane does not necessitate the use of a shielded enclosure as is implied in paragraph 4.2.1.2. Thus, in order to standardize the measurement test conditions, the use of a ground plane is recommended wherever practical (see comments, paragraph 4.2.2.4) even outside of a shielded enclosure. In this case the ground plane should be electrically tied to an earth ground in order to minimize the possibility of shock. For large equipment mounted in a metal test stand, it may be impractical to locate the equipment on a ground plane. In this case the metal test stand can be considered to form the ground plane. However, in order to perform conducted emission and susceptibility tests, the use of by-pass capacitors mounted to a ground system is necessary. Thus in order to allow for the use of by-pass capacitors in these cases it is recommended that a ground strap, bonded to the metal test stand at the location in which the power enters the equipment, be used. The 10 μf by-pass capacitors should be mounted to this ground strap at a point no greater than 1 meter from the power lead terminals of the test sample. For purposes of standardization, it is recommended that the strap be copper of thickness .25 mm, of width 20 cm and less than 1 meter long.

Bonding of Test Sample (4.2.2.4)

In the case of test samples having metal legs or parts of the chassis contacting the ground plane and in which no bonding straps are specified in the installation instructions, it has been found that the emission levels are erratic and strongly dependent upon the contact that the test sample is making with the ground plane. In order to standardize the measurement and have consistent data, it is recommended that if no bond is required between the test sample and ground plane, the test sample be located on a masonite sheet having a thickness of 3 mm and an area sufficiently large to support the test sample.

Isolation Transformer (4.2.3.2(c))

In this section an isolation transformer is listed as being required to break the RF circuit along the power line feeding the EMI meter. However, no specification as to the RF performance of this isolation transformer is given. Since most EMI meters contain RF filters on the power line feeds, it appears that there may be no need of an isolation transformer. However, it is recommended that further investigation be made into the need for such isolation and specification on RF isolation be documented.*

(4.2.3.3.1) (untitled paragraph)

In this section it appears that one is required to use a spectrum analyzer or at least have a CRT display of the spectrum for all measurements. However, following the experimental procedures outlined in Section 5, it appears that no use is made of this display and hence it is recommended that it be dropped as a requirement.

Calibration of Measuring Equipment (4.2.3.5)

In this section the reader is referred to MIL-STD-461 which in turn refers him to MIL C 45662! Why not be referred directly?*

Broadband-Narrowband Emissions (4.2.6)

The presence or absence of narrowband emission, as defined by MIL-STD-462, is not only a function of the characteristics of the spectrum emitted by the test sample but also a function of the frequency resolution of the measuring apparatus. Since this frequency resolution is not specified, measurements made with different apparatus or with the same apparatus but with different resolution settings may show differences in the number of narrowband emission lines. Thus in order to standardize the identification of types of emission it is

---

* A recently proposed revised edition, MIL-STD-462A, of MIL-STD-462 has corrected this criticism.

recommended that the following nominal bandwidths be employed in the tested frequency ranges.

Table 5.1

SUGGESTED NOMINAL BANDWIDTHS FOR IDENTIFICATION OF TYPES OF EMISSIONS

30 Hz - 20 kHz	BW = 30 Hz
20 kHz - 150 kHz	BW = 200 Hz
150 kHz - 30 MHz	BW = 5 kHz
30 MHz - 400 MHz	BW = 100 kHz
400 MHz - 16 Hz	BW = 400 kHz
1 GHz - 10 GHz	BW = 1 MHz

5.4.2 Comments on Experimental Procedures, Conducted Emissions, Test Procedures, Section 5 of MIL-STD-462

CE01 Conducted Emissions 30 Hz to 20 kHz Power Leads

A) Broadband emission tests are outlined in Section 4.2 of MIL-STD-462. However, no specification of the required frequency response of the current probe of the combination of the current probe and matching transformer is given. For many current probes, the frequency response in this range is not flat, but linearly frequency dependent, as shown in Fig. 13 of Report #1 "Test Method CE", 1968. Where the narrowband limit is flat with frequency (as in this frequency range with the present limit) the effect of the current probe characteristic is to give relatively higher weight to those components at higher frequency. It is recommended that an inverse filter (or matching transformer) be used to make the transfer response uniform over the frequency range.*

Where the narrowband limit varies inversely with frequency (as in the proposed limit) the increasing sensitivity at higher frequencies results in proper weighting of all components and no compensating filter is needed.

In line with comments in paragraph 5.3.3, it is recommended that this test be applied to common mode interference on all "signal" and "control" leads.

---

* Proposed MIL-STD-462A has suggested such a filter.

CE02 Conducted Emissions 30 Hz to 20 kHz Signal and Control Leads

A) Applicability

The statement of applicability in MIL-STD-462 implies that all signal and control leads of a piece of equipment must be measured. No good definition is given as to just which classes of leads are intended. It is, however, implied that the cables to be measured are those connecting separate chassis together, not cables from one part of a chassis to another. As mentioned in paragraph 5.3 it is recommended that this test be applied only to differential mode interference on "control" and "signal" lines. Some specifications for test circuits and jigs are necessary to separate properly the common mode and differential mode currents.

B) 10 μf Feedthrough Capacitors 3(d)

The apparatus specifications state the use of 10 μf feedthrough capacitors, but they are not shown in Fig. CE02-1, and no statement is made as to where they are to be used. The assumption may have been made that they are for use in measurements of emission interconnecting power leads as per CE01, but if the interpretation of paragraph (A) above is used, such testing is unnecessary and no feedthrough capacitors are required.*

CE03 Conducted Emission 20 kHz to 50 MHz Power Leads

A) Measurement Procedure

CE01 specifies a 20 kHz bandwidth of test equipment for broadband measurements while no specifications of bandwidth are given in CE03. It is recommended that the bandwidths specified in Table 5.1 be used when testing on the indicated frequency ranges and that a 1 MHz bandwidth be used as a normalization factor to compare with test limit of Fig. 14.

B) High Frequency Performance of Test Circuit

At the higher frequencies in the range of this test (i.e., above 3 MHz) the present test circuit, composed of the specified 10 μf feedthrough capacitor and the power leads from the test sample to the feedthrough capacitor, presents an impedance to the test sample which is inductive above 50 kHz and has a magnitude reaching several hundred ohms at 50 MHz. If the intent of this test is to measure effectively short circuit current of the test sample, one must know

* Proposed MIL-STD-462A does not specify the 10 μf as part of the apparatus.

whether the impedance levels of the equipment are sufficiently high compared to the test circuit. If this test circuit is retained, it is recommended that experiments be conducted that will establish the statistically expected values of test sample impedance. On the other hand the test network shown in Fig. 11 is considered to provide a better test impedance.

CE04 Conducted Emission 20 kHz to 50 MHz Control and Signal Leads

Comments listed under CE02 apply here.

CE05 Conducted Emission 30 Hz to 50 MHz Inverse Filter Method

The general validity of this test procedure is questioned. Furthermore, as written it is ambiguous in that both narrowband and broadband limits are referred to. No specific information is included on how one is to apply these limits in using this particular test.

In principle it appears that this test is designed to shorten test time by permitting a single measurement of broadband interference which covers each of the frequency ranges 30 Hz to 20 kHz and 20 kHz to 50 MHz or to permit searching for a single limit value while scanning the frequency range with a narrowband filter. In the former case, in theory, by using a filter with a characteristic that is the inverse of the limit value one could determine compliance with the broadband limit if the spectrum of the interference had the same shape as the limit. Since the frequency range covered is so broad, it is extremely unlikely that this will occur in any practical sense. If it did occur presumably one could determine compliance with the limit by measuring the peak value of the interference through the inverse filter and comparing it with the value obtained by integrating the limit curve properly. In the higher frequency range, this is an extremely complex procedure since the limit is a function of frequency and the phase characteristic of the filter must be taken into account. Furthermore, it is likely that the dominant contribution to the peak value will be from the flat portion of the spectrum above 2 MHz. This means that if the spectrum does not have the limit shape components could exceed the limit at low frequencies by substantial amounts and would not be detected if the components above 2 MHz were only slightly below the limit.

This type of test only has validity when applied to specific equipments whose emission spectra are well defined and for which a given peak voltage has been defined for which one can be assured that the limit is not exceeded at any frequency.

It is recommended that, unless the conditions for use of this test are more explicitly defined along with methods of arriving at a suitable limit (or limits if the frequency range is subdivided), the test be eliminated.

5.4.3 Conducted Susceptibility Test Procedures

CS01 Conducted Susceptibility 30 Hz to 50 kHz Power Leads

A) Power Line Frequency at Amplifier Output Terminals

Difficulties have been experienced from feedback of the power line frequency into the power amplifier. These include burning out the output section of the amplifier as well as causing distortion and modulation of the signal frequency by the power line frequency. It is recommended that a diagram of an alternate test setup using two identical transformers for power line bucking such as that shown on data sheet No. 6603 in the Solar Electronics Company catalog be included. The diagram shown in Fig. CS01-1 is most useful for test samples requiring dc supplies or low power ac loads, of less than perhaps 100 W.

CS02 Conducted Susceptibility 50 kHz to 400 MHz Power Lead

Figure CS02-1 should show more detail of coaxial cables and terminations to be used. Specifically, can the 50 Ω load shown, be the EMI meter input impedance, and, if so, should be EMI meter connection be made at the signal source or at the capacitor?*

At the higher end of the frequency range the lengths of the leads of the capacitor and of the connection from the feed-cable of the signal source to the capacitor can affect the results. It is recommended that the EMI cable connection be made as close to the capacitor as physically possible. See Fig. 16 for recommended cable arrangement.

CS03 Conducted Susceptibility 30 Hz to 10 GHz, Intermodulation, Two Signal

(3c) The requirement of low pass filters to remove all signal generator harmonics is unrealistic. It is recommended that 3c read "... reduce signal generator harmonics to levels which will not affect the measurements."

CS04-CS05 Conducted Susceptibility 30 Hz to 10 GHz, Rejection of Undesired Signals at Input Terminals (2 signal generator method), Cross Modulation

Comments made on test CS03 apply to CS04-CS05 tests.

---

* Proposed MIL-STD-462A does not show the 50 Ω load in Fig. CS02-1.

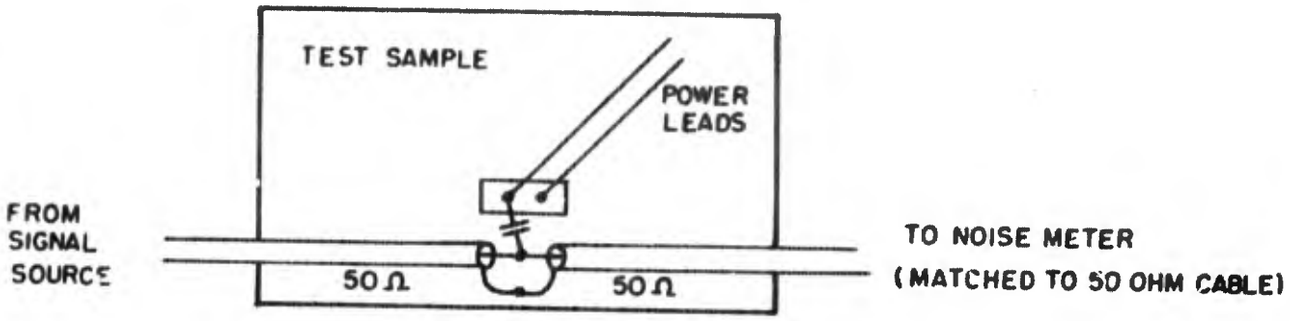

(a) Detailed component arrangement used for CS02

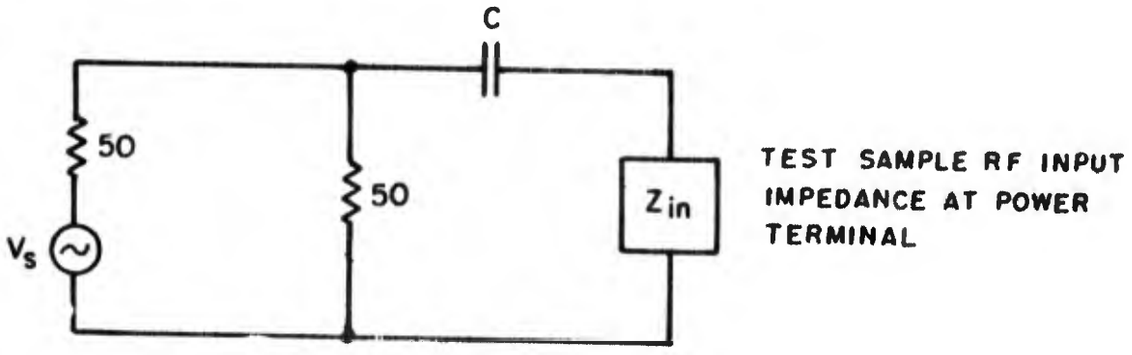

(b) Equivalent circuit

Figure 16 Suggested modified test arrangement for CS02

In addition, in CS04, Clause 1., Purpose, should read: "This method is used for determining the input terminal spurious responses and desensitization using two signal generators."

CS06 Conducted Susceptibility Spike (Power Leads)

Connecting the scope directly across the input terminals as suggested in Fig. CS01-1 will superimpose line frequency upon the spike display. In order to better view the spike and measure its characteristics, it is recommended that a rejection filter be placed between the test sample terminal and the scope. A nominal rejection of 40 dB of power line frequency would be suitable.

CS08 Conducted Susceptibility, 30 Hz to 10 GHz, Rejection of Undesired Signals at Input Terminals (1-Signal Generator Method)

Comment on CS03 applies.

5.5 More Complex Measurement Procedures

We have not treated here the possibility of measuring source parameters in addition to current into a known load. For example, an increase in the confidence of prediction of compatibility may result if the magnitude of the source impedance is measured as well.

Changing the test load impedance, as we have recommended, does not substantially increase the complexity of measurement; the optimum load is simply installed instead of the feedthrough capacitors and the corresponding limit curve is used. There is, however, an increase in accuracy. The tradeoff between accuracy and complexity, therefore, is quite clear-cut and the evaluation is easy to make.

In the case of multiple measurements, however, the situation is less straightforward. The measurement complexity is considerably increased. For example, an impedance-measuring device (either standard RF bridge or 2-current probe device) must be added to the required measuring equipment if source impedance magnitude is to be measured, and an additional set of data must be taken. In addition, another set of limits must be developed, specifying allowable combinations of current and impedance.

The tradeoff in this case between confidence of predicted compatibility and complexity is more difficult to assess. Assumptions of linearity and normality of distributions, which were adequate in evaluating the optimum terminating impedance, might lead to incorrect evaluations of relative accuracy vs complexity in this case. Our statistical data were not extensive enough nor was there sufficient time to find the actual distributions of predicted interference, without making these assumptions. Therefore, we have not made recommendations on the multiple-measurement techniques for these reasons.

SECTION 6

CONCLUSIONS AND RECOMMENDATIONS

6.1 Introduction

The examination of the proper basis for establishment of limits and methods of measurement to maintain electromagnetic compatibility has necessitated the recognition of the importance of many technical and state-of-the-art factors. The present specifications have been established after many years of experience, coupled with the requirements for obtaining agreement in areas where wide differences of opinion exist.

Under the circumstances, it is difficult, in a limited period of time, to give proper weight to the various special circumstances to which a given limit or technique is applicable. For this reason some of the conclusions reached must be recognized as tentative, being made on the basis of the best judgement in view of the available data.

6.2 Conclusions

In the following statements the major conclusions of this report are summarized. Specific conclusions are covered in the recommendations that follow.

1) On the basis of a direct conduction model which makes use of the expected value of line impedance, present emission and susceptibility limits appear much further apart than necessary. On the other hand, if one considers the possibility of a combined radiation-conduction coupling of a susceptible device to a transmitter, no obvious relationship between conducted emission and conducted susceptibility limits need exist. However, the latter situation will be analyzed more completely in the radiation phase of this study.

2) Two bases should be considered in the establishment of conducted emission limits:

a) the consistent pairs of levels of emission and susceptibility which can be economically maintained, either by meeting general limits, or permitted deviations from these limits in special cases, and

b) the level of emission which, when considered in terms of a realistic radiation model, can be tolerated in typical topological configurations of potential emitters and susceptible devices.

Using measured data in applying the former criterion and an assumed field value at a given distance in applying the latter, a consistent emission limit not much different from the present limit is obtained.

3) In order to obtain minimum spread in predicted emission currents, and hence optimize the confidence associated with a given emission limit, measurements of emission current should be made across an impedance equal to the expected value of the line impedance. Measurements with the present method (assumed to be a short circuit current method) require assigning a limit estimated to be about 6 dB more severe in order to obtain the same degree of protection from interference with the same confidence.

4) Present susceptibility limits are higher than many of the values measured on equipments which were tested. The proposed limit is more consistent with present practice, but does not satisfy the condition mentioned in item 1 above, where there is direct coupling from a transmitter antenna to a receiver power line.

5) Consideration should be given to divisions in limits and test procedures between signal and control lines and between common mode and differential modes of transmission.

6) Numerous editorial and technical amendments are needed in the texts of MIL-STD-461A and 462.

6.3 Recommendations

The recommendations are divided into two groups: those pertaining to limits and those pertaining to test methods. In the case where there is a relation between these, the limits specified assume the modified test method.

6.3.1 Limits

1) CE01, 03 Narrowband Power Lead Emission: The limit specified on Fig. 10 ($Z_M = Z_{MOPT}$) should be adopted in the frequency range up to 30 MHz. The limit could be extended to 50 MHz at the level at 30 MHz if desired, but evidence of the importance of the extended range was not available in this study.

2) CS01, 02 Narrowband Power Lead Susceptibility: The limit shown on Fig. 12 ($Z_M = Z_{MOPT}$) should be considered for adoption.

Special consideration is necessary for receivers whose power lines are expected to be exposed to direct radiation from transmitters. In this latter case provision should be made for

either (a) a separate limit of one volt out to 400 MHz (same as present limit) or (b) proper shielding of power circuits to reduce vulnerability to direct transmitter pickup. (Direct radiation pickup will be explored in the next phase of this study.)

3) CE01, 03, Broadband Power Lead Emission: The limit shown on Fig. 14 ($Z_M = Z_{MOPT}$) should be adopted.

4) Consideration should be given to the establishment of a broadband susceptibility limit (power lines) corresponding to the emission limit. Tentatively the limit should be 47 dB (in μV/MHz) above the emission limit (in μA/MHz). The wide differences in effective bandwidth of communications and digital devices requires further examination.

5) CE02, 04: These tests should be restricted to signal and control lead emission in the common mode only. The limits shall be the same as for power lead emission as given above.

6) CE06, CS03, 4, 5, 8: For signal leads in the differential mode, no change in the existing emission and susceptibility limits is proposed at this time. These tests should, furthermore, be applied to the inputs and outputs of other electronic equipment (e.g., sonar amplifiers) as well as to the antenna terminals of communication equipment as is now specified.

7) For "control" lines in the differential mode new limits should be established. The value of 90 dB/μV is suggested for the narrowband susceptibility limit and 38 dB/μA for the emission limit. Corresponding wideband limits could be 120 dB/μV/MHz and 68 dB/μA/MHz.

8) No recommendation for change is being made for CS06 and CS07. A recommendation on CE05 is given in Section 6.3.2.

6.3.2 Test Procedures

Two of the most significant of the preceding recommendations were to adopt a new test circuit and new limits. It is recognized, however, that certain problems remain in implementation. For example, although the proper equivalent circuit of the test circuit has been determined, the design of an actual network to provide the desired isolation, proper impedance, and still pass the power frequency, remains to be accomplished. Because the circuit is thus not an accomplished fact, included in the recommendations are some items which apply to the present measurement techniques along with those which should be incorporated when the new techniques are implemented.

1) CE01: If present limits are maintained the current probe should be required to have a flat frequency characteristic or should be properly compensated with a filter.

If the proposed limit is adopted the current probe should be required to have a linearly increasing frequency characteristic and its sensitivity calibrated at 10 kHz.

This test should also be required for common mode interference on all interconnecting "signal" and "control" cables.

The measurement procedure should be modified to include the new measurement impedance whose equivalent circuit is shown on Fig. 9.

2) CE02, 04: Rewrite to apply only to differential mode "signal" and "control" leads and modify to provide methods of performing test properly. The measurement impedance should be 50 ohms. Note 5(b) should be deleted and note 5(c) must be revised.

3) CE03: For broadband measurements, limit should be placed on the bandwidth of the measuring instrument: 200 Hz to 10 kHz is recommended, see Table 5.I.

The measurement load impedance should be modified to have the equivalent circuit shown in Fig. 9.

4) Test CE03: Should also be applied to measure common mode interference on "control" and "signal" lines.

5) CE05: This test should be deleted or the circumstances under which it can be used and method of interpreting limits carefully defined.

6) CS01: Statement 3b should read "... less than 10% drop." Add to description the method using 2 transformers as discussed in Section 5.4.3.

7) CS02: Figure 16 should be adopted to assure proper lead lengths in the test setup.

8) CS03, 04, 05, 06 and 08: Minor editorial and technical changes in the text as discussed in Section 5 are recommended.

APPENDIX 1

CONDUCTED EMISSION AND SUSCEPTIBILITY MEASUREMENT PROGRAM

A.1.1 Introduction

In order to form a basis for the critique on experimental test procedures, several test samples were subjected to as many CS and CE tests as time and available test equipment would allow. Although many of the tests were not implemented, a comprehensive review of each experimental test procedure outlined in MIL-STD-462 was made with a view toward anticipating any conceptual or practical difficulty that might arise if these tests were conducted. These reviews plus the experience gained by implementation of some test procedures formed the basis for the discussion in Section 5.

The following test samples were subjected to the tests reported here.

1)	R-390A/URR	HF receiver
2)	KWM-2A	Single sideband transceiver HF
3)	AN/GRC-27	UHF AM transmitter and receiver set
4)	BC-348	Receiver HF
5)	Drake 2B	Amateur band receiver HF
6)	TPS1-D	L-band radar

Except where indicated the test setups and experimental procedures recommended in MIL-STD-462 were used. Results and discussions on tests CE01 and CE03 are detailed in "EMC Data Collection Techniques," Technical Report NO. RADC-7R, December 1968.

A.1.2 CE02 and CE04 Control and Signal Leads, 30 Hz to 50 Hz

Below 20 kHz, no currents were detected on any control or signal leads of any of the equipment tested, although the instrumentation was sensitive to currents 20 dB or more below the limits for CE02. Above 20 kHz, such currents were found in several cases, always well below the MIL-STD-461 limits for CE04. With the KWM-2A and the R-390A it was possible to detect currents on the headphone cable, at several of the internal oscillator frequencies. The magnitude of the current was generally greater with the cable lying on the ground plane than with it suspended above the ground plane. For the T217 set, the cables between the transmitter and the modulator/power supply showed some broadband emission in the MF and HF range, probably due to fan motors, but they were generally well below the limits for CE04.

A.1.3 CE06 Antenna Terminal CE, 10 kHz to 12.4 GHz

A.1.3.1 Tests on the TPS-1D Radar

Test CE06 was performed with the radar operating in the receive mode only (key up). The only emission discovered was at the frequency of the local oscillator, 1380 MHz, and had a level of 33 dBμV. This measurement was not performed in the transmit mode (key down) due to lack of attenuators able to handle the power.

A.1.3.2 CE06 Tests on HF-UHF Receivers

This test was performed on the R-390 and R-278 receivers. A number of narrowband emissions were detected, for which the applicable limit is 34 dBμV into a matched load.

The R-390A HF receiver emitted only a -7 dBμV level signal, due to a local oscillator, in its 0.5 - 30 MHz operating range. It had several emissions in the VHF range, the greatest of which was +20 dBμV at 126 MHz. No emissions were detected from 200-1000 MHz.

The R278 VHF receiver produced only a local oscillator emission of 13 dBμV at 360 MHz, in the range 150 kHz - 1000 MHz.

Numerous and intense emissions are produced by the KWM-2A HF single sideband transceiver. In its operating range of 3.5 - 30 MHz, the output of the VFO, the local oscillator fundamental and its second harmonic, were detected having levels near or above the limit. Numerous strong emissions were found in the VHF region. Those in excess of the limit are listed in Table A.1-I.

Table A.1-I

ANTENNA TERMINAL EMISSION FROM KWM-2A

Frequency of Emission	Levels of Emission	Possible Source of Emission
2.6 MHz	+33 dBμV	(VFO)
8.5	40	(local oscillator fundamental)
17.0	51	(local oscillator injection)
25.3	31	(3 × local oscillator)
34	41	(4 × local oscillator)
78	49	--
87	54	--

The Drake 2A HF amateur band receiver exhibited emissions only at the local oscillator frequency of 18.0 MHz. The level of this emission, +40 dBμV, is in excess of the limit.

A.1.4 CS01 Power Lead, 30 Hz to 50 kHz

Several receivers were tested for susceptibility in the frequency range 30 Hz to 50 kHz when signals are injected onto the power lines. The test setup used is that specified by MIL-STD-462.

A test sample was considered susceptible if a spurious output was detected on a pair of earphones when the injected signal power level was increased from 0 level. The level at which the spurious response was barely detectable was recorded and compared with the levels specified in MIL-STD-461. In general spurious responses were detected on all test samples except the R390 receiver. However, in all cases the level needed to cause barely detectable interference was well above the limits specified by MIL-STD-461 except for the Drake 2A receiver which was susceptible at the limit level at its 50 kHz third intermediate frequency.

The CS01 test was attempted on the TPS1-D radar but it proved impossible, with the equipment on hand, to reduce the power line voltage within the test equipment without exceeding the capacity of the motor-generator set supplying power to the radar. The audio test generator used for performing this measurement required the power line voltage at its output terminals to be as small as possible. In practice less than one or two volts would suffice. A scheme using two transformers was attempted, Fig. A.1.1. This requires the use of a dummy load of dissipation rating equal to the radar. The addition of this load on the generator plus the voltage drop across transformer #1 caused the voltage at the radar to be much too low to operate.

Two other schemes using two transformers were considered as shown in Figs. A.1.2 and A.1.3.

The scheme of Fig. A.1.2 was similar to the scheme of Fig. A.1.1 except that the turns ratio of the second transformer was adjusted to produce the same secondary voltage as transformer #1 without using a high power load. This would prevent the overloading of the generator. However, the impedance of transformer #2 was much greater than that of transformer #1. This meant that almost all of the audio voltage appeared across transformer #2 instead of across transformer #1.

The second scheme, shown in Fig. A.1.3, was to shift the phase of a second phase of the 3 phase generator using a resistor-inductor network to produce a current through transformer #2 equal

in magnitude and opposite phase to that through transformer #1, thus removing the power line voltage at the output terminals of the audio generator. This, as the first scheme, failed because of generator overload and excessive voltage drop across transformer #1. These problems point out the need for further study in testing equipment that is powered by limited electrical supplies.

A.1.5 CS02 Power Lead, 50 kHz to 400 MHz

A.1.5.1 Tests on HF and UHF Receivers

The CS02 power line susceptibility test was made on a number of receivers in the range 150 kHz to 400 MHz. MIL-STD-462 being unclear about the details of the test setup, the configuration shown on Fig. 16.a was used. The equivalent circuit shown on Fig. 16.b indicates that the noise meter forms a 50 Ω load at the termination of the signal source cable, and this is shunted by the coupling capacitor in series with the RF input impedance Z at the power terminal. The noise meter reads the voltage across R.

Signals were injected at a number of arbitrarily chosen receiver operating frequencies, as well as intermediate frequencies. As in CS01 the amplitude is raised until an output is just discernable.

Representative values of susceptibility levels for several receivers are shown on Table A.1-II.

Table A.1-II

SUSCEPTIBILITY LEVELS AT FREQUENCIES ARBITRARILY SPOTTED IN THE RECEIVING BAND OF THE TEST SAMPLES
(Specified Lower Limit +120 dBμV)

Drake 2A HF Amateur band Receiver		BC 348 HF Receiver	
7.2 MHz	+40 dBμV	2.0 MHz	+55 dBμV
14.2	+45	5.0	35
21.2	+34	10.0	40
28.2	+32	15.0	65
KWM-2A Single Sideband HF Transceiver		**R-390A HF Receiver**	
3.7 MHz	+30 dBμV	0.60 MHz	+110 dBμV
7.1	55	4.6	85
14.3	40	14.6	100
21.1	45	25.6	100
		0.455	120

cont.

Table A.1-II (cont.)

R-278B/GR
VHF Receiver

2.20 MHz	+ 96 dBμV	
3.21	82	
3.99	87	
45.9	96	(1st IF)
9.9	90	(2nd IF)
2.05	>100	(3rd IF)

Discussion of Results

The R-390A, which is the least susceptible of the units tested, has a double pi section feedthrough filter in its power connections. The frequency range was not swept, so it is possible that there are other susceptible frequencies. None of these units appears to meet the limit stated in 6.5 of MIL-STD-461 "when subjected to 1 volt from a 50 ohm source" (1 volt = +120 dBμV).

A.1.5.2 CS02 Tests in TPS1-D Radar

The TPS1-D radar was also subjected to the test procedure outlined in MIL-STD-462, utilizing pulse modulation of the output of a 5 watt source synchronized to the base repetition rate of the radar, observations were made on the PPI and A scope for false echoes. These echoes have been observed at various frequencies in the range 50 kHz to 400 MHz.

The radar proved to be most susceptible to interfering signals having a frequency equal to the radar IF frequency. However, this was the only frequency at which the level of susceptibility fell below that specified by MIL-STD-461. The level was -69 dBm at 58.5 MHz.

A.1.6 CS08 Signal Input Terminal, 30 Hz to 10 GHZ

A.1.6.1 HF and UHF Receivers

a) In-Band Tests

The CS08 test for rejection of undesired signal at the antenna terminal was performed on the R278 and R390 receivers. The specification limit requires 80 dB rejection of undesired signals in any tuning band, and no response to a 0 dBmW signal outside the tuning band.

The R-278 had several responses to in-band signals indicating less than 80 dB rejection. Table A.1.III shows the responses when the receiver is tuned to 310.0 MHz.

Table A.1-III

REJECTION OF IN-BAND SIGNALS

	292 MHz	85 dB
	297	80
	302	65
	307	65
f_o =	310	0
	317	60
	322	75
	327	75
	332	80

In general, there seems to be weak in-band responses at 5 MHz intervals. These have not been explained.

b) Out-of-band signals produced a few responses in excess of the limit. For example, when tuned to 221.1 MHz, responses were found at 620 MHz at -5 dBmW and 580 MHz at -15 dBmW. No other responses were found to 4 GHz.

Tests for rejection of below-band signals were inconclusive. Many responses were found for which a generator harmonic falls at the operating frequency. It was not determined whether these harmonics were present in the generator output or were created in the receiver.

The R-390 was essentially free of responses to undesired signals in the tuning range, at the specification limit of 80 dB.

The most surprising result was the large number of spurious responses to above-band signals of the R-390 receiver. For example, with the receiver tuned to 7.6 MHz, the above-band responses in Table A.1.IV were found.

With the receiver tuned for 1.0 MHz, it was susceptible to a 69.5 MHz signal at -98 dBmW, only a few dB above the minimum signal strength at the operating frequency.

Tests for below-band susceptibility were inconclusive as for the R-278, but no response was found which was not traceable to generator harmonics.

Table A.1.IV

OUT OF BAND SUSCEPTIBILITY LEVELS
R390A

30.5 MHz	0 dBmW	93.0 MHz	-33 dBmW
38.0	-17	95.0	-16
39.0	0	97.0	- 5
41.8	-30	108.5	- 5
55.0	- 3	110.0	-35
56.0	0	112.0	-29
59.0	-57	115.0	-11
60.7	-29	146.0	- 8
63.7	- 5	124.0	-18
76.2	-62	125.0	-13
78.0	-38	127.5	-37

A.1.6.2 TPS1-D Radar

The test procedure in MIL-STD-462 was followed for these measurements with the exception of the low pass filters. No such filters were available. The measurements were made over the frequency range of 10 MHz to 10 GHz.

The susceptibility levels are listed in Table A.1.V. The operating frequency of the radar was 1320 MHz and the radar's measured sensitivity of -110 dBm at that frequency is listed in the table for reference. As the radar has an 80 dB down estimated bandwidth of less than 20 MHz, this frequency is the only one listed which is within the normal passband of the radar receiver.

The tuning range of the receiver is from 1.20 GHz to 1.35 GHz. Within this band the susceptibility limit level is 80 dB above the input required to produce standard response at the tuned frequency, which for this radar is -110 dBm. Outside the tuning range the susceptibility limit level is 0 dBm. Within the tuning range no response was detected which exceeded the limit level of -30 dBm.

In this test, as in all other susceptibility measurements on the radar, the susceptibility "standard response" was the minimum visible echo produced on the radar indicator screens.

The presence of responses at frequencies down to 1/17 of the operating frequency are due in part to the radar itself and partly due to the lack of a low pass filter on the generator output. It is felt that these responses indicate that the radar has excessive inherent responses to frequencies which have the operating frequency as a harmonic.

Table A.1.V

CONDUCTED SUSCEPTIBILITY LEVELS OF TPS-1D RADAR
FROM THE ANTENNA TERMINALS

Frequency MHz	Level dBm	Remarks
58.5	-11	IF frequency
78	- 7	1320 MHz is 17th harmonic of 78 MHz
83	-20	" " " 16th " " 83 "
89	-24	" " " 15th " " 89 "
95	-24	" " " 14th " " 95 "
102.5	-29	" " " 13th " " 102.5"
112	-37	" " " 12th " " 112 "
122	-32	" " " 11th " " 122 "
133	-36	" " " 10th " " 133 "
148	-37	" " " 9th " " 148 "
166	-27	" " " 8th " " 166 "
190	-20	" " " 7th " " 190 "
220	-39	" " " 6th " " 220 "
264	-44	" " " 5th " " 264 "
330	-34	" " " 4th " " 330 "
440	-70	" " " 3rd " " 440 "
480	- 5	1440 MHz is 3rd harmonic of 480 MHz
660	-22	1320 MHz is 2nd harmonic of 660 MHz
880	-11	
1320	-110	Operating frequency f_o (LO = 1380 MHz)
1350	-30	1350 x 2 = 2700 2 x ^{o}LO = 2760
1440	-39	LO + 60 MHz
2080	- 2	
2700	-43	2 x LO = 2760 MHz; 2760 - 2700 = 60
2820	-37	2 x LO = 2760 MHz; 2820 - 2760 = 60
3420	-12	spurious response
3480	0	spurious response
3800	- 4	spurious response
3860	- 4	spurious response

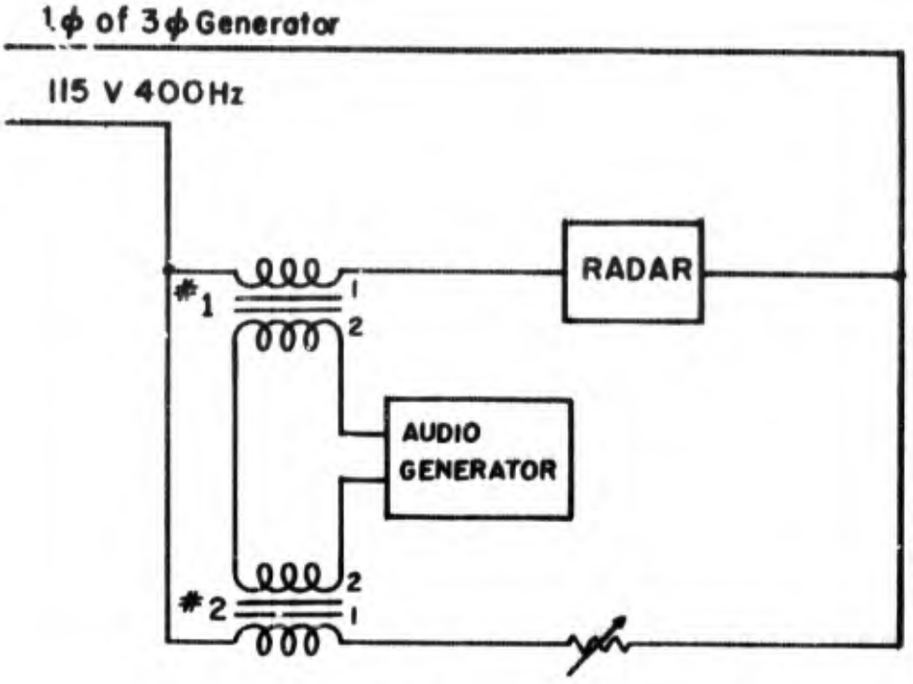

Figure A.I.1 First CSOI Test Setup, TPS-ID Radar

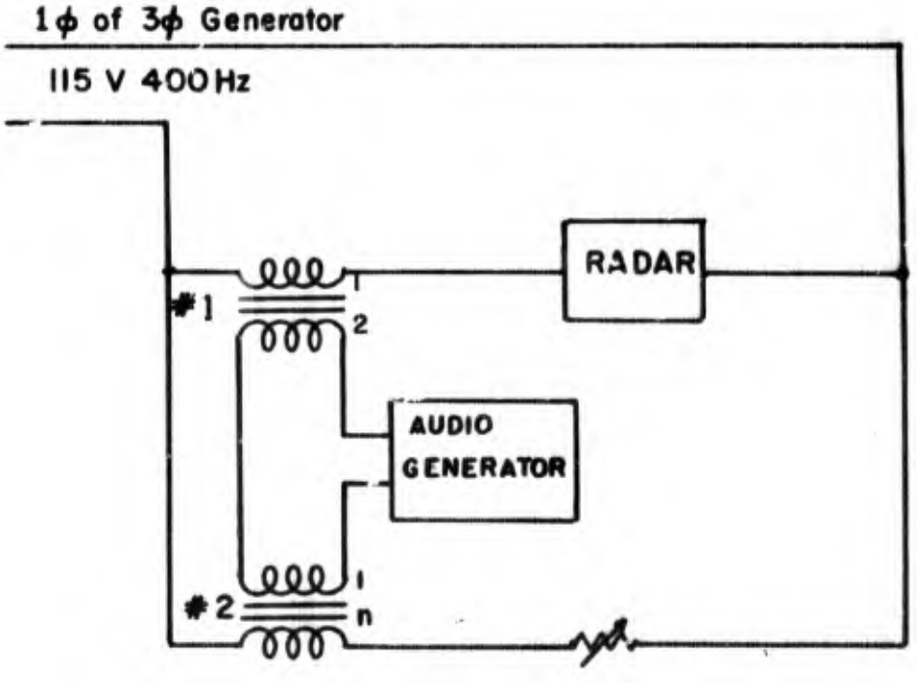

Figure A.I.2 Second CSOI Test Setup, TPS-ID Radar

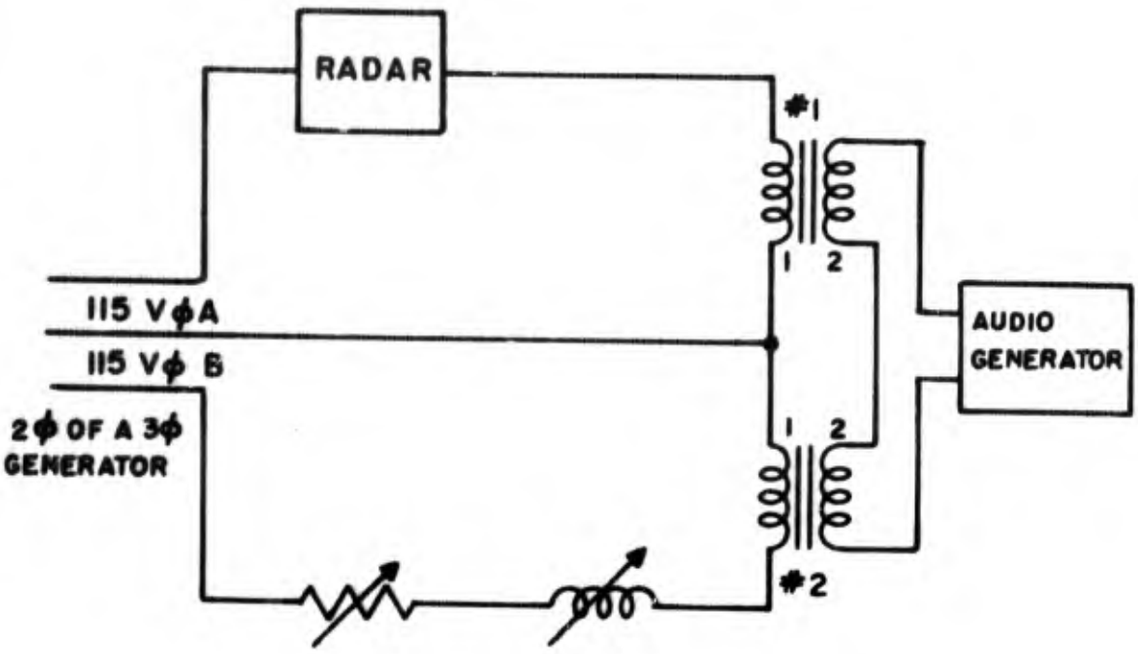

Figure A.1.3 Third CSO1 Test Setup TPS ID Radar

Appendix 2

POWER LINE IMPEDANCE MEASUREMENTS

A.2.1 Introduction

As discussed in the first interim report, the power line is modeled as a three-terminal device, with an impedance between each of the three terminals as shown in Fig. A.2.1. These three impedances may be calculated from three related impedances: Z', Z", and Z"'. The effective impedance between L and ground, with H shorted to ground is just the parallel combination of Z_2 and Z_3, and is defined to be Z'. Similarly, if L is shorted to ground, the impedance between H and ground is defined as Z"', and if H is shorted to L, the impedance between H and ground is defined as Z".

Thus, one has the three simultaneous equations:

$$Z' = \frac{Z_2 Z_3}{Z_2 + Z_3}$$

$$Z'' = \frac{Z_1 Z_3}{Z_1 + Z_3}$$

$$Z''' = \frac{Z_1 Z_2}{Z_1 + Z_2}$$

If these are solved for Z_1, Z_2 and Z_3, one obtains

$$Z_1 = \frac{2}{\frac{1}{Z''} + \frac{1}{Z'''} - \frac{1}{Z'}}$$

$$Z_2 = \frac{2}{\frac{1}{Z'} + \frac{1}{Z'''} - \frac{1}{Z''}}$$

$$Z_3 = \frac{2}{\frac{1}{Z'} + \frac{1}{Z''} - \frac{1}{Z'''}}$$

Thus, values for Z', Z", and Z"' at a given frequency completely determine Z_1, Z_2 and Z_3 at that frequency.

In practice, the shorting of two terminals of a live line was accomplished using a capacitor whose impedance was always less than 1 ohm over the frequency range for which it was used. Thus,

a 10 microfarad capacitor was used for the frequency range 10 kHz to 0.5 MHz and a one microfarad capacitor was used for the range 0.5 MHz to 50 MHz (see Figs. A2.2 and A2.5). The capacitor was changed in the latter range to avoid problems connected with internal resonances in the larger capacitor, and to reduce the 60 hertz current flowing into the capacitor. The diagram of the circuit used for the measurements of Z', Z'', and Z''' in the frequency range 10 kHz to 10 MHz is shown in Fig. A.2.3. The current probe was a Stoddart type 91550-1, the spectrum analyzer was a Singer type SPA-3a and the unit oscillator was a General Radio type 1001-a. A diagram of the switch box (S.B.) constructed for the measurements in this frequency range is shown in Fig. A.2.4, and the three circuits corresponding to the switch positions are shown in Fig. A.2.5.

The "blocking" capacitor (C_B) was used to block the 60 cycle voltage of the line in order to protect the unit oscillator.

The oscillator was modeled as a constant voltage source in series with an internal resistance, as shown in Fig. A.2.6. The voltage source was calibrated to a constant value E_i using an oscilloscope to measure the open-circuit voltage of the generator. The internal resistance R_i was then found to be 10 ohms using an impedance bridge.

If the generator open circuit voltage E_i is kept constant, the scale readings are proportional to the admittance

$$\left(\frac{1}{R_i + Z}\right)$$

since the spectrum analyzer reading is proportional to the current measured by the current probe.

The spectrum analyzer responds according to the voltage developed at its input terminals. For the current probe used the voltage developed at the analyzer input is not constant in the frequency range 10 kHz to 1 MHz for a constant probe input current. The correction chart shown in Fig. A.2.7 was therefore required to correct admittance values measured.

The correction factors from this chart properly apply only if the output of the probe is an open circuit. Since the output impedance in the test case was the finite input impedance of the spectrum analyzer, the validity of the correction factors was checked in the following manner. A known input current to the probe at 80 kHz (20 log Z_t = 0 dB at this frequency) was adjusted to a full scale reading on the spectrum analyzer. At some other frequency in the range 10 kHz to 1 MHz, the same current as at 80 kHz was applied to the probe input and produced a reading on the spectrum analyzer.

This reading multiplied by the correction factor at the given frequency should correspond to a full scale reading, if the assumption that the spectrum analyzer does not appreciably load the probe output is valid. This was found to be the case at frequencies in this range. The spectrum analyzer is adjusted to full scale with Z shorted. Thus, full scale deflection corresponds to an admittance of $Y_i = \frac{1}{R_i} = 0.1\text{mho}$. With the short on Z removed, the deflection corresponds to the magnitude of $\left(\frac{1}{R_i + Z}\right)$.

Depending on the magnitude of the measured impedance, the internal resistance of 10 ohms is either considered or neglected. If the magnitude of Z', Z'', or Z''' is greater than 100 ohms, the internal resistance is neglected since it is at most 10%, and usually less than 5% of the magnitude of the impedance measured. Thus, the magnitude of the impedances Z', Z'', and Z''' is determined by the ratio of the generator open circuit voltage divided by the measured current.

If the magnitude of Z', Z'', or Z''' is less than 100 ohms, it is divided into its real and imaginary parts. The internal impedance of 10 ohms is then subtracted from the real part and the new magnitude is computed from the new real and (old) imaginary parts.

The phase used in the above calculation is measured at representative frequency points using an impedance bridge. These phase points are then connected, providing an estimate for the phase at the magnitude points between the points of phase measurement.

Thus, Z', Z'', and Z''' were obtained for the frequency range 10 kHz to 10 MHz.

A diagram of the circuit used for the measurements in the frequency range 10 MHz to 50 MHz is shown in Fig. A.2.2. The impedance bridge was a General Radio type 916-A, the unit oscillator was a General Radio type 1211-C, and the detector was a Singer spectrum analyzer type SPA-12.

In the frequency range 10 MHz to 50 MHz, a 1 microfarad capacitor was used to block the 60 cycle voltage of the line in order to prevent the transformer in the bridge from being driven into a saturated region of its magnetization curve. The shorting and blocking capacitors contributed negligible impedances in comparison with the line impedances being measured.

The switch box used in the frequency range below 10 MHz could not be used above this frequency because it showed a resonant condition at approximately 14 MHz. Therefore, the capacitors and the impedance bridge were directly connected to the line through an ordinary power plug, using leads which were no longer than 2 inches.

This offered an additional improvement by reducing the inductive reactance.

For this frequency range, the real and imaginary parts of Z', Z'', and Z''', rather than magnitudes alone, were determined at each frequency of measurement.

The driving point impedances Z_1, Z_2 and Z_3 were found at four locations within the Moore School. The mean and standard deviation of the driving point impedances are shown in Figures A.2.8, A.2.9 and A.2.10. The mean was calculated at each frequency by averaging the values of the driving point impedance at the four locations. The standard deviation (defined as

$$\sum_{i=1}^{n} (x_1 - m_x)^2 \left[(x-\mu)^2\right]^{1/2}$$

where the x_i's are the sample points at each frequency and m is the mean) was also calculated at each frequency.

At low frequencies--that is, from 10 kHz to 400 kHz, the mean value of the impedance rises and the standard deviation is small. The line has external loads at various distances from the measurement point. These loads have greater effect on the driving point impedance if they are closer to the input terminals. Since in this frequency range the impedances are small, the number and location of the loads have a relatively small effect. This supports the fact that the standard deviation is small.

At intermediate frequencies, 400 kHz to 13 MHz, the calculated standard deviation becomes large, casting some doubt on the reliability of the averages calculated with only four points. There is no question that more data are needed, but a glance at the data shown in Figures A.2.8, 9, 10, reveals the tendency of the impedance magnitude to rise to a level of about 150 to 200 ohms and to remain at that value throughout this frequency range.

At high frequencies, 13 MHz to 50 MHz, the impedance magnitude falls and the standard deviation becomes smaller too. At these frequencies the loads on the power line far from the point of measurement have, in all likelihood, a minimal effect. And since all loads in the immediate vicinity of the measurement point were removed, the variability from one line to another can be expected to be smaller.

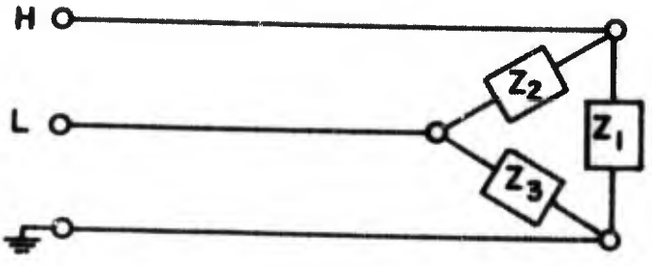

Figure A2-1 Impedance Model of Three Conductor Power Line

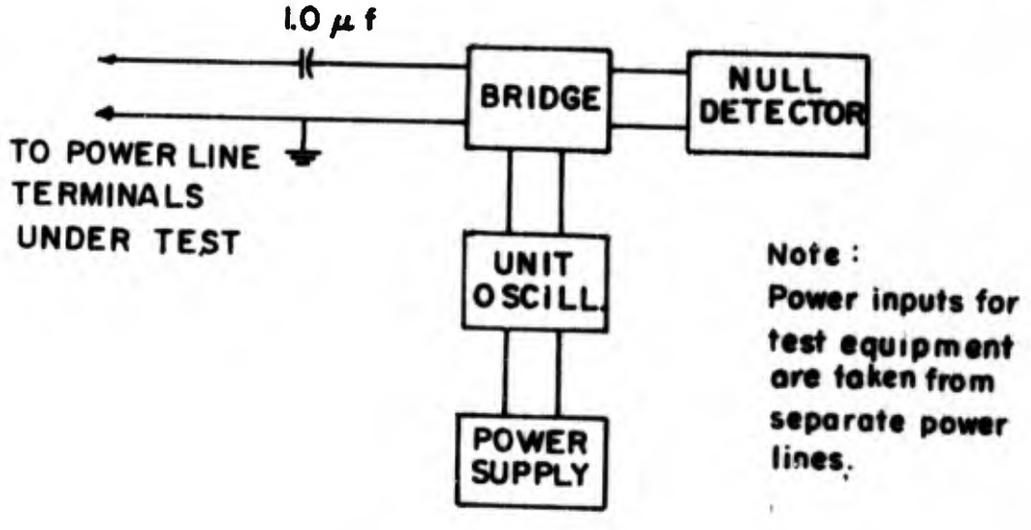

Figure A2-2 Impedance Measurement Circuit
10 MHz – 50 MHz

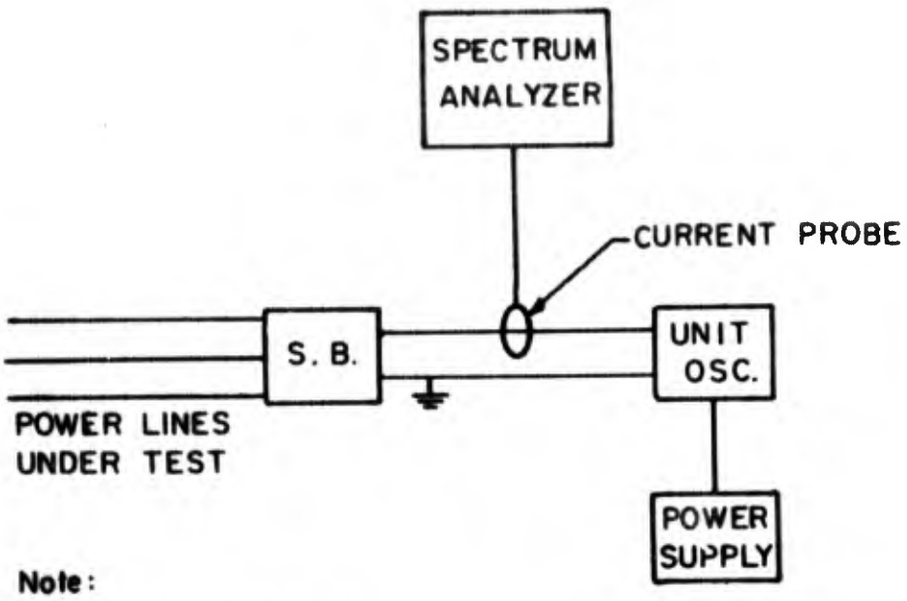

Note:

Power inputs to test equipment are taken from seperate power lines.

Figure A2-3 Impedance Measurement Circuit
10 kHz - 10 MHz

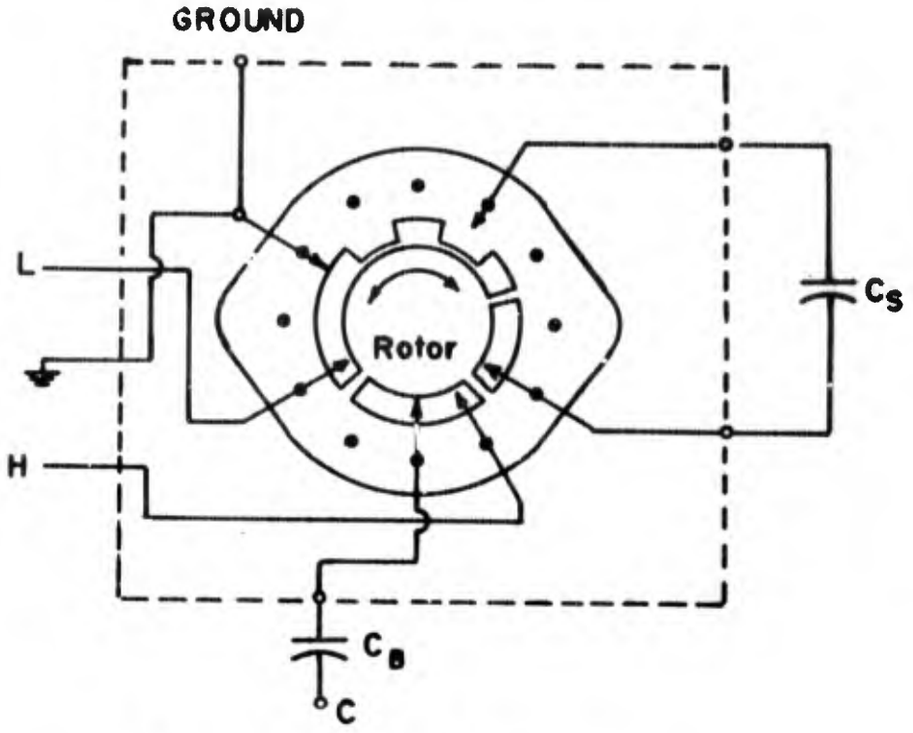

Figure A2-4 Switch Box

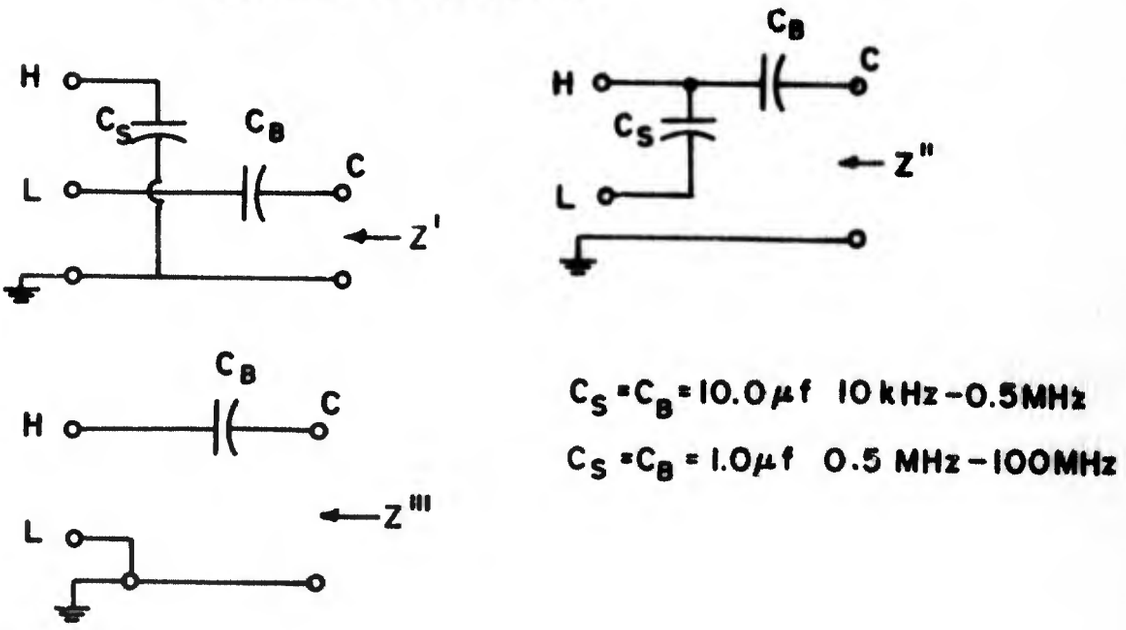

$C_S = C_B = 10.0\mu f$ 10 kHz – 0.5 MHz

$C_S = C_B = 1.0\mu f$ 0.5 MHz – 100 MHz

Figure A2-5 Circuits obtained from switch box of figure A.2-4

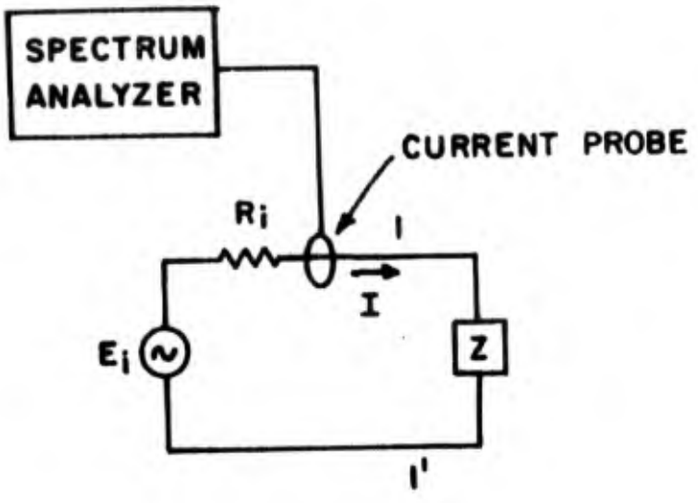

Figure A2-6 Measurement Circuit

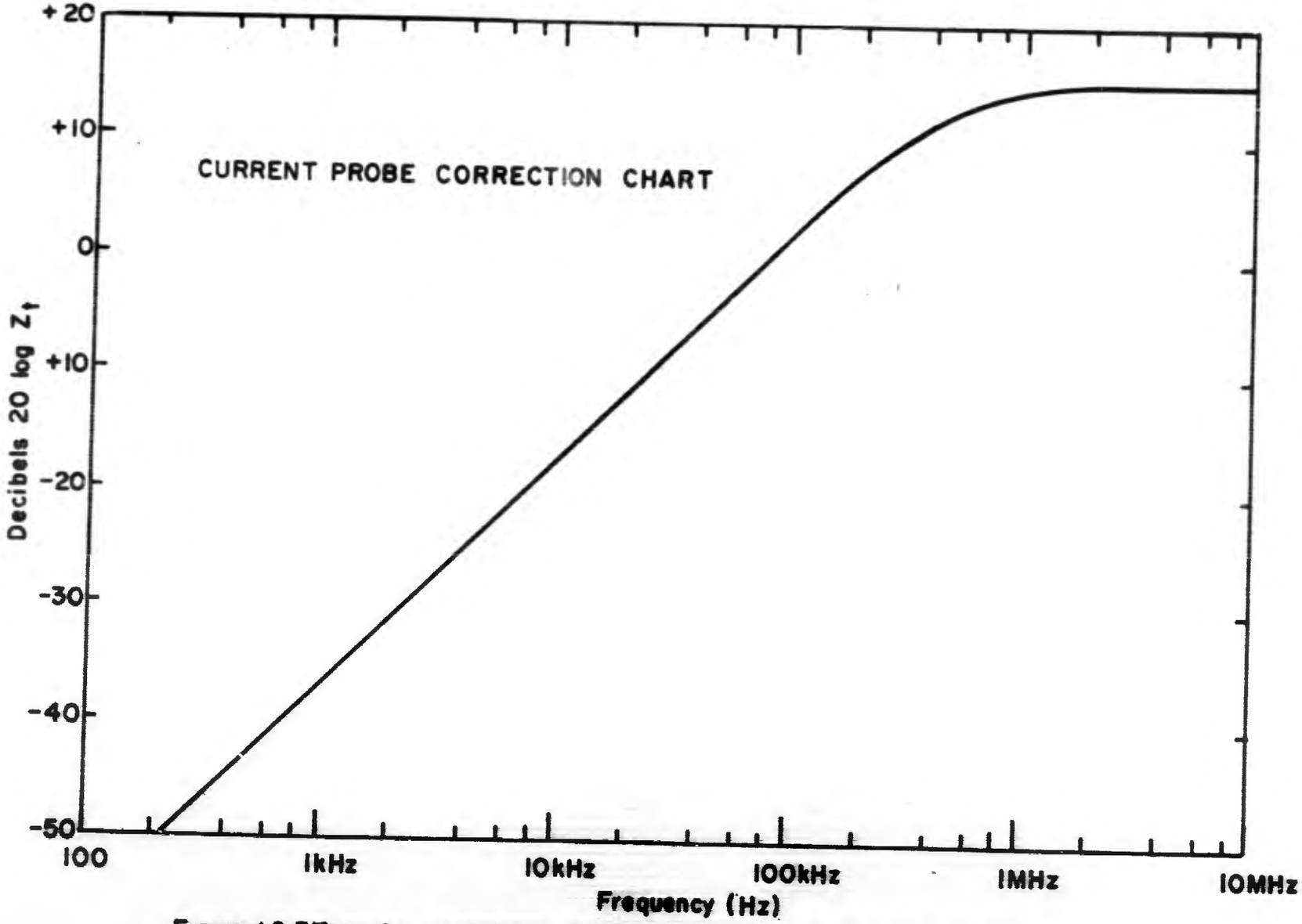

Figure A2-7 Transfer Impedance Referenced to One Ohm vs. Frequency

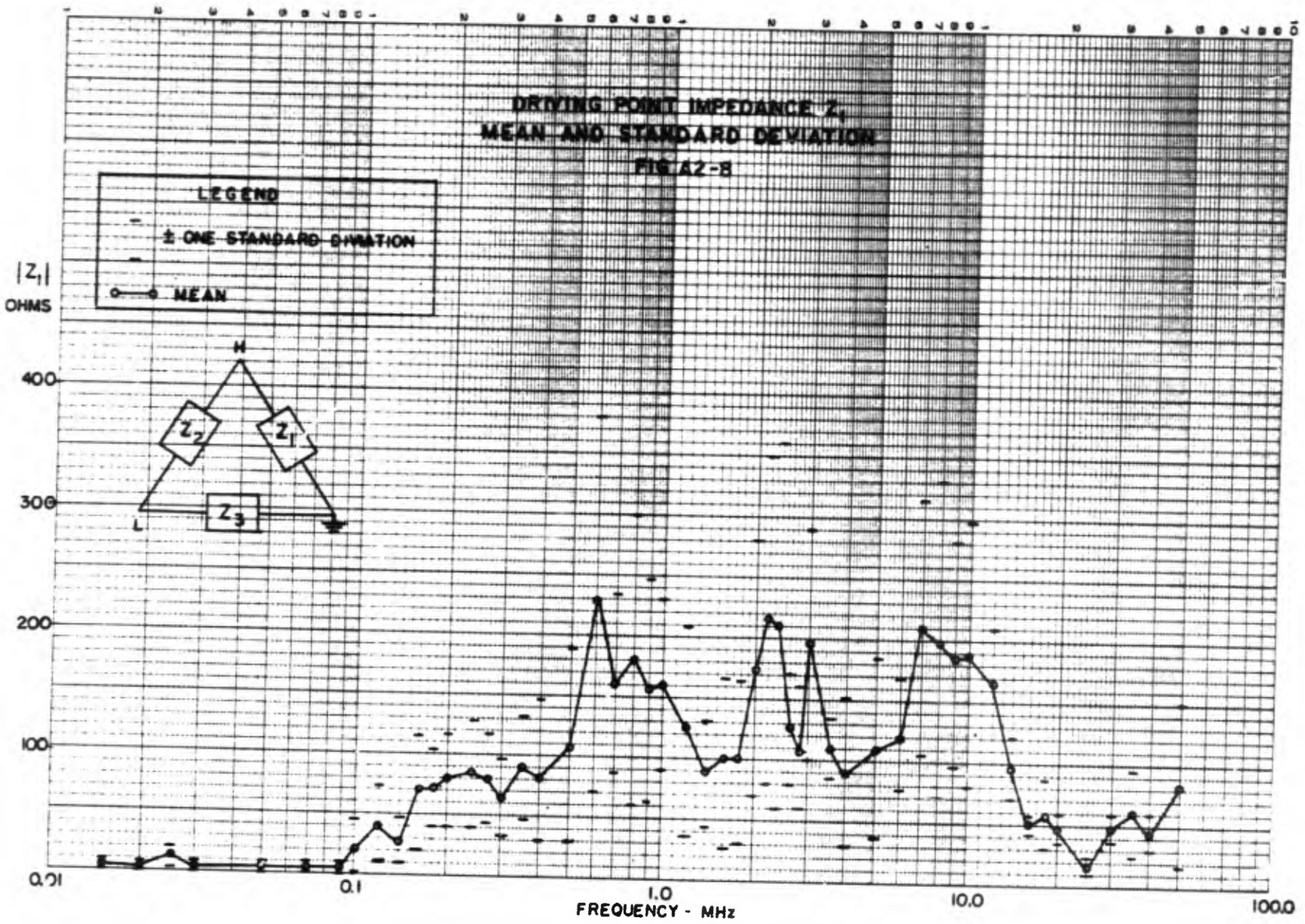
DRIVING POINT IMPEDANCE Z_1
MEAN AND STANDARD DEVIATION
FIG A2-8
LEGEND
± ONE STANDARD DEVIATION
MEAN
$|Z_1|$
OHMS
400
300
200
100
H
L
Z_2
Z_1
Z_3
0.01
0.1
1.0
10.0
100.0
FREQUENCY - MHz

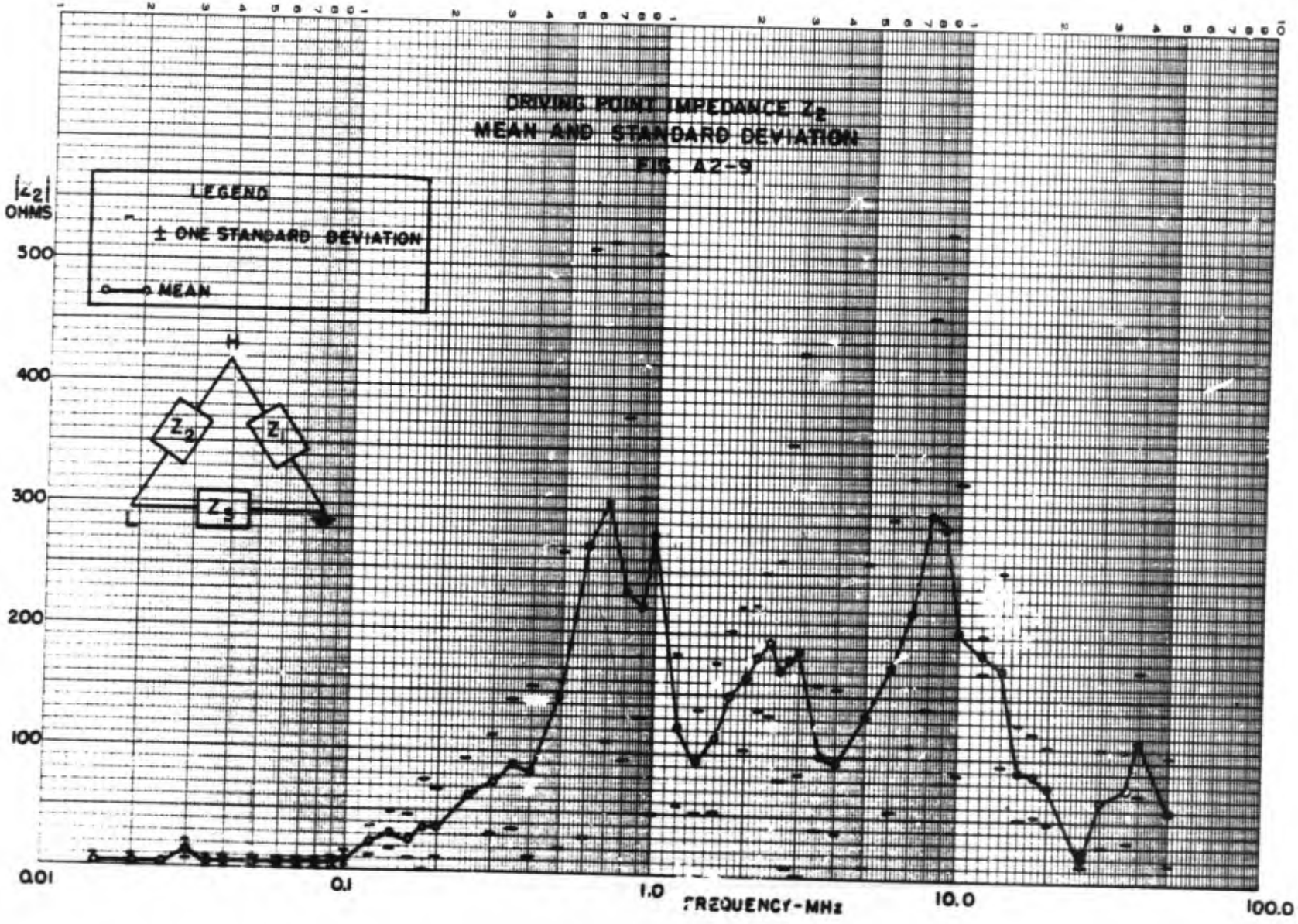
DRIVING POINT IMPEDANCE Z_2
MEAN AND STANDARD DEVIATION
FIG. A2-9
LEGEND
± ONE STANDARD DEVIATION
MEAN
$|Z_2|$ OHMS
500
400
300
200
100
0.01
0.1
1.0
10.0
100.0
FREQUENCY-MHz
H
L
Z_2
Z_1
Z_3

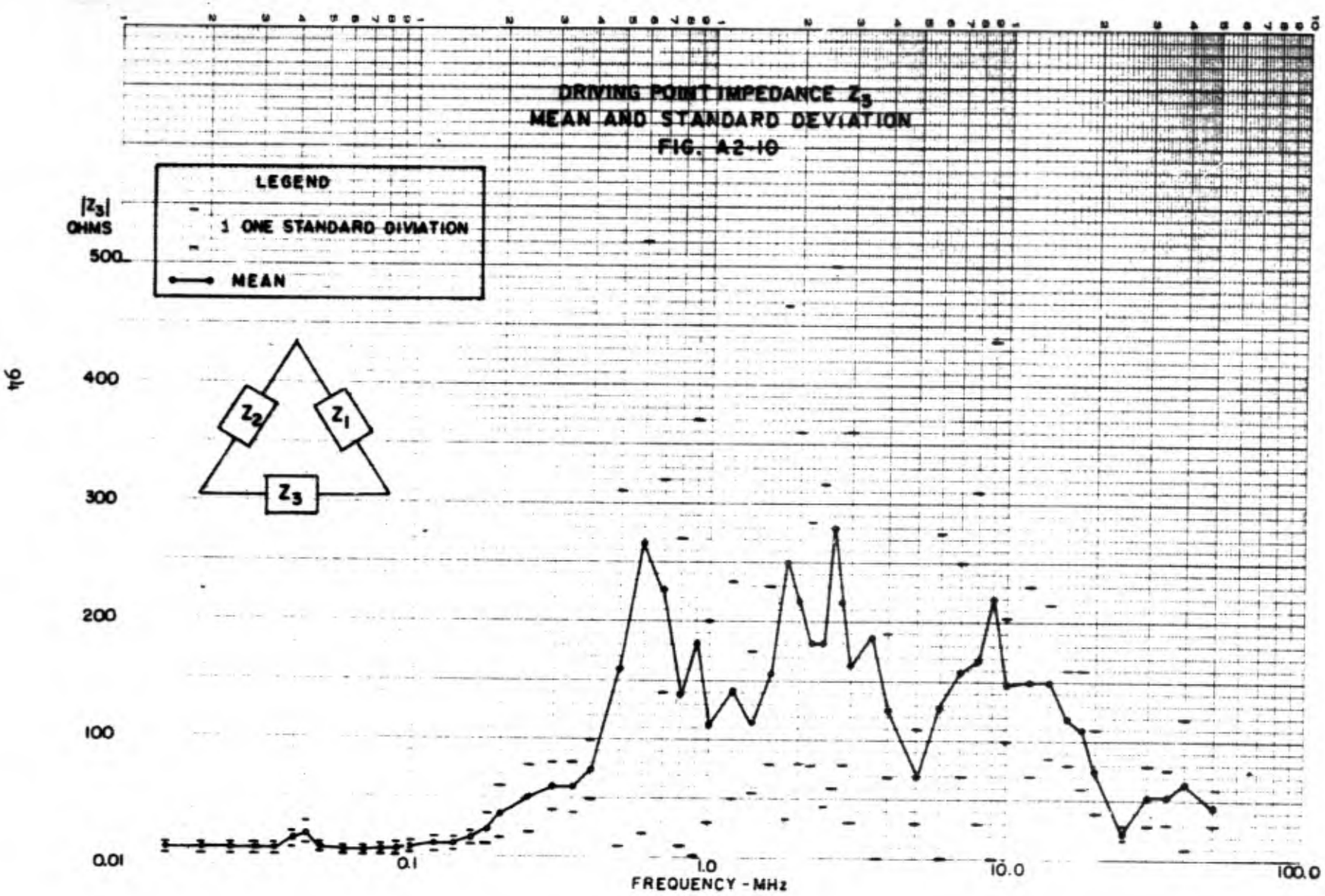
DRIVING POINT IMPEDANCE Z_3
MEAN AND STANDARD DEVIATION
FIG. A2-10
LEGEND
1 ONE STANDARD DIVIATION
MEAN
$|Z_3|$ OHMS
500
400
300
200
100
0.01
0.1
1.0
10.0
100.0
FREQUENCY - MHz
Z_2
Z_1
Z_3

APPENDIX 3

EQUIPMENT IMPEDANCE MEASUREMENTS

A.3.1 Introduction

It is the purpose of this section to report measurement procedures and preliminary data on test sample power line input impedance which is needed to complement the analysis of section 4. Although a large sample size of input impedance data is required in order to obtain reasonable statistical estimates, the data reported here on 5 pieces of equipment may provide a crude estimate on some of the statistical paramcters.

A.3.2 General Considerations

As has been previously reported [1], the input impedance, at the power line terminals of a piece of equipment, can be represented by a generalized circuit configuration such as depicted in Fig. A.3.1, in which Z_{12} is the impedance across the power lines 1 and 2, and Z_{10}, Z_{20} are the impedances from line to ground. Thus, in order to completely characterize the input impedance all three impedances must be measured.

Since the impedance measurements may be made in conjunction with conducted emission and susceptibility tests, it is desirable to use the same test setup and equipment wherever possible. Thus the test setup used is shown in Fig. A.3.2. In order to insure a 3-terminal situation the ground lead of the power line is bonded to the ground plane and the power leads are placed a fixed distance apart and above the ground plane. In addition, the test sample chassis is bonded to the ground plane. About 75 cm distance from the equipment terminals, 10 μF bypass capacitors are placed in order to isolate the power line impedance from the test sample impedance. The injector and receptor probes of the impedance bridge (Solar Mod. 6362-2) are connected into the line as shown in Fig. A.3.2.

Measured values of shunt impedance [2] of the bypass capacitors and preliminary data on power line impedances [3] indicates that the bypass capacitors effectively isolate the measured impedance from the

---

1. "EMC Data Collection Techniques, Report No. 1, Test Method CE," Dec. 1968, University of Pennsylvania.
2. "The Performance of 10 μF Power Line Feedthrough Capacitors," by D. E. Groff, Technical Report, Moore School Report 69-19, Univ. of Pa., February 1969.
3. Ibid, Section VII.

power line impedance in the frequency range of measurement (i.e., 100 kHz-30 MHz). In addition, the shunt impedance of the capacitors, in the above specified frequency range, is less than one ohm and will be assumed to be small in comparison to the impedance levels of the remainder of the circuit.* Thus a simplified diagram of the impedance network can be that depicted in Fig. A.3.3.

The Solar bridge is used to measure the driving point impedances at the locations indicated in Fig. A.3.3. The impedances which are measured, are the following loop impedances.

$$Z_{\ell_1} \approx \frac{Z_{12}\, Z_{10}}{Z_{12} + Z_{10}}$$

$$Z_{\ell_2} \simeq \frac{Z_{12}\, Z_{20}}{Z_{12} + Z_{20}}$$

$$Z_{\ell_3} \simeq \frac{Z_{10}\, Z_{20}}{Z_{10} + Z_{20}}$$

With the above three measured values, the test sample impedances Z_{10}, Z_{20}, and Z_{12} can be computed.

It should be noted that the impedances Z_{10}, Z_{12}, Z_{20} include the impedance of the power line lead inductance.

A.3.3 Experimental Procedure and Data

All equipments (test samples, impedance bridge and RIFI meter) were placed on a ground plane located in a shielded enclosure. A block diagram of the experimental setup is given in Fig. A.3.4. Details of the connection of power lines and grounding are given in Fig. A.3.2. In order to measure, for example, the impedance Z_{ℓ_1} as seen from line 1, the probe was clamped around line 1, the signal generator set to the desired frequency and the bridge was tuned for a null on the RIFI meter. The impedance magnitude and phase of the impedance Z_{ℓ_1}

* Measurements have shown the 10 μF capacitors resonant with the line (between capacitor and equipment) inductance at a frequency of about 50 kHz).

is read directly off the dials of the bridge. The same procedure is used to obtain Z_{ℓ_1}. However, Z_{ℓ_3} is the impedance measured in the ground return and hence it is impossible to place the probe around it. Under the assumption that only unbalanced current exists in the ground plane and the two power lines, the impedance as measured with the probe clamped around both wires, is equivalent to the impedance measured if the probe were clamped around the ground return current.

Data were obtained for the following pieces of equipment:

1)	BC-343-N	HF receiver
2)	R-278B/GR	UHF receiver (200-400 MHz)
3)	KWM-2A	single sideband transceiver HF
4)	TPS1-D	L-band radar set*
5)	R 390A/URR	HF receiver
6)	BC-348R	HF receiver
7)	T-217A/GR	UHF transmitter

The resistive and reactive parts of the measured impedances Z_{ℓ_1}, Z_{ℓ_2}, Z_{ℓ_3} are plotted in Figs. A.3.5 - A.3.10.

A.3.4 Discussion of Results

The data for the resistive part of the measured impedances show considerable difference between test samples for frequencies below 10 MHz. However, in all cases the resistive impedance has a value which rarely exceeds 100 ohms in the frequency band 1-20 MHz.

The reactive part of the impedance shows a trend of increasing inductance for frequencies above 8 MHz. The values of inductive reactance above this frequency compare favorably with the computed reactive impedance of the power line lead inductance of approximately 1 μH. It is expected that reactances, measured in lines 1 and 2, should show smaller levels of inductive reactance as the frequency is decreased. This is borne out by Figs. A.3.8 and 9, with the exception of data for BC-342-N, and BC-348-R. The data for KWM-2A appear to be anomalous in the frequency range; further checks should be made on the measurements before any conclusions are made. The increasing capacitive reactance of BC-342-N and BC-348-R for decreasing frequencies may be indicative of an open circuit in the power line.

---

* The radar set is powered by a 400 Hz motor generator set.

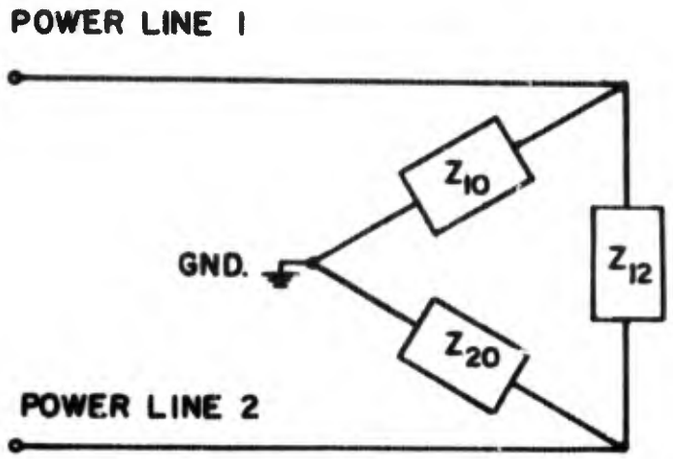

Figure A, 3.1 Power line Input Impedance of an Emission Source.

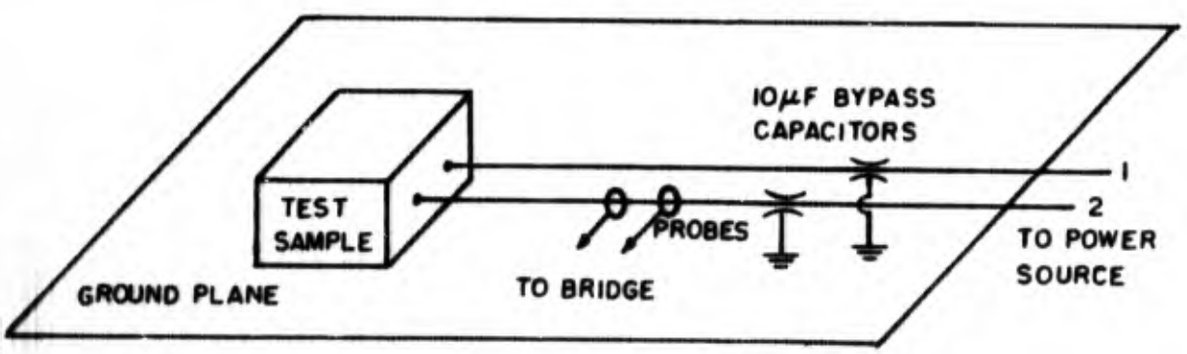

Figure A.3.2 Test Setup

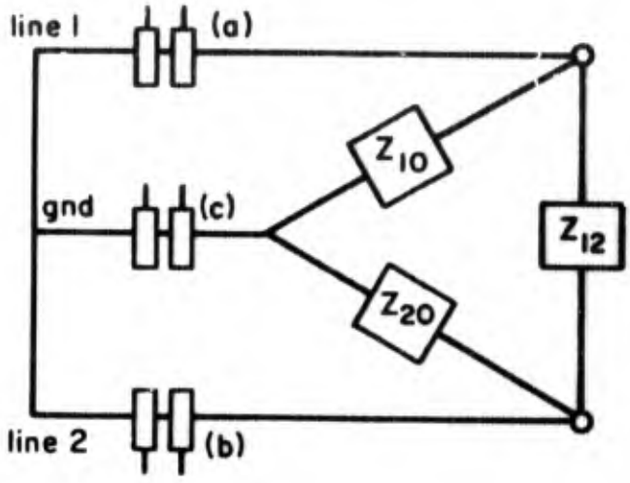

Figure A·3·3 Impedance Probe Locations

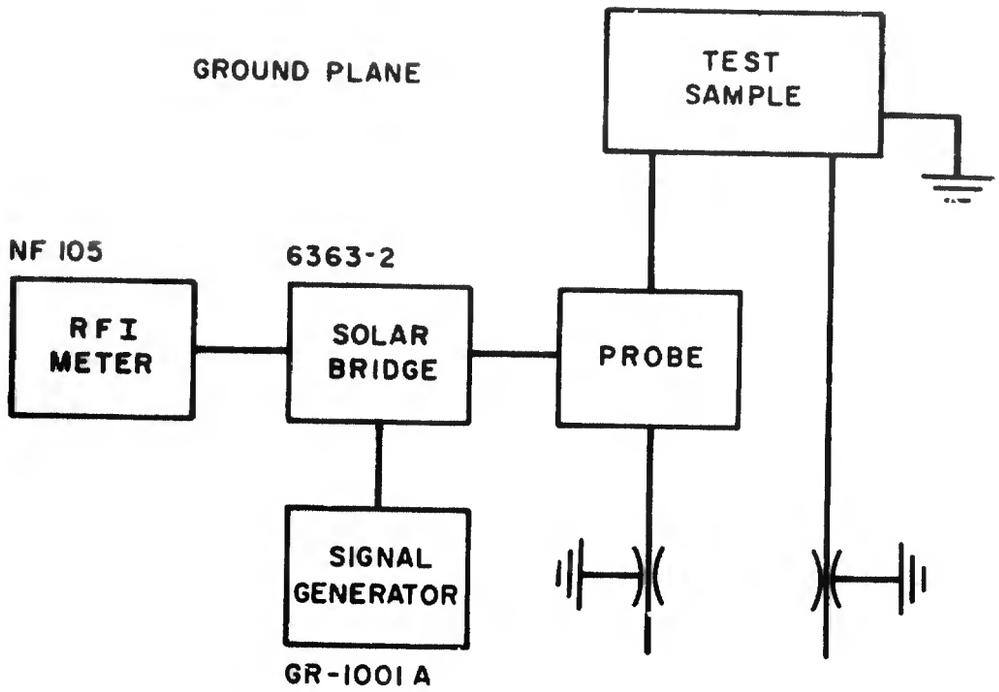

Figure A·3·4 Block Diagram of Test Setup

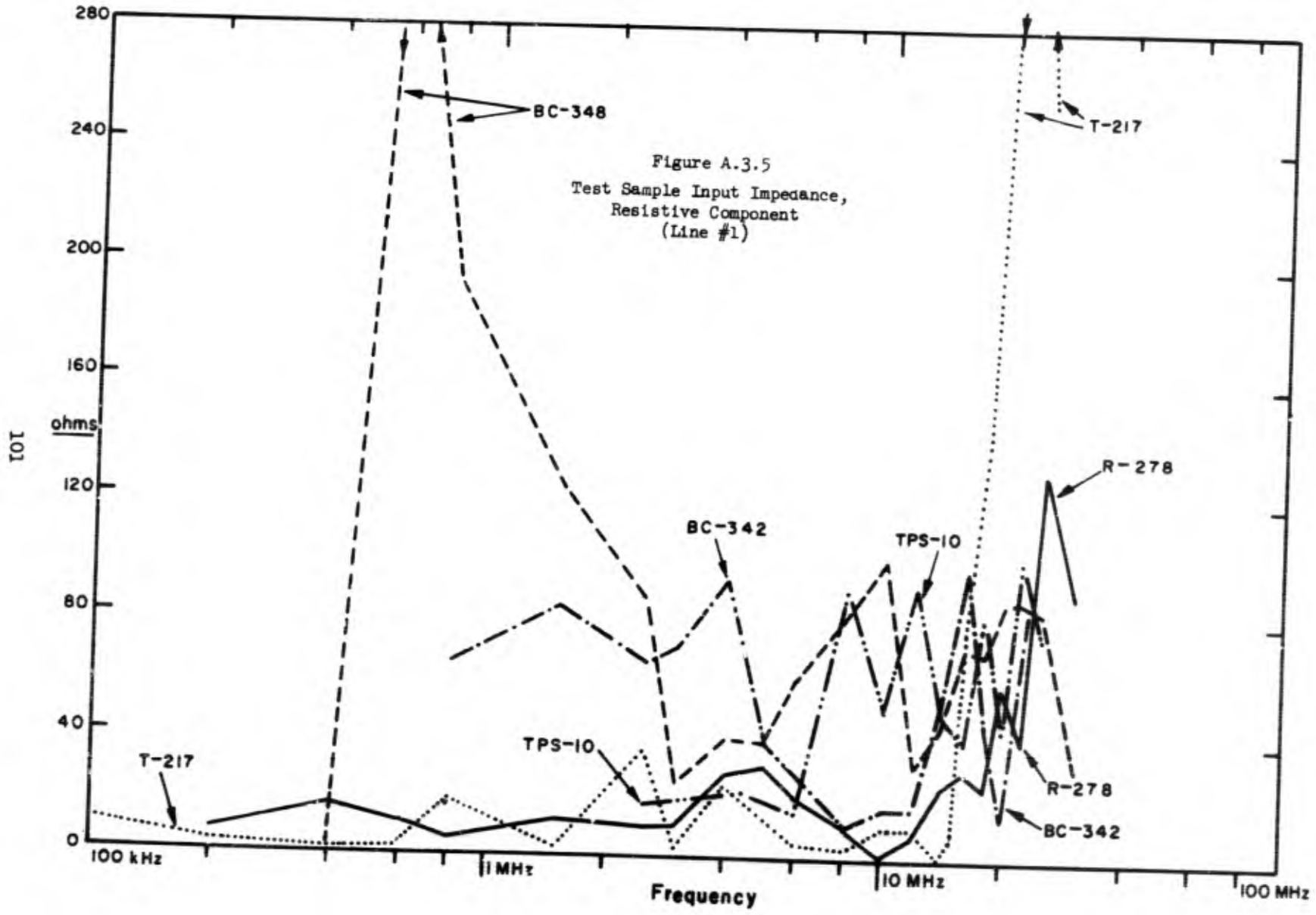

Figure A.3.5
Test Sample Input Impedance,
Resistive Component
(Line #1)

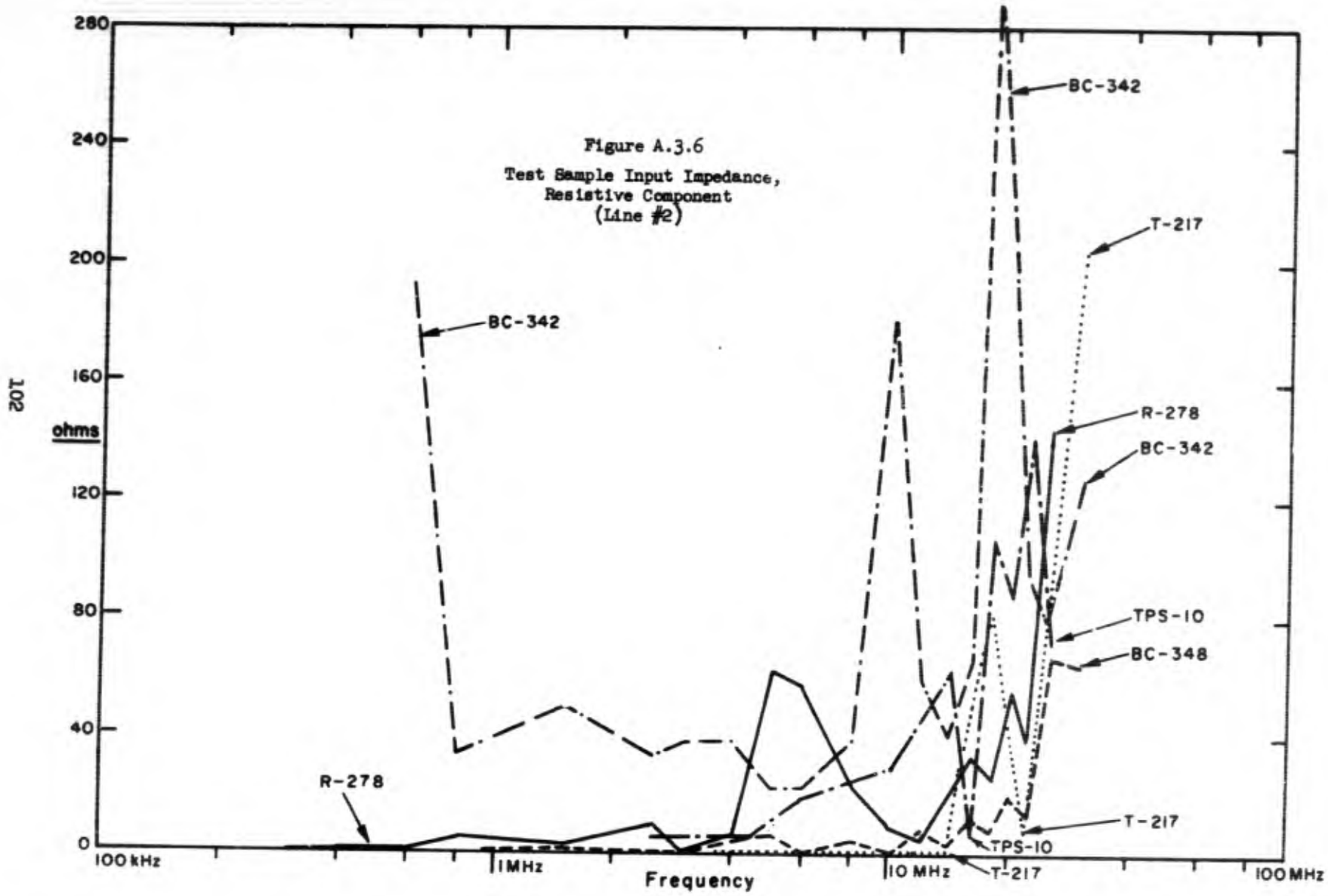

Figure A.3.6

Test Sample Input Impedance,
Resistive Component
(Line #2)

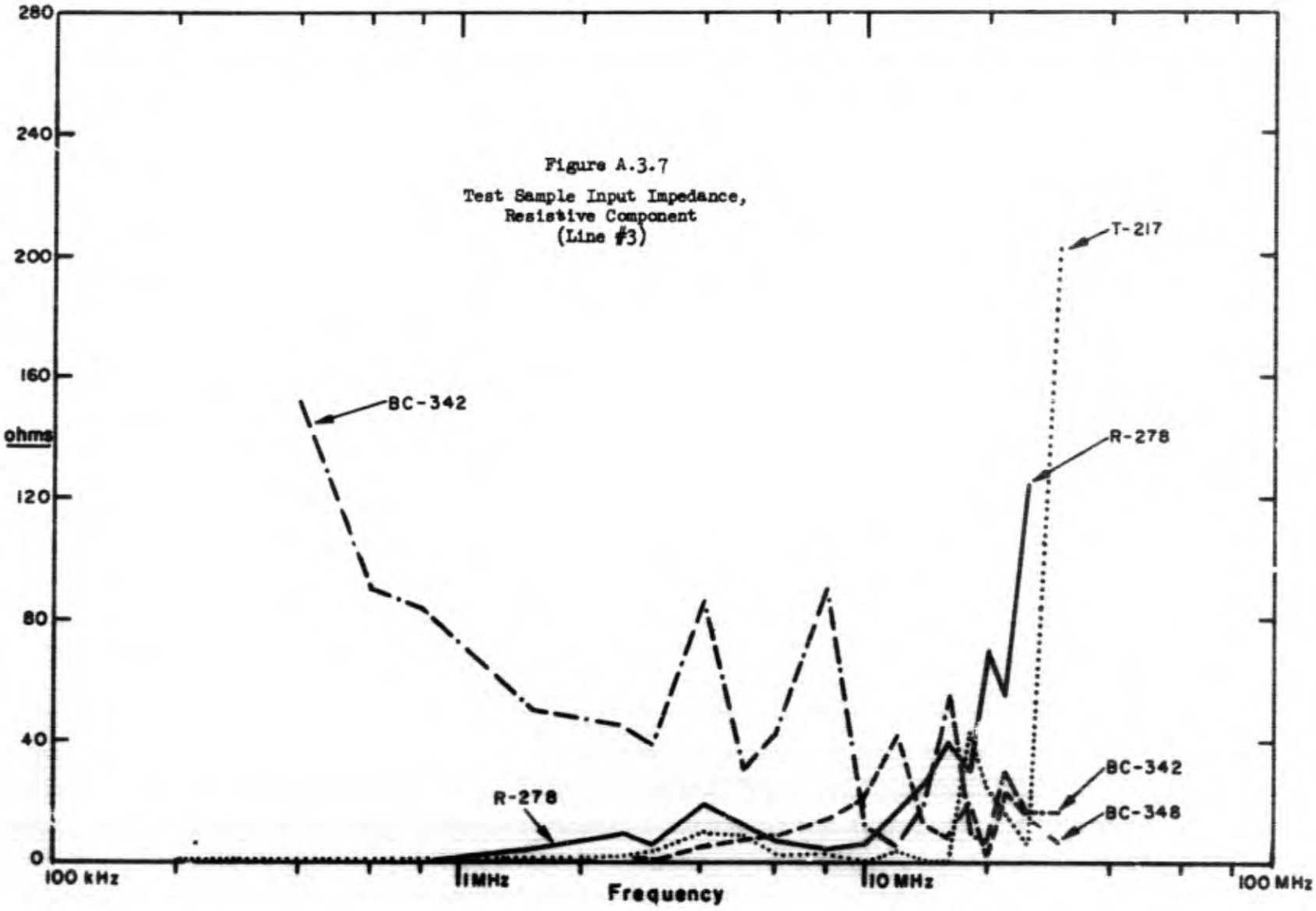

Figure A.3.7

Test Sample Input Impedance,
Resistive Component
(Line #3)

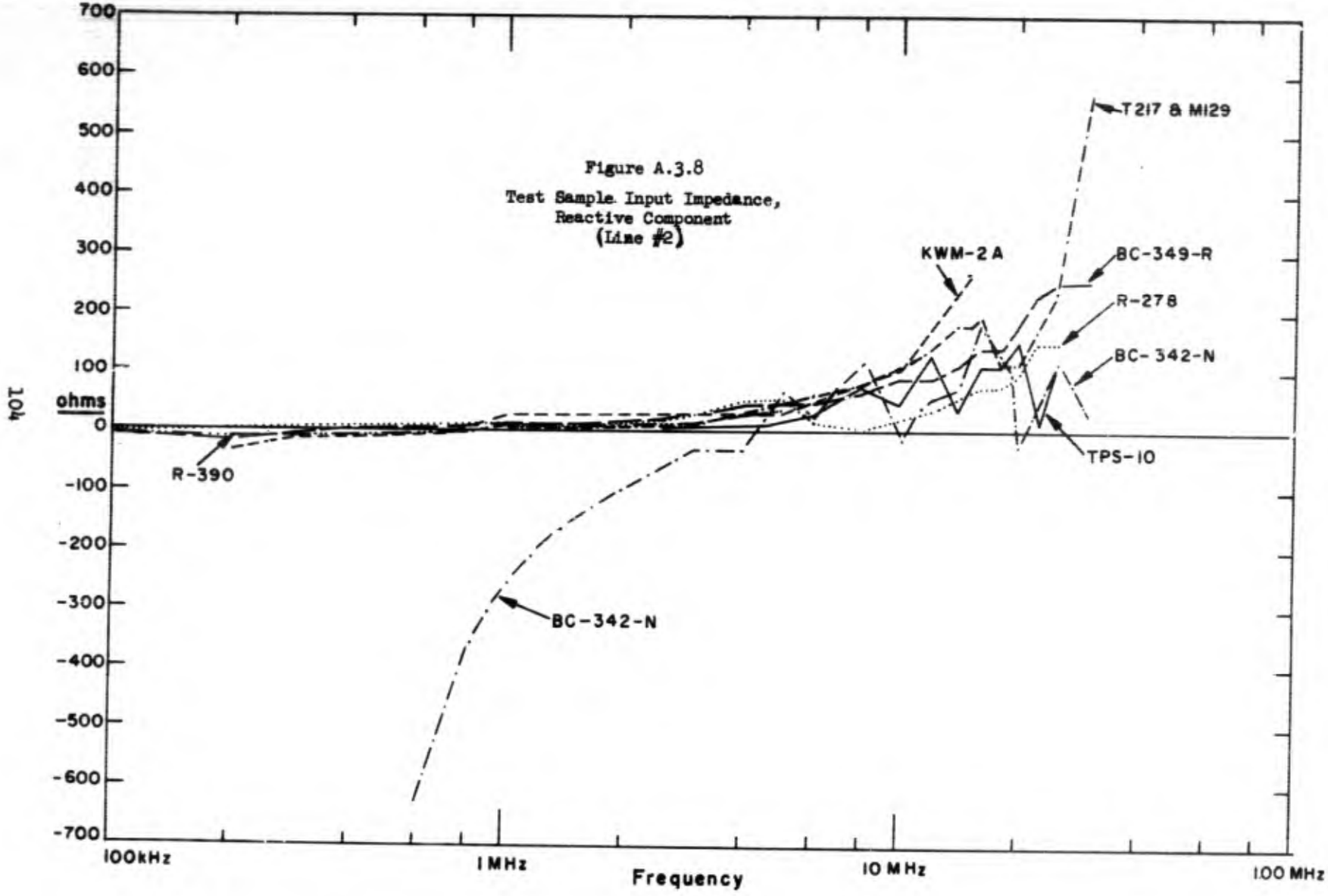

Figure A.3.8

Test Sample Input Impedance,
Reactive Component
(Line #2)

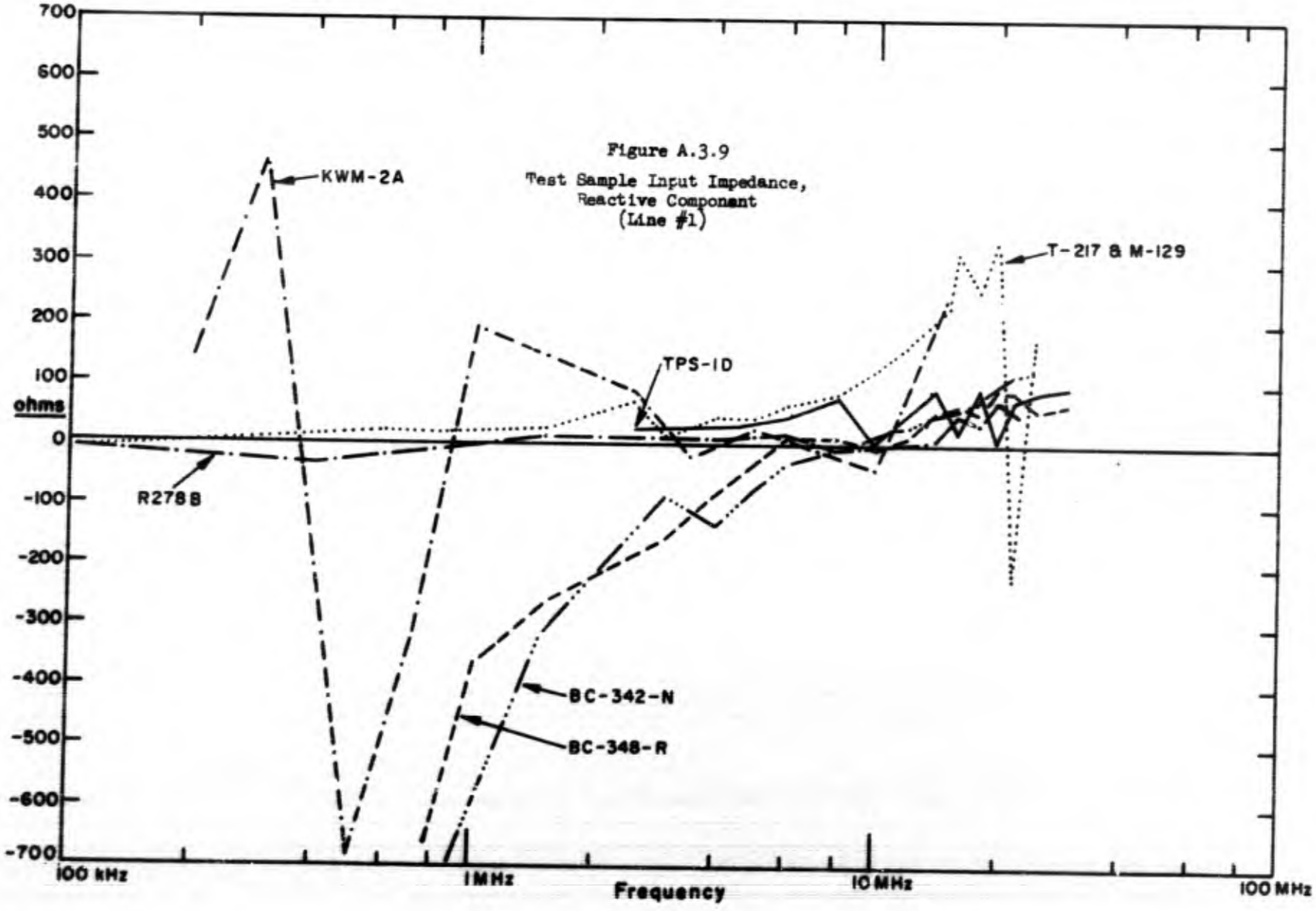

Figure A.3.9
Test Sample Input Impedance,
Reactive Component
(Line #1)

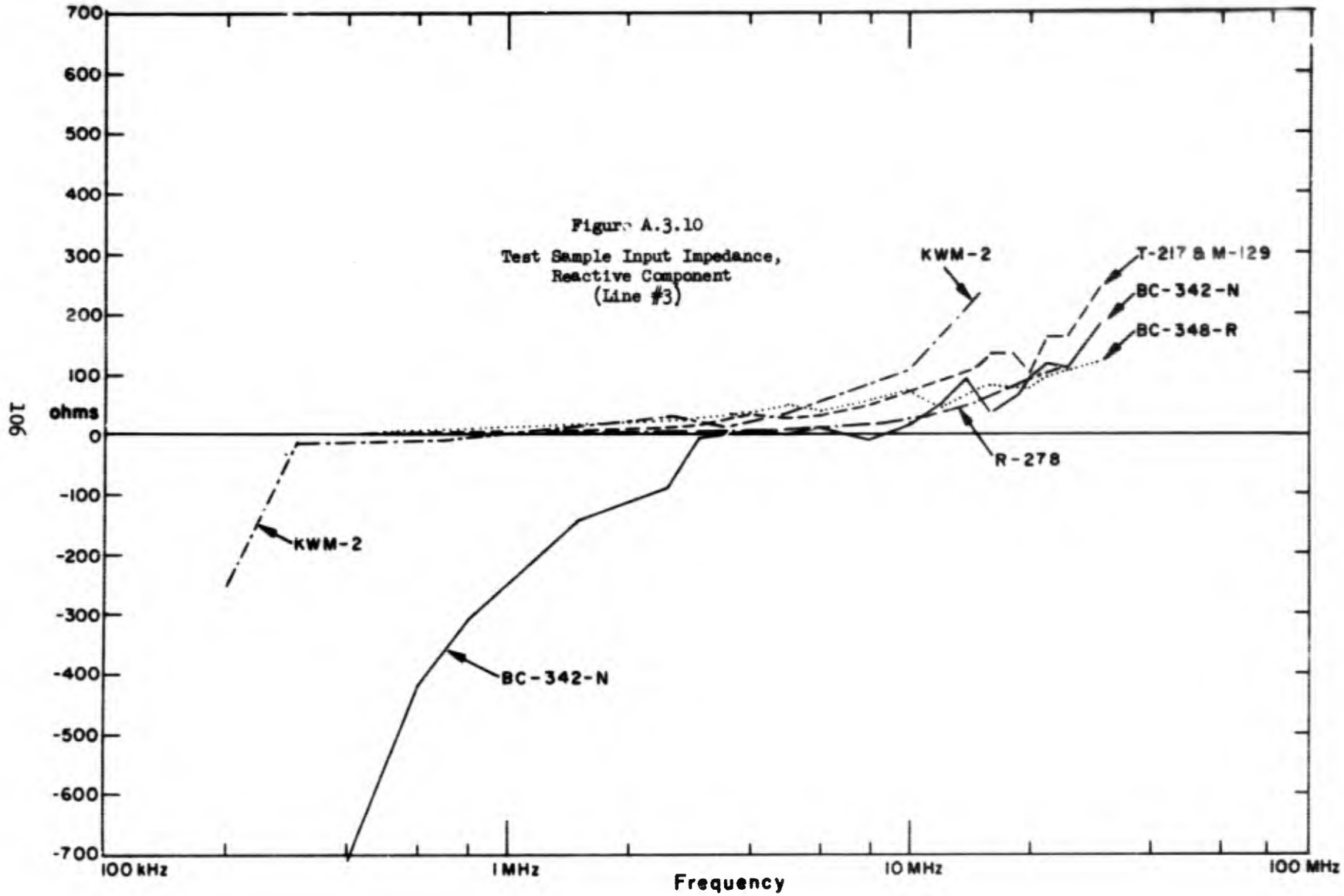

Figure A.3.10

Test Sample Input Impedance,
Reactive Component
(Line #3)

APPENDIX 4

MINIMIZATION AND COMPUTATION OF VARIANCES OF ACTUAL CURRENT AND VOLTAGE

A.4.1 Introduction

In this section are presented the details of some computations whose results are used in the sections on emission and susceptibility limits.

In particular, expressions are derived for the variances of the actual line current and voltage produced by an interference source, which are then minimized with respect to Z_M, and their values are computed for different values of Z_M.

A.4.2 Expressions for the Variances

Recalling eqs. 3.3.3 and 3.3.5 of Section 3.3, the actual line current and voltage, I_T and V_T, are given respectively by

$$I_T = I_M \left| \frac{Z_S + Z_M}{Z_S + Z_T} \right| = I_M A_M \qquad (A.4.1)$$

$$V_T = I_M \left| Z_T \right| \left| \frac{Z_S + Z_M}{Z_S + Z_T} \right| = I_M \left| Z_T \right| A_M = I_M C_M \qquad (A.4.2)$$

where I_M = magnitude of current measured from source when terminated by Z_M

Z_S = impedance of source

Z_T = actual terminating impedance of source

$$A_M = \left| \frac{Z_S + Z_M}{Z_S + Z_T} \right| \qquad (A.4.3)$$

$$C_M = \left| Z_T \right| \left| \frac{Z_S + Z_M}{Z_S + Z_T} \right| = \left| Z_T \right| A_M \qquad (A.4.4)$$

Assuming I_M and Z_M are known quantities, we seek to find the variances of I_T and V_T about the fixed mean values $\bar{I}_T$ and $\bar{V}_T$ respectively. These variances may be written

$$\mathrm{Var}(I_T) = \bar{I}_T^{\,2}\ \mathrm{Var}\left(\frac{I_T}{\bar{I}_T}\right) \tag{A.4.5}$$

$$\mathrm{Var}(V_T) = \bar{V}_T^{\,2}\ \mathrm{Var}\left(\frac{V_T}{\bar{V}_T}\right) \tag{A.4.6}$$

Now,

$$\frac{I_T}{\bar{I}_T} = \frac{I_M A_M}{\overline{I_M A_M}}\ ; \quad \frac{V_T}{\bar{V}_T} = \frac{I_M C_M}{\overline{I_M C_M}}$$

Since I_M is assumed known,

$$\overline{I_M A_M} = I_M \bar{A}_M$$

and

$$\overline{I_M C_M} = I_M \bar{C}_M$$

so that

$$\frac{I_T}{\bar{I}_T} = \frac{A_M}{\bar{A}_M} \equiv A$$

$$\frac{V_T}{\bar{V}_T} = \frac{C_M}{\bar{C}_M} \equiv C$$

and

$$\mathrm{Var}(I_T) = \bar{I}_T^{\,2}\ \mathrm{Var}(A) \tag{A.4.7}$$

$$\mathrm{Var}(V_T) = \bar{V}_T^{\,2}\ \mathrm{Var}(C) \tag{A.4.8}$$

Thus, the variances of concern are the normalized variances Var(A) and Var(C). Once these have been calculated, the variance about any mean value may be calculated from (A.4.7) and (A.4.8).

A.4.3 Expressions for the Normalized Variances Using Linear Approximation

Since $A \equiv \frac{A_M}{\bar{A}_M}$ and $C \equiv \frac{C_M}{\bar{C}_M}$,

we have

$$\mathrm{Var}(A) = \frac{1}{\bar{A}_M^2}\,\mathrm{Var}(A_M) \tag{A.4.9}$$

$$\mathrm{Var}(C) = \frac{1}{\bar{C}_M^2}\,\mathrm{Var}(C_M) \tag{A.4.10}$$

By eqs. A.4.3 and A.4.4,

$$A_M = \left|\frac{Z_S + Z_M}{Z_S + Z_T}\right| = \sqrt{\frac{(R_S + R_M)^2 + (X_S + X_M)^2}{(R_S + R_T)^2 + (X_S + X_T)^2}} \tag{A.4.11}$$

$$C_M = \left|Z_T\right| A_M = \sqrt{R_T^2 + X_T^2}\,\sqrt{\frac{(R_S + R_M)^2 + (X_S + X_M)^2}{(R_S + R_T)^2 + (X_S + X_T)^2}} \tag{A.4.12}$$

where $Z_S = R_S + jX_S$

$Z_T = R_T + jX_T$

$Z_M = R_M + jX_M$.

R_S, X_S, R_T, and X_T are random variables. Finding the variance of A_M and C_M in general is thus quite difficult. We, therefore, approximate A_M and C_M by assuming they vary linearly with these variables about their mean values:

$$A_M - \bar{A}_M = \Delta A_M \approx \left.\frac{\partial A_M}{\partial R_S}\right|_{\bar{A}_M} \cdot \Delta R_S + \left.\frac{\partial A_M}{\partial X_S}\right|_{\bar{A}_M} \cdot \Delta X_S$$

$$+ \left.\frac{\partial A_M}{\partial R_T}\right|_{\bar{A}_M} \cdot \Delta R_T + \left.\frac{\partial A_M}{\partial X_T}\right|_{\bar{A}_M} \cdot \Delta X_T \qquad \text{(A.4.13)}$$

$$C_M - \bar{C}_M = \Delta C_M \approx \left.\frac{\partial C_M}{\partial R_S}\right|_{\bar{C}_M} \cdot \Delta R_S + \left.\frac{\partial A_M}{\partial X_S}\right|_{\bar{C}_M} \cdot \Delta X_S$$

$$+ \left.\frac{\partial C_M}{\partial R_T}\right|_{\bar{C}_M} \cdot \Delta R_T + \left.\frac{\partial C_M}{\partial X_T}\right|_{\bar{C}_M} \cdot \Delta X_T \qquad \text{(A.4.14)}$$

where

$$\left.\frac{\partial A_M}{\partial R_S}\right|_{\bar{A}_M} \equiv \left.\frac{\partial A_M}{\partial R_S}\right|_{\substack{R_S = \bar{R}_S,\ R_T = \bar{R}_T \quad \text{, etc.,} \\ X_S = \bar{X}_S,\ X_T = \bar{X}_T}}$$

$$\Delta R_S = R_S - \bar{R}_S \text{ , etc.,}$$

and

$\bar{R}_S$ = mean value of R_S, etc.

Then, we have

$$\mathrm{Var}(A_M) = (\overline{\Delta A}_M)^2 = \left(\frac{\partial A_M}{\partial R_S}\right)^2_{\bar{A}_M} \sigma_{R_S}^2 + \left(\frac{\partial A_M}{\partial X_S}\right)^2_{\bar{A}_M} \sigma_{X_S}^2$$

$$+ \left(\frac{\partial A_M}{\partial R_T}\right)^2_{\bar{A}_M} \sigma_{R_T}^2 + \left(\frac{\partial A_M}{\partial X_T}\right)^2_{\bar{A}_M} \sigma_{X_T}^2 \qquad \text{(A.4.15)}$$

$$\mathrm{Var}(C_M) = (\overline{\Delta C}_M)^2 = \left(\frac{\partial C_M}{\partial R_S}\right)^2_{\bar{C}_M} \sigma_{R_S}^2 + \left(\frac{\partial C_M}{\partial X_S}\right)^2_{\bar{C}_M} \sigma_{X_S}^2$$

$$+ \left(\frac{\partial C_M}{\partial R_T}\right)^2_{\bar{C}_M} \sigma_{R_T}^2 + \left(\frac{\partial C_M}{\partial X_T}\right)^2_{\bar{C}_M} \sigma_{X_T}^2 \qquad \text{(A.4.16)}$$

where $\sigma_{R_S}^2 = \mathrm{Var}(R_S)$, etc., assuming independence of R_S, X_S, R_T, and X_T.

Since

$$C_M = |Z_T| A_M \ ,$$

then

$$\left.\frac{\partial C_M}{\partial R_S}\right|_{\bar{C}_M} = \bar{A}_M \left.\frac{\partial |Z_T|}{\partial R_S}\right|_{\bar{C}_M} + |\bar{Z}_T| \left.\frac{\partial A_M}{\partial R_S}\right|_{\bar{C}_M}$$

$$\vdots$$

$$\left.\frac{\partial C_M}{\partial X_T}\right|_{\bar{C}_M} = \bar{A}_M \left.\frac{\partial |Z_T|}{\partial X_T}\right|_{\bar{C}_M} + |\bar{Z}_T| \left.\frac{\partial A_M}{\partial X_T}\right|_{\bar{C}_M}$$

Now,

$$\frac{\partial |Z_T|}{\partial R_S} = \frac{\partial |Z_T|}{\partial X_S} = 0$$

so that

$$\mathrm{Var}(C_M) = |\bar{Z}_T|^2 \left[\left(\frac{\partial A_M}{\partial R_S} \right)^2_{\bar{C}_M} \sigma_{R_S}^2 + \ldots + \left(\frac{\partial A_M}{\partial X_T} \right)^2_{\bar{C}_M} \sigma_{X_T}^2 \right]$$

$$+ \frac{\bar{A}_M^2}{|\bar{Z}_T|^2} \left[\bar{R}_T^2 \sigma_{R_T}^2 + \bar{X}_T^2 \sigma_{X_T}^2 \right]$$

$$= |\bar{Z}_T|^2 \mathrm{Var}(A_M) + \frac{\bar{A}_M^2}{|\bar{Z}_T|^2} \left[\bar{R}_T^2 \sigma_{R_T}^2 + \bar{X}_T^2 \sigma_{X_T}^2 \right] \quad \text{(A.4.17)}$$

where we have used the relationship

$$|Z_T| = \sqrt{R_T^2 + X_T^2} \quad .$$

Equation A.4.17 tells us that $\mathrm{Var}(C_M)$ can be computed once $\mathrm{Var}(A_M)$ is known, and need not be computed independently.

From eqs. A.4.9 and A.4.10, we find the normalized variances:

$$\mathrm{Var}(A) = \frac{1}{\bar{A}_M^2} \mathrm{Var}(A_M) = \left(\frac{1}{\bar{A}_M} \frac{\partial A_M}{\partial R_S} \right)^2_{\bar{A}_M} \sigma_{R_S}^2 + \ldots + \left(\frac{1}{\bar{A}_M} \frac{\partial A_M}{\partial X_T} \right)^2_{\bar{A}_M} \sigma_{X_T}^2 \quad \text{(A.4.18)}$$

$$\mathrm{Var}(C) = \frac{1}{\bar{C}_M^2} \mathrm{Var}(C_M) = \frac{1}{(|\bar{Z}_T| \bar{A}_M)^2} \mathrm{Var}(C_M)$$

$$= \frac{1}{\bar{A}_M^2} \mathrm{Var}(A_M) + \frac{1}{|\bar{Z}_T|^4} \left[\bar{R}_T^2 \sigma_{R_T}^2 + \bar{X}_T^2 \sigma_{X_T}^2 \right]$$

$$= \mathrm{Var}(A) + \frac{1}{|\bar{Z}_T|^4} \left[\bar{R}_T^2 \sigma_{R_T}^2 + \bar{X}_T^2 \sigma_{X_T}^2 \right] \quad \text{(A.4.19)}$$

The second term on the right of A.4.19 is independent of Z_M. Consequently, the value of Z_M which minimizes Var(A) will also minimize Var(C).

By assumption, the mean value of A_M is given by

$$\bar{A}_M = \left| \frac{\bar{Z}_S + Z_M}{\bar{Z}_S + \bar{Z}_T} \right| = \sqrt{\frac{(\bar{R}_S + R_M)^2 + (\bar{X}_S + X_M)^2}{(\bar{R}_S + \bar{R}_T)^2 + (\bar{X}_S + \bar{X}_T)^2}} \tag{A.4.20}$$

We now compute the partial derivatives called for in A.4.18 and multiply them by $1/\bar{A}_M$ as given by A.4.20. The results are

$$\frac{1}{\bar{A}_M} \frac{\partial A_M}{\partial R_S}\bigg|_{\bar{A}_M} = \left[\frac{(\bar{R}_S + R_M)[(\bar{R}_T - R_M)(\bar{R}_S + \bar{R}_T) + (\bar{X}_S + \bar{X}_T)^2] - (\bar{X}_S + X_M)^2(\bar{R}_S + \bar{R}_T)}{|\bar{Z}_S + Z_M|^2 \cdot |\bar{Z}_S + \bar{Z}_T|^2} \right] \tag{A.4.21}$$

$$\frac{1}{\bar{A}_M} \frac{\partial A_M}{\partial X_S}\bigg|_{\bar{A}_M} = \left[\frac{(\bar{X}_S + X_M)[(\bar{X}_T - X_M)(\bar{X}_S + \bar{X}_T) + (\bar{R}_S + \bar{R}_T)^2] - (\bar{R}_S + R_M)^2(\bar{X}_S + \bar{X}_T)}{|\bar{Z}_S + Z_M|^2 \cdot |\bar{Z}_S + \bar{Z}_T|^2} \right] \tag{A.4.22}$$

$$\frac{1}{\bar{A}_M} \frac{\partial A_M}{\partial R_T}\bigg|_{\bar{A}_M} = - \frac{\bar{R}_S + \bar{R}_T}{|\bar{Z}_S + \bar{Z}_T|^2} \tag{A.4.23}$$

$$\frac{1}{\bar{A}_M} \frac{\partial A_M}{\partial X_T}\bigg|_{\bar{A}_M} = - \frac{\bar{X}_S + \bar{X}_T}{|\bar{Z}_S + \bar{Z}_T|^2} \tag{A.4.24}$$

Substituting eqs. A.4.21 thru A.4.24 into A.4.18, we obtain the expression for Var(A). Var(C) is then found from A.4.19.

A.4.4 Value of Z_M Minimizing the Normalized Variances

The value of Z_M minimizing Var(A) can be determined by inspection of eqs. A.4.21 thru A.4.24. These quantities are squared, multiplied by positive quantities, and added to obtain Var(A) by eq. A.4.18. The last two terms of A.4.18 are independent of Z_M (see A.4.23 and A.4.24). Thus, if there were a value of Z_M that could make the first two terms zero simultaneously, this would result in the minimum value of Var(A), since these terms, being squares of real quantities, cannot be negative

By inspection of eqs. A.4.21 and A.4.22, there is such a value of Z_M. It is given by

$$\left.\begin{aligned} R_M &= \overline{R}_T \\ X_M &= \overline{X}_T \end{aligned}\right\} \qquad \text{(A.4.25)}$$

or

$$Z_M = \overline{R}_T + j\overline{X}_T \qquad \text{(A.4.26)}$$

That is, Var(A) is minimized when Z_M is the average value of the actual terminating impedance $\overline{Z}_T = \overline{R}_T + j\overline{X}_T$.

In accordance with the statements just following A.4.19, this value also minimizes Var(C).

This is thus the value of Z_M, by eqs. A.4.7 and A.4.8, which will minimize the variances of I_T and V_T about any mean values, given that I_M is known.

This result is used in Section 3.3.4, where the optimum terminating impedance for emission measurement is discussed.

A.4.5 Computation of the Statistics of Z_T

In the next section, actual values of the normalized variances will be computed. For these computations the mean and variance of R_T and X_T, the resistance and reactance of the actual terminating impedance Z_T will be required. Z_T, it may be recalled, is the parallel combination of the line and load impedance, or

$$Z_T = \frac{Z_L Z_R}{Z_L + Z_R} \qquad \text{(A.4.27)}$$

We assume means and variances for Z_L and Z_R. From A.4.27 we then find the means and variances of Z_T, using a linear approximation as above.

Letting

$$Z_T = R_T + jX_T$$

$$Z_L = R_L + jX_L$$

$$Z_R = R_R + jX_R$$

and using A.4.27, we have

$$R_T = \frac{R_R(R_L^2 + X_L^2) + R_L(R_R^2 + X_R^2)}{(R_L + R_R)^2 + (X_L + X_R)^2} \qquad \text{(A.4.28)}$$

$$X_T = \frac{X_R(R_L^2 + X_L^2) + X_C(R_R^2 + X_R^2)}{(R_L + R_R)^2 + (X_C + X_R)^2} \qquad \text{(A.4.29)}$$

Using a linear approximation as above, i.e., assuming that R_T and X_T vary linearly from their mean values as functions of R_L, X_L, R_R, and X_R, we have, assuming these variables are statistically independent,

$$\overline{R}_T = \frac{\overline{R}_R(\overline{R}_L^2 + \overline{X}_L^2) + \overline{R}_L(\overline{R}_R^2 + \overline{X}_R^2)}{(\overline{R}_L + \overline{R}_R)^2 + (\overline{X}_L + \overline{X}_R)^2} \qquad \text{(A.4.30)}$$

$$\overline{X}_T = \frac{\overline{X}_R(\overline{R}_L^2 + \overline{X}_L^2) + \overline{X}_L(\overline{R}_R^2 + \overline{X}_R^2)}{(\overline{R}_L + \overline{R}_R)^2 + (\overline{X}_C + \overline{X}_R)^2} \qquad \text{(A.4.31)}$$

$$\sigma_{R_T}^2 = \mathrm{Var}(R_T) = \left(\frac{\partial R_T}{\partial R_R}\right)^2_{\overline{R}_T} \sigma_{R_R}^2 + \left(\frac{\partial R_T}{\partial R_L}\right)^2_{\overline{R}_T} \sigma_{R_L}^2 + \left(\frac{\partial R_T}{\partial X_R}\right)^2_{\overline{R}_T} \sigma_{X_R}^2 + \left(\frac{\partial R_T}{\partial X_L}\right)^2_{\overline{R}_T} \sigma_{X_L}^2 \qquad \text{(A.4.32)}$$

$$\sigma_{X_T}^2 = \mathrm{Var}(X_T) = \left(\frac{\partial X_T}{\partial R_R}\right)^2_{\bar{X}_T} \sigma_{R_R}^2 + \ldots + \left(\frac{\partial X_T}{\partial X_L}\right)^2_{\bar{X}_T} \sigma_{X_L}^2 \qquad \text{(A.4.33)}$$

where the subscripts $\bar{R}_T$ and $\bar{X}_T$ indicate that these derivatives are evaluated at the mean values of R_R, R_L, X_R, and X_L.

The values of these derivatives are listed below.

$$\left.\frac{\partial R_T}{\partial R_R}\right|_{\bar{R}_T} = \frac{(\bar{R}_L^2 + \bar{X}_L^2) + 2\bar{R}_L \bar{R}_R}{D} - \frac{2N_R}{D^2}(\bar{R}_L + \bar{R}_R) \qquad \text{(A.4.34)}$$

$$\left.\frac{\partial R_T}{\partial R_L}\right|_{\bar{R}_T} = \frac{(\bar{R}_R^2 + \bar{X}_R^2) + 2\bar{R}_L \bar{R}_R}{D} - \frac{2N_R}{D^2}(\bar{R}_L + \bar{R}_R) \qquad \text{(A.4.35)}$$

$$\left.\frac{\partial R_T}{\partial X_L}\right|_{\bar{R}_T} = \frac{2\bar{R}_R \bar{X}_L}{D} - \frac{2N_R}{D^2}(\bar{X}_L + \bar{X}_R) \qquad \text{(A.4.36)}$$

$$\left.\frac{\partial R_T}{\partial X_R}\right|_{\bar{R}_T} = \frac{2\bar{R}_L \bar{X}_R}{D} - \frac{2N_R}{D^2}(\bar{X}_L + \bar{X}_R) \qquad \text{(A.4.37)}$$

$$\left.\frac{\partial X_T}{\partial R_R}\right|_{\bar{X}_T} = \frac{2\bar{R}_R \bar{X}_L}{D} - \frac{2N_X}{D^2}(\bar{R}_L + \bar{R}_R) \qquad \text{(A.4.38)}$$

$$\left.\frac{\partial X_T}{\partial R_L}\right|_{\bar{X}_T} = \frac{2\bar{R}_L \bar{X}_R}{D} - \frac{2N_X}{D^2}(\bar{R}_L + \bar{R}_R) \qquad \text{(A.4.39)}$$

$$\left.\frac{\partial X_T}{\partial X_L}\right|_{\bar{X}_T} = \frac{2\bar{X}_R\,\bar{X}_L + (\bar{R}_R^{\,2} + \bar{X}_R^{\,2})}{D} - \frac{2N_X}{D^2}(\bar{X}_L + \bar{X}_R) \qquad \text{(A.4.40)}$$

$$\left.\frac{\partial X_T}{\partial X_R}\right|_{\bar{X}_T} = \frac{2\bar{X}_R\,\bar{X}_L + (\bar{R}_L^{\,2} + \bar{X}_L^{\,2})}{D} - \frac{2N_X}{D^2}(\bar{X}_L + \bar{X}_R) \qquad \text{(A.4.41)}$$

where $D = (\bar{R}_L + \bar{R}_R)^2 + (\bar{X}_L + \bar{X}_R)^2$

$$N_R = \bar{R}_R(\bar{R}_L^{\,2} + \bar{X}_L^{\,2}) + \bar{R}_L(\bar{R}_R^{\,2} + \bar{X}_R^{\,2})$$

$$N_X = \bar{X}_R(\bar{R}_L^{\,2} + \bar{X}_L^{\,2}) + \bar{X}_L(\bar{R}_R^{\,2} + \bar{X}_R^{\,2})$$

Identical Statistics Case

To obtain numerical values, we make the assumption (which is in agreement with the data in Sections A.2 and A.3) that the means of the resistances are equal, the means of the reactances are equal, and that the variances of the resistances and the reactances are equal. That is, that

$$\left.\begin{aligned} \bar{R} &= \bar{R}_S = \bar{R}_L = \bar{R}_R \\ \bar{X} &= \bar{X}_S = \bar{X}_L = \bar{X}_R \\ \sigma^2 &= \sigma_{R_S}^{\,2} = \sigma_{X_S}^{\,2} = \sigma_{R_L}^{\,2} = \sigma_{X_L}^{\,2} = \sigma_{R_R}^{\,2} = \sigma_{X_R}^{\,2} \end{aligned}\right\} \qquad \text{(A.4.42)}$$

Substituting these relationships into the above equations, we find

$$\left.\begin{aligned} \bar{R}_T &= \frac{\bar{R}}{2} \qquad \text{(A.4.43)} \\ \bar{X}_T &= \frac{\bar{X}}{2} \qquad \text{(A.4.44)} \end{aligned}\right\} \quad \bar{Z} = \frac{\bar{R} + j\bar{X}}{2}$$

$$\sigma_{R_T}^2 = \sigma_{X_T}^2 = \frac{\sigma^2}{8} \qquad (A.4.45)$$

In other words, the mean actual terminating impedance is one-half the mean source, line, or load impedance, and its variance is one-eighth that of the common variance of the resistances and reactances.

A.4.6 Computation of the Normalized Variances

Actual values of the normalized variances of current and voltage are used in Section 4.2.3, for comparing accuracies of measurement techniques, in Section 4.3 for deriving emission limits and in Section 4.4 for deriving susceptibility limits. In this section, we derive the general expressions used in making these computations.

Minimum Values

We recall eqs. A.4.18 and A.4.19 for Var(A) and Var(C), and the ensuing discussion on minimum values. At $\text{Var}(A)_{\min}$, the first two terms in A.4.18 are zero, so that

$$\text{Var}(A)_{\min} = \left(\frac{1}{\bar{A}_M}\frac{\partial A_M}{\partial R_T}\right)^2_{\bar{A}_M} \sigma_{R_T}^2 + \left(\frac{1}{\bar{A}_M}\frac{\partial A_M}{\partial X_T}\right)^2 \sigma_{X_T}^2 \qquad (A.4.46)$$

$$\text{Var}(C)_{\min} = \text{Var}(A)_{\min} + \frac{1}{|\bar{Z}_T|^4}\left[\bar{R}_T^2\,\sigma_{R_T}^2 + \bar{X}_T^2\,\sigma_{X_T}^2\right] \qquad (A.4.47)$$

Making the identical statistics assumption (see previous section), these expressions reduce to

$$\text{Var}(A)_{\min} = \frac{\sigma^2}{18(\bar{R}^2 + \bar{X}^2)} \qquad (A.4.48)$$

$$\text{Var}(C)_{\min} = \frac{8\sigma^2}{9(\bar{R}^2 + \bar{X}^2)} = 16\ \text{Var}(A)_{\min} \qquad (A.4.49)$$

where the meaning of σ^2, $\bar{R}$, and $\bar{X}$ is described in eq. A.4.42.

Relative Values

In turns out that computing the ratios $\mathrm{Var}(A)/\mathrm{Var}(A)_{min}$ and $\mathrm{Var}(C)/\mathrm{Var}(C)_{min}$ is easier than the direct computation of $\mathrm{Var}(A)$ and $\mathrm{Var}(C)$. Then, once the minimum values are known, a simple multiplication provides $\mathrm{Var}(A)$ and $\mathrm{Var}(C)$.

From eqs. A.4.46 and A.4.18,

$$\mathrm{Var}(A) = \left(\frac{1}{\bar{A}_M}\frac{\partial A_M}{\partial R_S}\right)^2 \sigma_{R_S}{}^2 + \left(\frac{1}{\bar{A}_M}\frac{\partial A_M}{\partial X_S}\right)^2 \sigma_{X_S}{}^2 + \mathrm{Var}(A)_{min}$$

so that

$$\frac{\mathrm{Var}(A)}{\mathrm{Var}(A)_{min}} = \frac{\left(\frac{1}{\bar{A}_M}\frac{\partial A_M}{\partial R_S}\right)^2 \sigma_{R_S}{}^2 + \left(\frac{1}{\bar{A}_M}\frac{\partial A_M}{\partial X_S}\right)^2 \sigma_{X_S}{}^2}{\left(\frac{1}{\bar{A}_M}\frac{\partial A_M}{\partial R_T}\right)^2 \sigma_{R_T}{}^2 + \left(\frac{1}{\bar{A}_M}\frac{\partial A_M}{\partial X_T}\right)^2 \sigma_{X_T}{}^2} + 1 \qquad \text{(A.4.50)}$$

From eqs. A.4.47 and A.4.19,

$$\mathrm{Var}(C) - \mathrm{Var}(C)_{min} = \mathrm{Var}(A) - \mathrm{Var}(A)_{min}$$

so that

$$\frac{\mathrm{Var}(C)}{\mathrm{Var}(C)_{min}} = \frac{\mathrm{Var}(A) - \mathrm{Var}(A)_{min}}{\mathrm{Var}(C)_{min}} + 1 \qquad \text{(A.4.51)}$$

Again assuming identical statistics (eq. A.4.42),

$$\frac{\mathrm{Var}(A)}{\mathrm{Var}(A)_{min}} = \frac{8}{\bar{R}^2 + \bar{X}^2} \cdot \frac{1}{\left[(\bar{R} + R_M)^2 + (\bar{X} + X_M)^2\right]^2} \left\{ \left[(\bar{R} + R_M)\left[\bar{R}\left(\frac{\bar{R}}{2} - R_M\right) + \bar{X}^2\right] - \bar{R}(\bar{X} + X_M)^2 \right]^2 + \left[(\bar{X} + X_M)\left[\bar{X}\left(\frac{\bar{X}}{2} - X_M\right) + \bar{R}^2\right] - \bar{X}(\bar{R} + R_M)^2 \right]^2 \right\} + 1 \qquad \text{(A.4.52)}$$

$$\frac{\mathrm{Var}(C)}{\mathrm{Var}(C)_{min}} = \frac{\mathrm{Var}(A) - \mathrm{Var}(A)_{min}}{16\ \mathrm{Var}(A)_{min}} + 1 = \frac{1}{16}\left[\frac{\mathrm{Var}(A)}{\mathrm{Var}(A)_{min}} - 1\right] + 1$$

$$= \frac{1}{16}\left[\frac{\mathrm{Var}(A)}{\mathrm{Var}(A)_{min}} + 15\right] \qquad (A.4.53)$$

Computation for $Z_M = 0$ and ∞

For $Z_M = 0$ ($R_M = X_M = 0$), eqs. A.4.52 and A.4.53 become

$$\frac{\mathrm{Var}(A)}{\mathrm{Var}(A)_{min}} = 2\,\frac{\overline{R}^6 + \overline{X}^6}{(\overline{R}^2 + \overline{X}^2)^3} + 1 \qquad (A.4.54)$$

$$\frac{\mathrm{Var}(C)}{\mathrm{Var}(C)_{min}} = 8\,\frac{\overline{R}^6 + \overline{X}^6}{(\overline{R}^2 + \overline{X}^2)^3} + 1 \qquad (A.4.55)$$

For $Z_M \to \infty$ ($R_M = X_M \to \infty$), eqs. A.4.52 and A.4.53 become

$$\frac{\mathrm{Var}(A)}{\mathrm{Var}(A)_{min}} = 9 \qquad (A.4.56)$$

$$\frac{\mathrm{Var}(C)}{\mathrm{Var}(C)_{min}} = \frac{3}{2} \qquad (A.4.57)$$

A.4.7 Summary

In this section the normalized variances of the actual current and voltage at the output of a source with a random impedance $Z_S = R_S + jX_S$ have been computed, given a random load Z_T, and that the current I_M into a known load Z_M is known. I.e., given I_M and Z_M

$$\mathrm{Var}(A) = \frac{1}{\overline{I}_T^{\,2}}\,\mathrm{Var}(I_T)$$

and

$$\mathrm{Var}(C) = \frac{1}{\bar{V}_T^2}\,\mathrm{Var}(V_T)$$

The General Expressions for these quantities are given as eqs. A.4.18 and A.4.19, assuming a linear approximation, i.e., assuming that the quantities are linear functions of their variables about their mean values.

The Minimizing Value of Z_M, that value which minimizes Var(A) and Var(C), is the average value of Z_T, the random terminating impedance (eqs. A.4.25 and A.4.26).

The Mean and Variance of Z_T in terms of line and load statistics are given in general in eqs. A.4.30 thru A.4.33, and for the case where source, line, and load impedances have the same statistics, in eqs. A.4.43 - A.4.45.

Values for the Normalized Variances are given in general for eqs. A.4.46, A.4.47, A.4.50, and A.4.51, for the equal-statistics case in eqs. A.4.48, A.4.49, A.4.52, and A.4.53, for $Z_M = 0$ in eqs. A.4.48, A.4.49, A.4.54, and A.4.55, and for $Z_M = \infty$ in eqs. A.4.48, A.4.49, A.4.56, and A.4.57, where $\bar{R}$, $\bar{X}$, and σ^2 are given in eq. A.4.42.

APPENDIX 5

CHARACTERISTIC IMPEDANCE AND VOLTAGE ATTENUATION MEASUREMENTS ON TRANSMISSION LINES

A.5.1 Introduction

Presented in this section are the results of characteristic impedance and voltage attenuation measurements made on power transmission lines set up in the Moore School laboratory. Measurements were made using Romex cable and cable in rigid conduit. Lines of 70' length were set up and all measurements were taken with the lines lying on the laboratory floor. The following instruments were used to make the measurements:

1) Empire Device Noise and Field Intensity meter, Model NF-114

2) GR type 116-A RF bridge

3) Federal Manufacturing and Engineering Corp. Type CFD-60006A RF Standard Signal Oscillator Unit

4) GR Unit Oscillator, Type 1211-C

5) Hewlett-Packard Model 410-B Wide-Band VTVM

6) GR Unit Oscillator Model 1210-C.

A.5.2 Termination

In practice, lines are terminated in an effective impedance which may vary considerably under various conditions of use. To simulate conditions close to what is considered to be an average condition in practice, the voltage attenuation measurements were made on the lines under terminated conditions. 100-Ω terminating resistors were used. This figure was selected simply because it is fairly close to the characteristic impedance of normal lines. If the lines were not terminated, high peaks would have been obtained in the voltage transfer ratio of the line. This is evident from the voltage transfer ratio of a dissipationless unterminated line, which is given as

$$\frac{V_2}{V_1} = K = \frac{1}{\cosh YZ\ell} = \frac{1}{\cosh YZ_o\ell} \qquad (A.5.1)$$

where V_1 = input voltage to the line

V_2 = output voltage

Z_o = characteristic impedance of the line

ℓ = length of the line

Y = admittance per unit length of the line = $j\omega c$.

Substituting $Y = j\omega c$ in (A.5.1) we get

$$K = \frac{1}{\cos \omega Z_o \ell c} = \frac{1}{\cos \frac{\omega}{\omega_o}} \qquad \text{(A.5.2)}$$

where

$$\omega_c = \frac{1}{Z_o \ell c} \qquad \text{(A.5.3)}$$

Equation A.5.2 suggests that K is infinite wherever $\frac{\omega}{\omega_o} = \frac{(2n+1)}{2}\pi$. In practice, some dissipation is always present in the line, and that limits the magnitude of the peak to a finite value. A typical experimental setup for voltage attenuation measurement is shown in Fig. A.5.1. Except in a couple of cases, a 50-Ω cable was used for bringing the signal at the receiving end of the line back to the sending end for measurement purposes.

Characteristic impedance of the line was determined by measuring the input impedance of the line with the far end open and short circuited and then taking the square root of the product of the two impedances. A typical experimental setup for characteristic impedance measurement is shown in Fig. A.5.2.

The voltage attenuation of a line terminated in its own characteristic impedance is given as

$$\frac{V_2}{V_1} = e^{-\nu \ell} \qquad \text{(A.5.4)}$$

where ν is the propagation constant of the line. In general

$$\nu = \alpha + j\beta \tag{A.5.5}$$

where

$$\alpha = \sqrt{\frac{RG - \omega^2 LC + \sqrt{(RG - \omega^2 LC)^2 + \omega^2 (LG + RC)}}{2}} \tag{A.5.6}$$

and

$$\beta = \sqrt{\frac{\omega^2 LC - RG + \sqrt{(RG - \omega^2 LC)^2 + \omega^2 (LG + RC)^2}}{2}} \tag{A.5.7}$$

where L = inductance per unit length of the line

C = capacitance per unit length of the line

R = resistance per unit length of the line

G = conductance per unit length of the line.

Hence, so far as only the magnitude of $\frac{V_2}{V_1}$ is concerned, it is given as

$$K = \left| \frac{V_2}{V_1} \right| = e^{-\alpha \ell} \tag{A.5.8}$$

From (A.5.6) and (A.5.8) it may be seen that for a lossless line, K is constant with frequency. However, this is not true in practice, especially at high frequencies. Due to skin effect, resistance (R) of the line is quite appreciable at high frequencies and, therefore, its effect cannot be neglected. Also, the effective resistance of the line increases at high frequencies if a steel conduit is used. The functional dependence of the ac resistance of the line to its dc resistance is given as

$$\frac{R_{ac}}{R_{dc}} = A \sqrt{f} \tag{A.5.9}$$

where A is a constant which depends upon the physical dimensions of the line. Equations A.5.6 and A.5.9 indicate that α is some function of the driving frequency and it increases with frequency. Hence, K is expected to decay with frequency. As may be seen from the results of voltage attenuation measurements on transmission line made of Romex wire (Fig. A.5.3) and the same on a transmission line with steel conduit under two different termination conditions (Figs. A.5.4, A.5.5 and A.5.6), K does decay with frequency, but some oscillations

are present in the K-f curves. These oscillations are due to the mismatch between the actual characteristic impedance of the line, which may be seen from the results of characteristic impedance measurements on Romex wire presented in Fig. A.5.7 and the same on transmission lines with steel conduits for various pipe sizes and gounding conditions presented in Figs. A.5.10 through A.5.12, and the actual terminating resistance. The reactive and resistive components of the line with steel conduit under two different terminating conditions with the far end of the line open and short-circuited are shown in Figs. A.5.8 and A.5.9. The frequency dependence of the line parameters and hence the characteristic impedance of the line are evident from these curves.

The results of characteristic impedance (Z_o) measurements show that Z_o remains practically constant up to a certain frequency, after which it becomes a frequency-dependent function. This may also be attributed to the increase in effective resistance of the line at high frequencies. When the effect of R and G is negligible, the characteristic impedance is given as

$$Z_o = \sqrt{\frac{L}{C}} \tag{A.5.10}$$

whereas when the loss components cannot be neglected, the characteristic impedance is given as

$$Z_o = \sqrt{\frac{R + j\omega L}{G + j\omega c}} = \sqrt{\frac{(RG + \omega^2 LC) + j\omega(LG - RC)}{(G^2 + \omega^2 c^2)}} \tag{A.5.11}$$

Equation A.5.11 indicates the dependence of Z_o upon frequency.

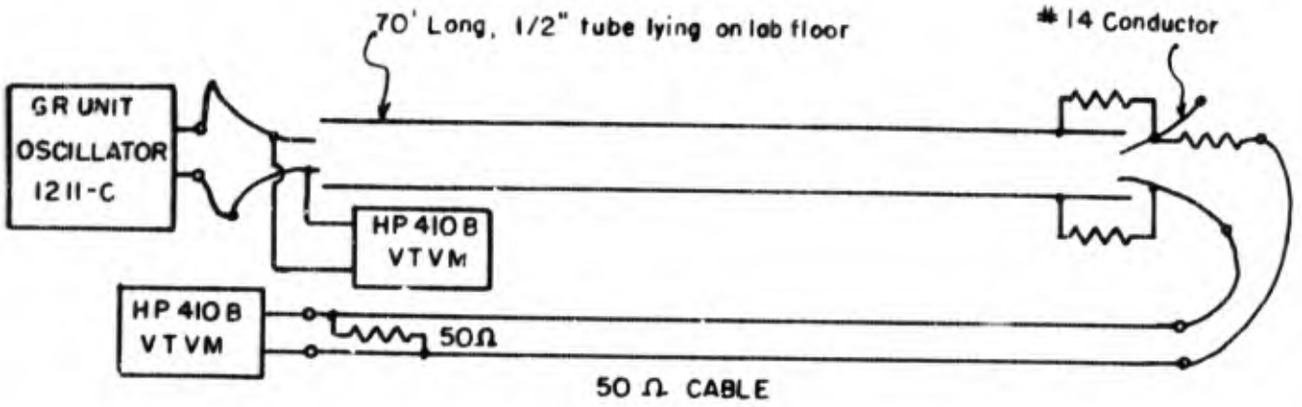

Figure A 5.1 EXPERIMENTAL SETUP FOR VOLTAGE ATTENUATION MEASUREMENTS.

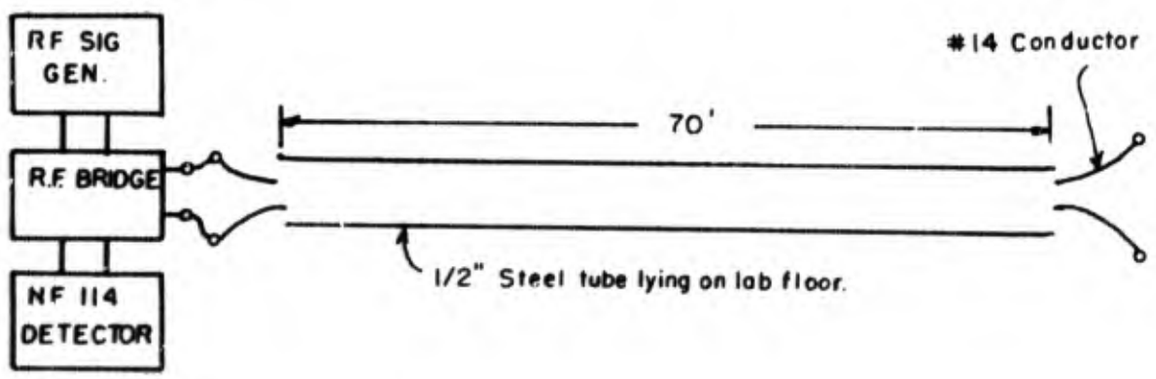

Figure A.5.2 TYPICAL EXPERIMENTAL SETUP FOR CHARACTERISTIC IMPEDANCE MEASUREMENTS

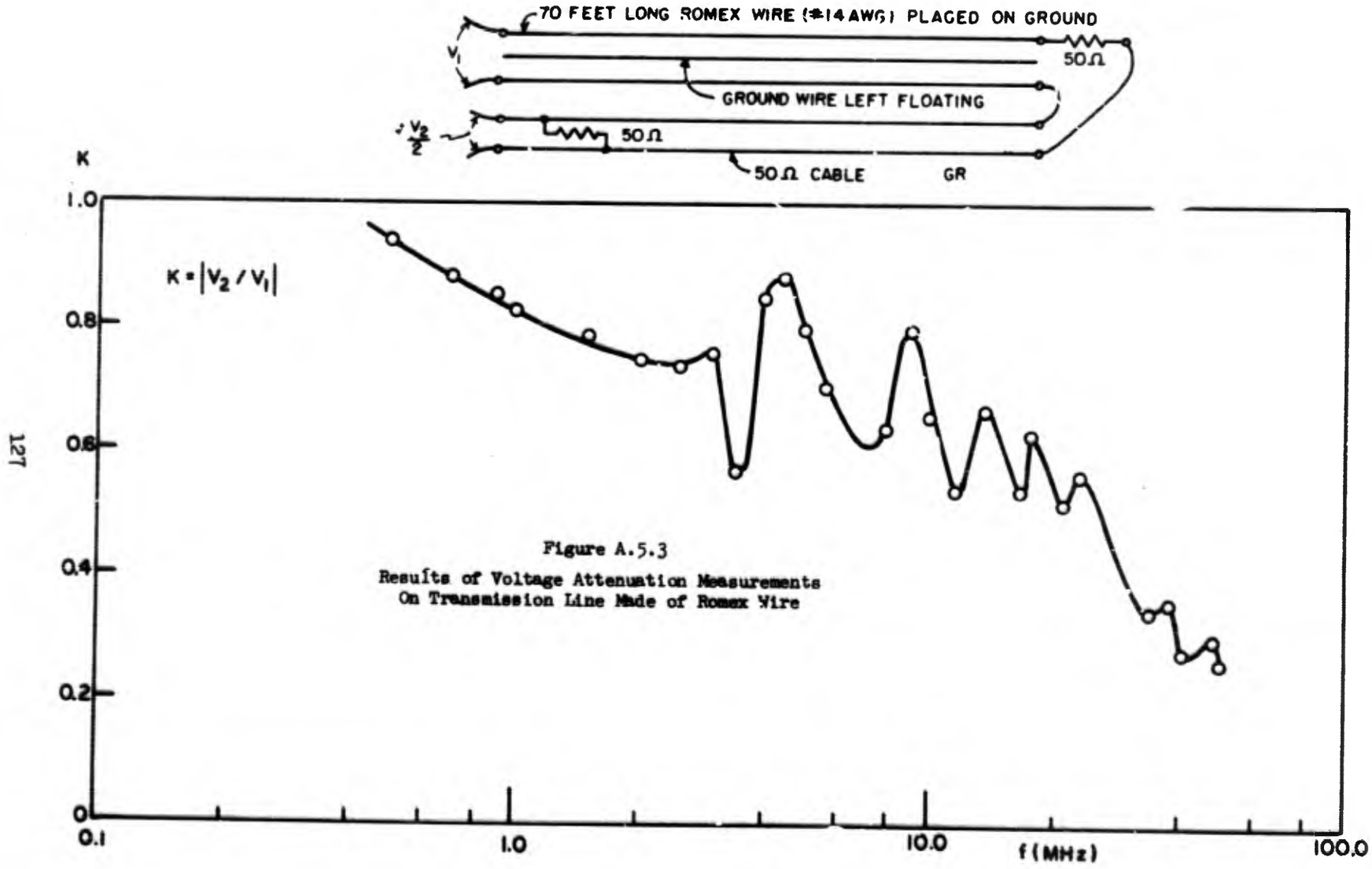

Figure A.5.3
Results of Voltage Attenuation Measurements
On Transmission Line Made of Romex Wire

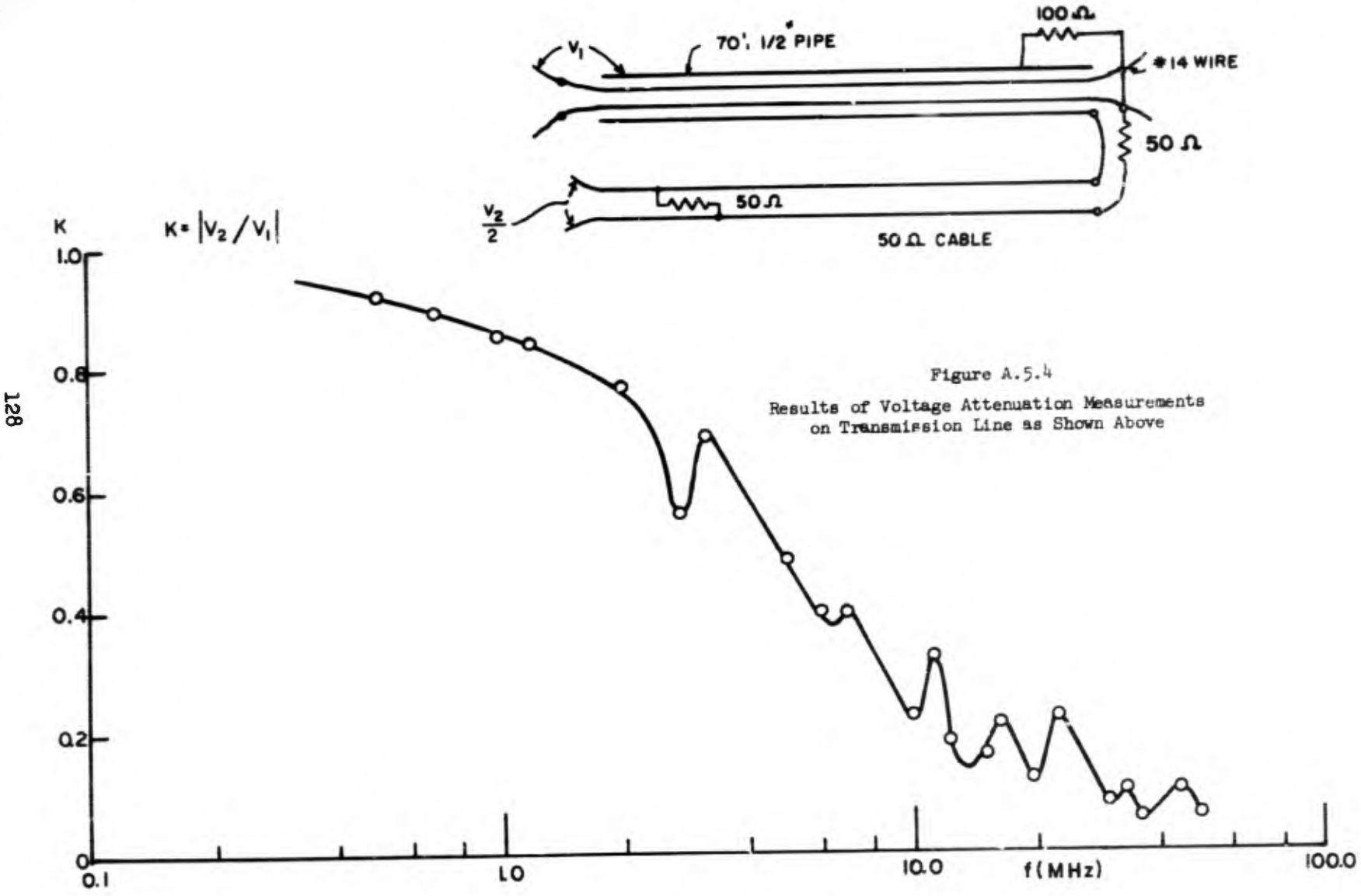

Figure A.5.4

Results of Voltage Attenuation Measurements on Transmission Line as Shown Above

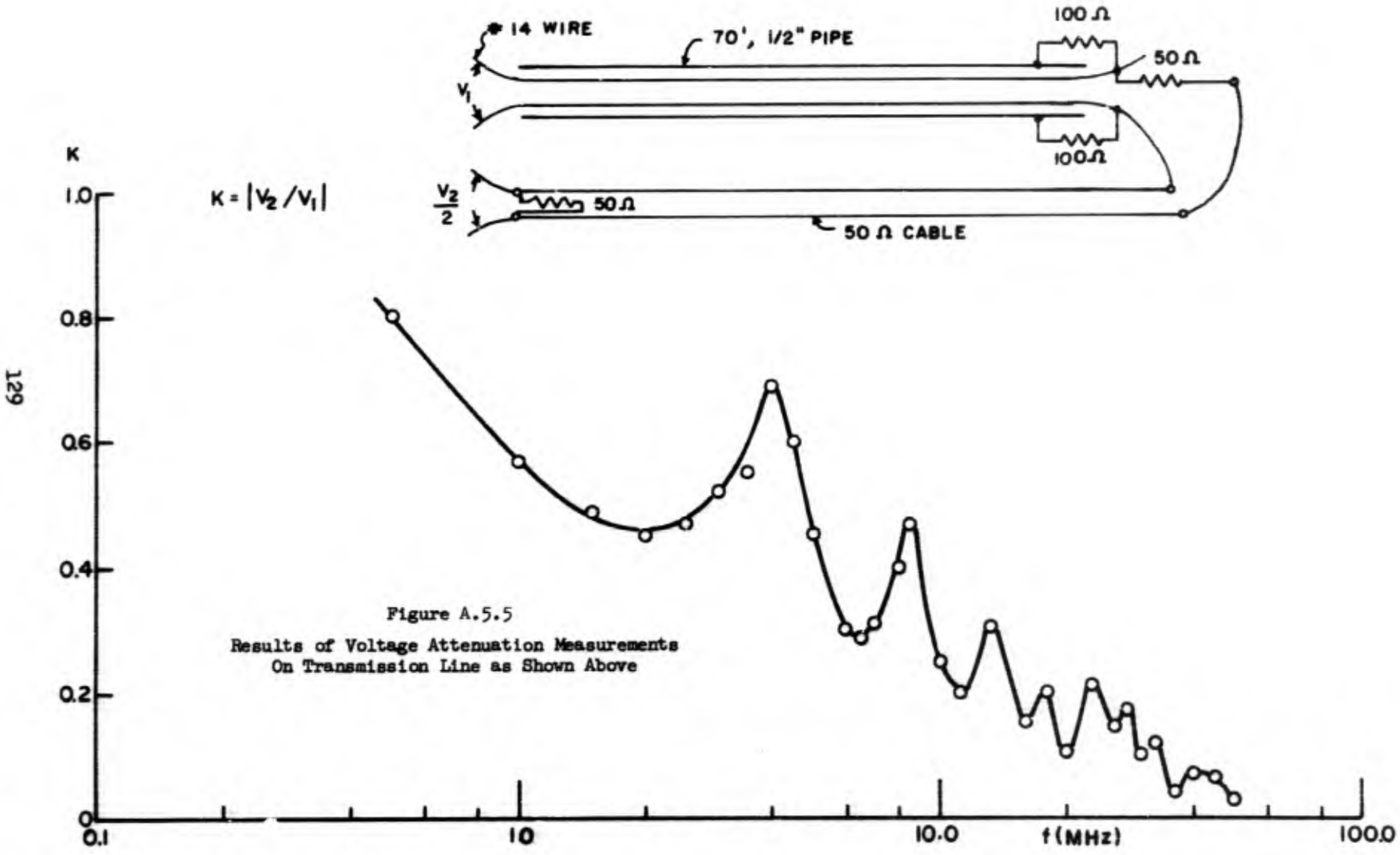

Figure A.5.5

Results of Voltage Attenuation Measurements
On Transmission Line as Shown Above

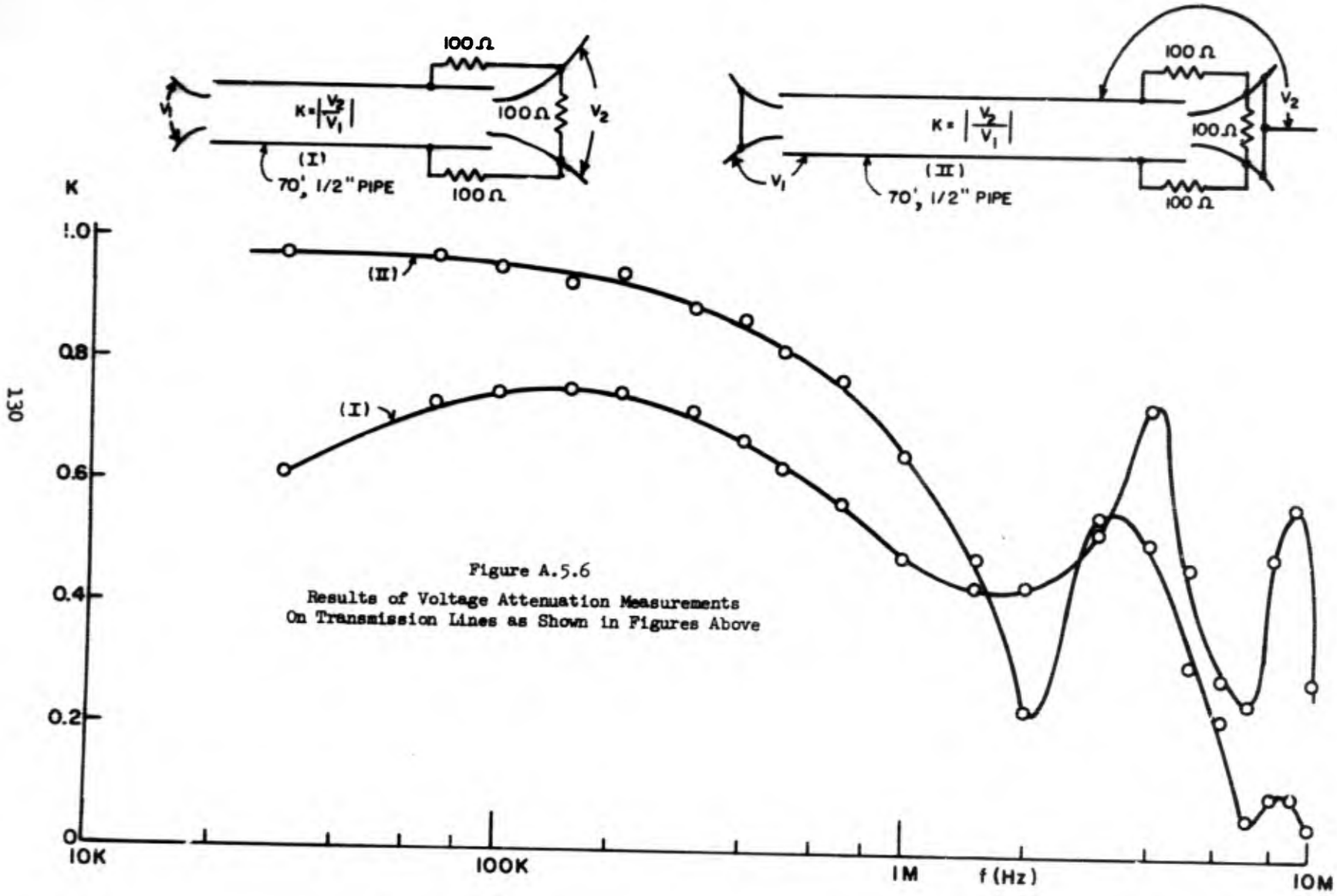

Figure A.5.6

Results of Voltage Attenuation Measurements On Transmission Lines as Shown in Figures Above

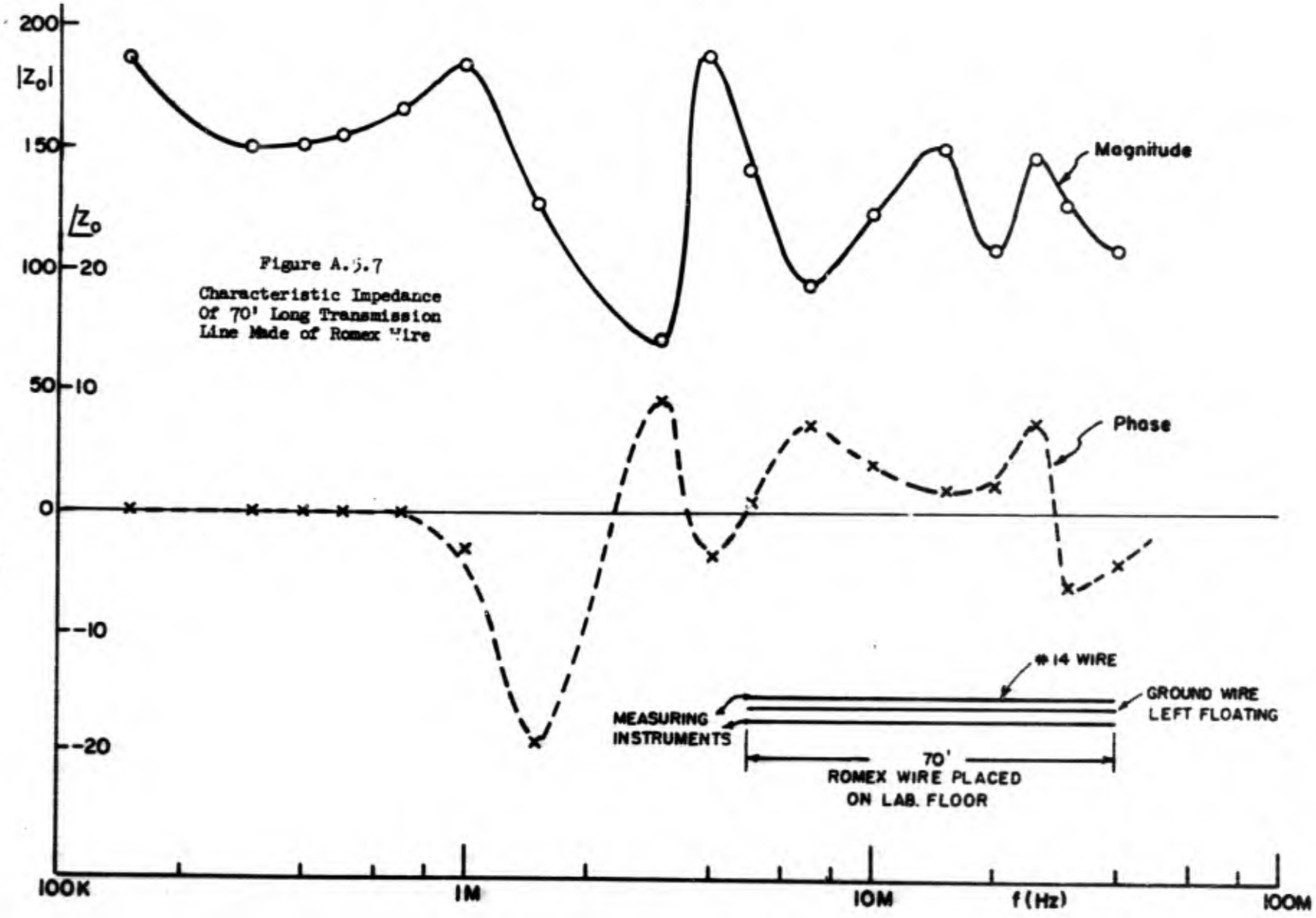

Figure A.5.7

Characteristic Impedance
Of 70' Long Transmission
Line Made of Romex Wire

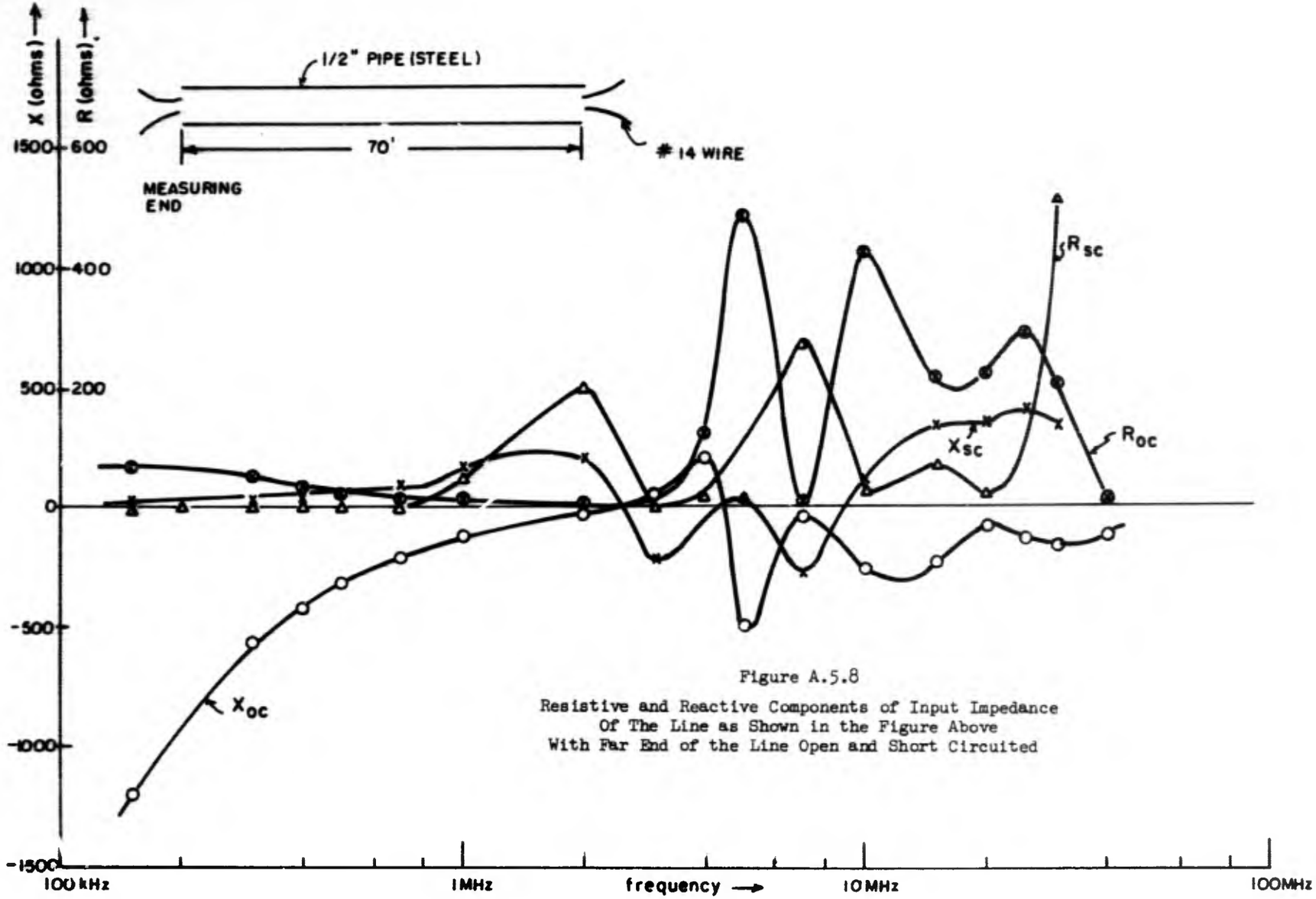

Figure A.5.8

Resistive and Reactive Components of Input Impedance
Of The Line as Shown in the Figure Above
With Far End of the Line Open and Short Circuited

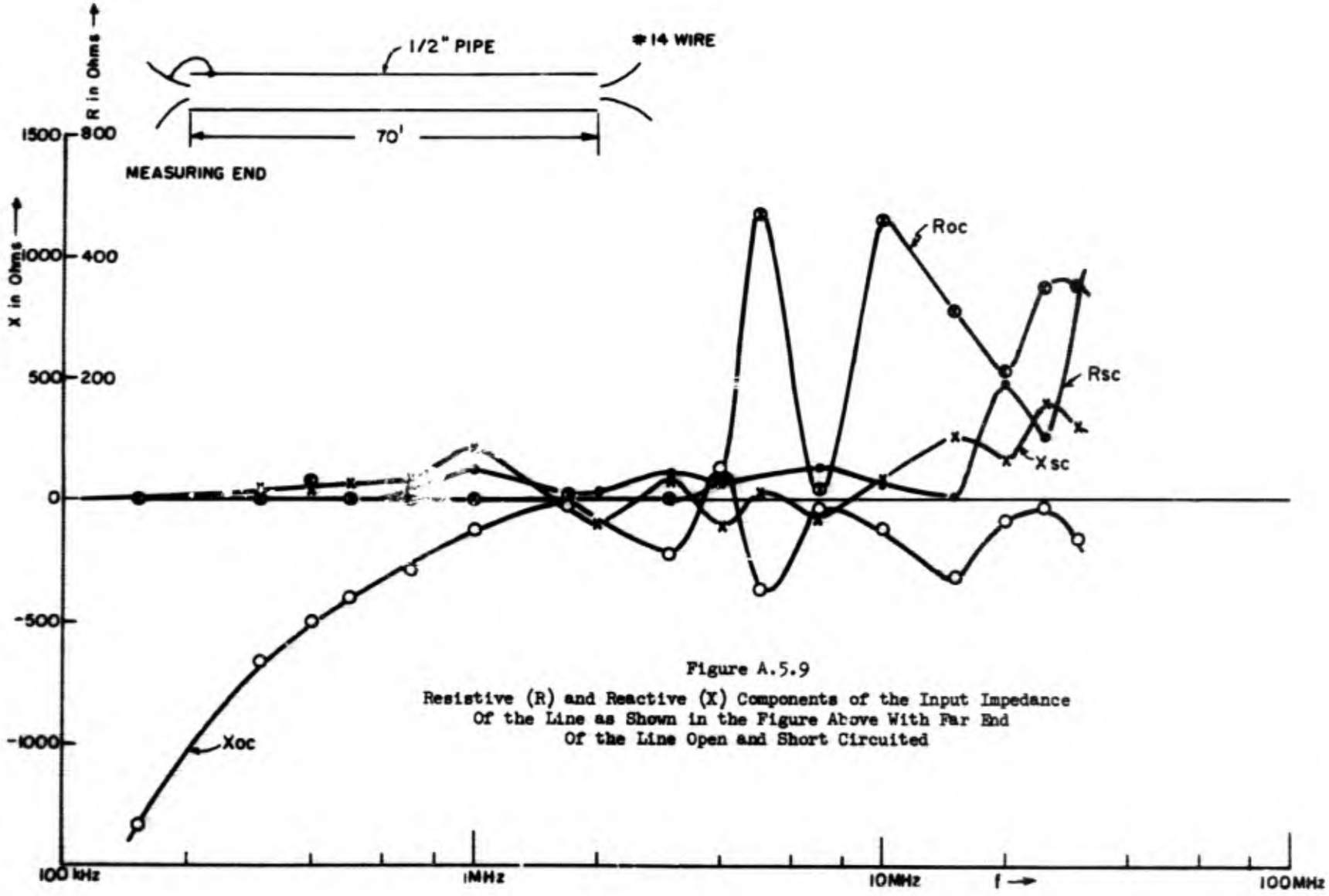

Figure A.5.9

Resistive (R) and Reactive (X) Components of the Input Impedance
Of the Line as Shown in the Figure Above With Far End
Of the Line Open and Short Circuited

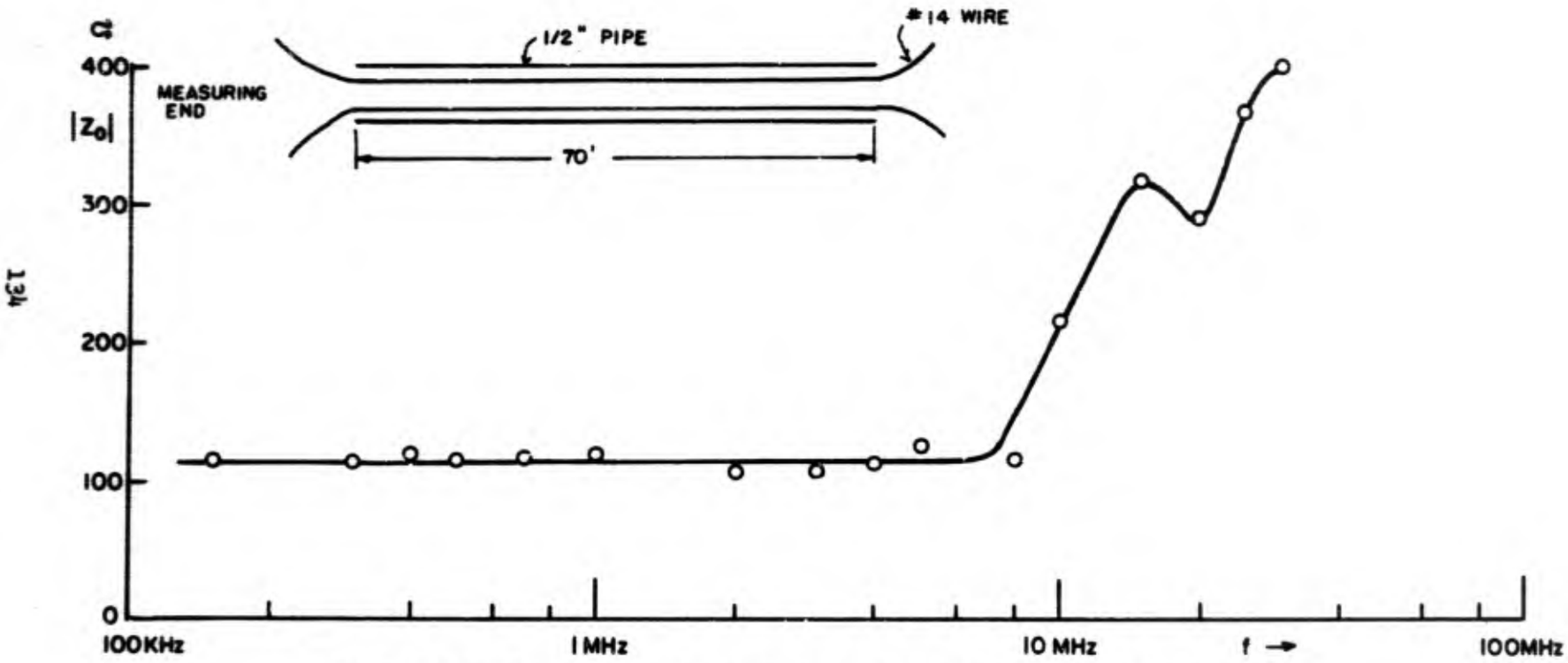

Figure A.5.10 Characteristic Impedance of the Line as Shown in the Figure Above

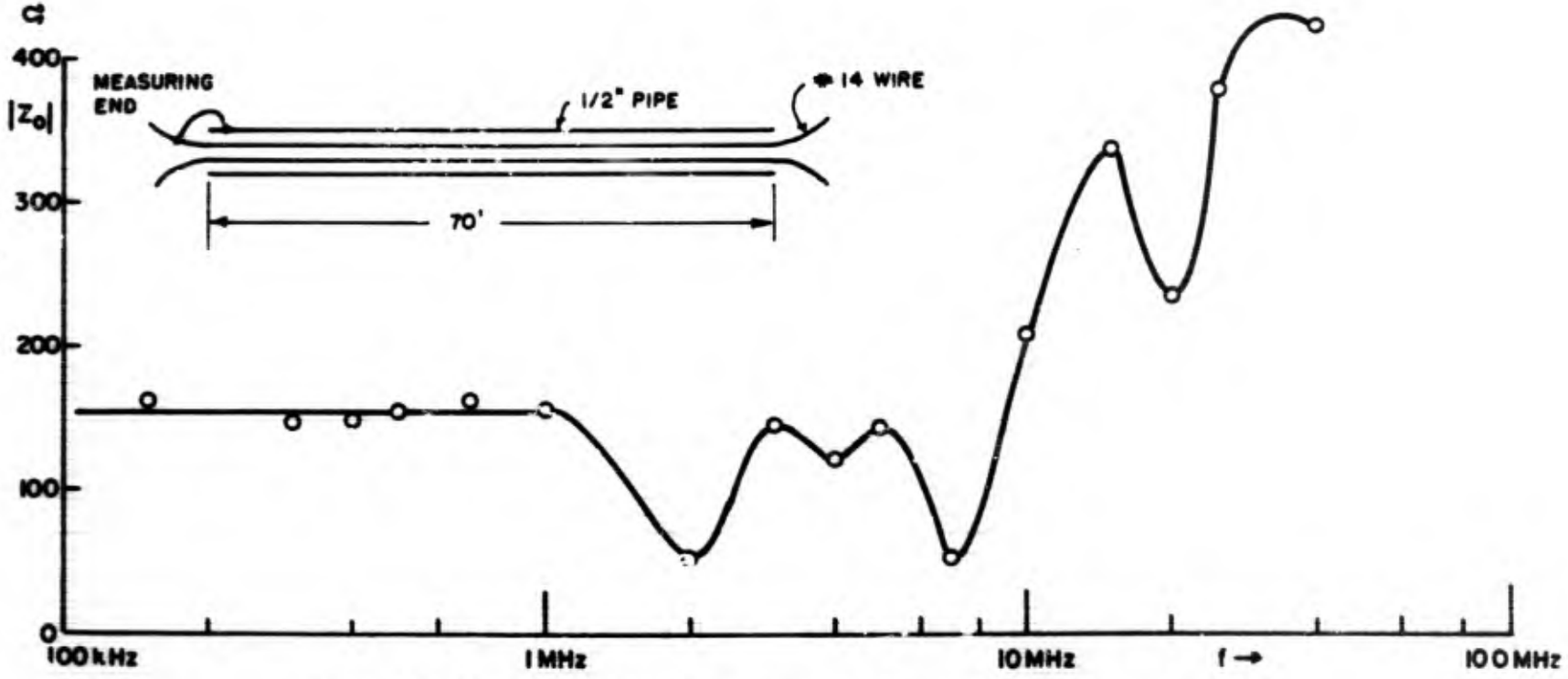

Figure A.5.11 Characteristic Impedance of the Line as Shown in Figure Above

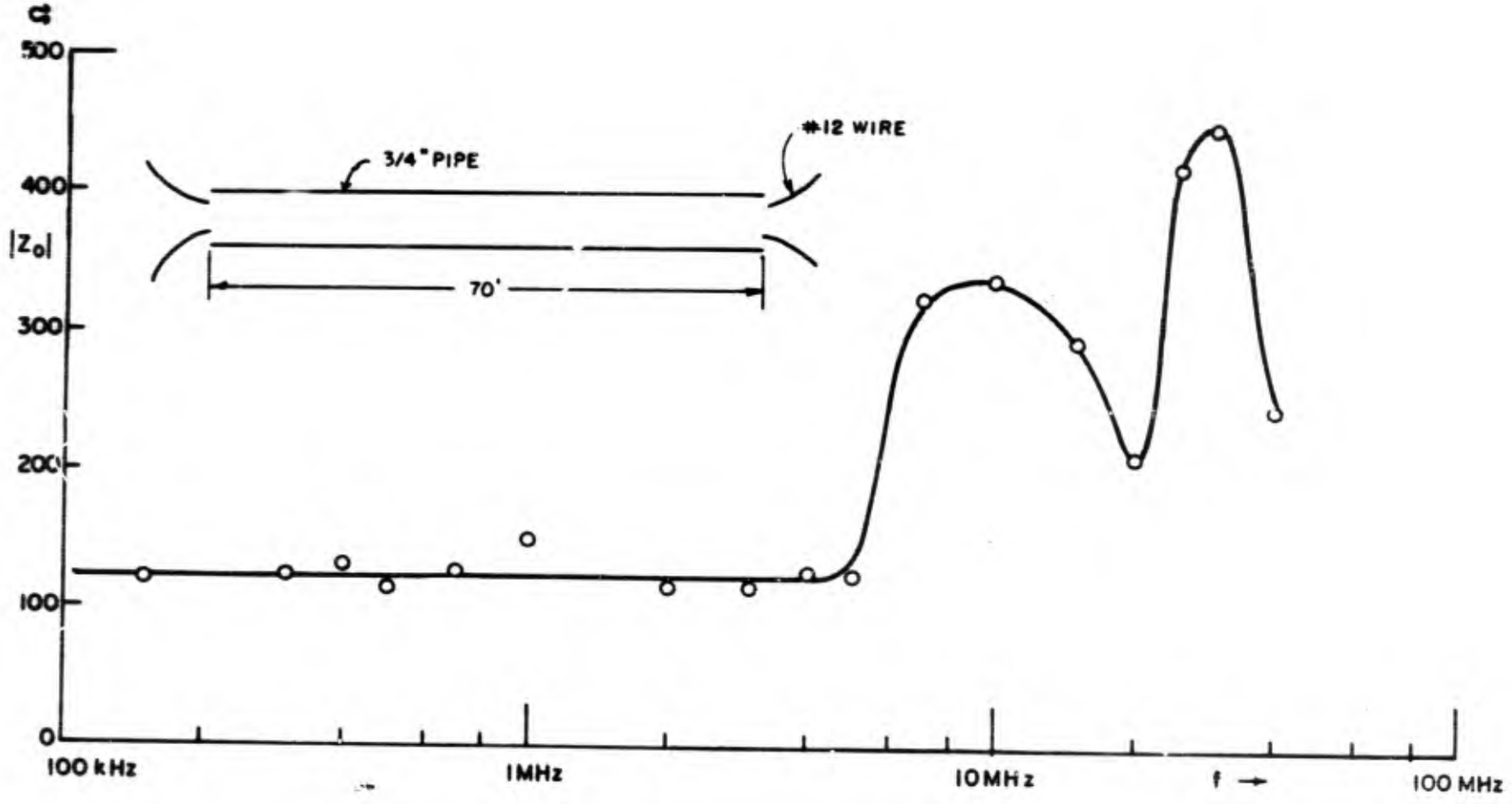

Figure A.5.12 Characteristic Impedance of the Line as Shown in Figure Above

UNCLASSIFIED

Security Classification

DOCUMENT CONTROL DATA - R & D

(Security classification of title, body of abstract and indexing annotation must be entered when the overall report is classified)

1. ORIGINATING ACTIVITY (Corporate author)
University of Pennsylvania
The Moore School of Electrical Engineering
Philadelphia, Pennsylvania 19104

2a. REPORT SECURITY CLASSIFICATION
UNCLASSIFIED

2b. GROUP
N/A

3. REPORT TITLE
EMC DATA COLLECTION TECHNIQUES
Test Methods CE and CS

4. DESCRIPTIVE NOTES (Type of report and inclusive dates)
Interim Report 2 (2 Nov 68 to 2 May 69)

5. AUTHOR(S) (First name, middle initial, last name)
Fred Haber
K.H. Dolle
R.M. Showers, et al

6. REPORT DATE	7a. TOTAL NO. OF PAGES	7b. NO. OF REFS
June 1969	136	5

8a. CONTRACT OR GRANT NO.	9a. ORIGINATOR'S REPORT NUMBER(S)
F30602-68-C-0178	Moore School Report No. 69-22
b. PROJECT NO. 4540	
c. Task 454001	9b. OTHER REPORT NO(S) (Any other numbers that may be assigned this report) RADC-TR-69-181
d.	

10. DISTRIBUTION STATEMENT
This document is subject to special export controls and each transmittal to foreign governments or foreign nationals may be made only with prior approval of RADC (EMCVM-1), GAFB, NY 13440.

11. SUPPLEMENTARY NOTES	12. SPONSORING MILITARY ACTIVITY
	Rome Air Development Center (EMCVM-1) Griffiss Air Force Base, New York 13440

13. ABSTRACT

An evaluation of the present specifications for conducted interference in MIL-STD-461A and 462 is reported. The basis for setting limits is reviewed, and the test methods presently called for are applied to several types of communications and radar equipment. Statistical data on power line and equipment internal impedances permit a comparison of present emission and susceptibility limits and permit the computation of new limits by inserting data into a theoretical interference model.

A radiation model is used to arrive at an absolute limit of current from an interference source. This limit is converted to a measured emission current limit through use of a statistical circuit model, assuming an allowable 2.3% probability of interference. A corresponding susceptibility limit is derived.

From the standpoint of efficiency in predicting compatibility, the optimum value of emission test load impedance is the average actual load impedance, and not a short circuit as is presently used. Limits derived for both test terminations, and accuracies of the two techniques are compared.

Certain new emission and susceptibility limits are proposed and specific recommendations are presented on test methods.

DD FORM 1 NOV 68 1473

UNCLASSIFIED

Security Classification

14. KEY WORDS	LINK A		LINK B		LINK C	
	ROLE	WT	ROLE	WT	ROLE	WT
Interference, conducted Interference Limits, conducted Specifications Test Methods, Electromagnetic Compatibility Impedance, Power Line Impedance, Equipment Internal						

AFLC—Griffiss AFB NY 5 Aug 69-135